



ZMNH



**IDENTIFICATION AND CHARACTERIZATION OF
INTRACELLULAR BINDING PARTNERS OF
THE CHL1 (CLOSE HOMOLOGUE OF L1)
NEURAL CELL RECOGNITION MOLECULE**

DISSERTATION

zur Erlangung des Grades eines
Doktors der Naturwissenschaften
(doctor rerum naturalium)
der Fakultät für Biologie der Universität Bielefeld

vorgelegt von

Melanie Richter

Bielefeld, Januar 2002

Name: Melanie Richter

Titel der Dissertation: Identification and Characterization of
Intracellular Binding Partners of the
CHL1 (Close Homologue of L1)
Neural Cell Recognition Molecule

Gutachter: Prof. Dr. Melitta Schachner
Priv. Doz. Dr. Joerg W. Bartsch

I.	INTRODUCTION.....	1
I.1.	The immunoglobulin superfamily of cell adhesion molecules (CAMs)	1
I.2.	Neuronal cell adhesion molecules of the immunoglobulin superfamily	4
I.3.	The cell adhesion molecule L1	8
I.4.	The L1 subfamily of neuronal IgSF molecules	9
I.5.	A new member of L1-related proteins: The close homologue of L1 (CHL1).....	13
II.	AIM OF THE STUDY	17
III.	MATERIAL.....	19
III.1.	Chemicals	19
III.2.	Solutions and buffers.....	19
III.3.	Bacterial media	26
III.4.	Cell culture media.....	26
III.5.	Bacterial strains and cell lines	27
III.6.	Molecular weight standards	28
III.7.	Plasmids	29
III.8.	Antibodies.....	30
IV.	METHODS	32
IV.1.	Cell culture of cell lines	32
IV.1.1.	Stable transfected CHO cells	32
IV.1.2.	Cell culture of stable transfected CHO cells	32
IV.1.3.	Transient transfection of cells.....	32

IV.1.4.	Lysis of transfected cells	33
IV.1.5.	Co-immunoprecipitation from transiently transfected CHO or N2A cells.....	33
IV.2.	Cell culture of primary hippocampal neurons.....	34
IV.2.1.	Preparation of dissociated hippocampal cultures	34
IV.2.2.	Neuritogenesis of hippocampal neurons.....	35
IV.2.3.	Transfection of hippocampal neurons	35
IV.3.	Immunocytochemistry.....	36
IV.3.1.	Immunocytochemistry of living cells	36
IV.3.2.	Fixation of cells	36
IV.3.3.	Immunocytochemistry of fixed CHO cells and hippocampal neurons.....	36
IV.4.	Immunohistochemistry	37
IV.5.	Generation of polyclonal antiserum from rabbit.....	38
IV.5.1.	Immunization.....	38
IV.5.2.	Preparation of serum from blood.....	38
IV.5.3.	Preparation of IgG fraction from crude serum	38
	Preparation of IgG fraction with saturated ammonium sulfate (SAS)	38
	Preparation of IgG fraction with ProteinA sepharose	39
IV.5.4.	Affinity purification of IgG fraction.....	39
	Coupling of mouse CHL1-Fc and human IgG to CNBr-activated sepharose ..	39
	Affinity purification.....	39
IV.6.	Molecular biology	40
IV.6.1.	Bacterial expression system (pQE 30, Qiagen).....	40
IV.6.2.	Production of competent bacteria	40
IV.6.3.	Transformation of bacteria	41
IV.6.4.	Plasmid isolation of E.coli.....	41
	Small scale plasmid isolation of E. coli (Miniprep)	41
	Large scale plasmid isolation of E. coli (Maxiprep)	42
IV.6.5.	Enzymatic modification of DNA.....	42
	Digestion of DNA.....	42

	Dephosphorylation of plasmid DNA	42
	Ligation of DNA fragments.....	43
IV.6.6.	Polymerase chain reaction (PCR).....	43
IV.6.7.	DNA gel electrophoresis	44
IV.6.8.	Extraction of DNA fragments from agarose gels	44
IV.6.9.	Purification of DNA fragments	45
IV.6.10.	Determination of DNA concentrations.....	45
IV.6.11.	DNA sequencing.....	45
IV.6.12.	Site-directed mutagenesis	45
IV.7.	Proteinbiochemistry	47
IV.7.1.	One-dimensional SDS-polyacrylamide gel electrophoresis	47
IV.7.2.	Two-dimensional SDS-polyacrylamide gel electrophoresis	48
IV.7.3.	Coomassie staining of polyacrylamide gels	48
IV.7.4.	Silver staining of polyacrylamide gels	48
IV.7.5.	Electrophoretic transfer of proteins on nitrocellulose membranes (Western blotting)	49
IV.7.6.	Immunological detection of proteins on nitrocellulose membranes.....	49
IV.7.7.	Overlay approach.....	49
IV.7.8.	Immunological detection using enhanced chemiluminescence (ECL).....	50
IV.7.9.	Enzyme-linked Immunosorbent assay (ELISA).....	50
IV.7.10.	Expression of recombinant proteins in <i>Escherichia coli</i>	51
IV.7.11.	Expression in <i>E. coli</i> using the pQE-system.....	51
IV.7.12.	Expression in <i>E. coli</i> using the pET-system	52
IV.7.13.	Lysis of bacteria.....	52
	Sonification.....	52
	French press	52
IV.7.14.	Expression of recombinant proteins in stable transfected CHO cells	53
IV.7.15.	Determination of protein concentration (BCA).....	53
IV.7.16.	Brain homogenisation.....	53
IV.7.17.	Preparation of membrane subfractions	54
IV.7.18.	Affinity chromatography	55

Coupling gels for ligand immobilization.....	55
Affinity chromatography	56
IV.7.19. Immunoprecipitation	56
V. RESULTS	57
V.1. Production of recombinant CHL1-Fc and CHL1-ICD _{his6}	57
V.2. Affinity chromatography of brain homogenates using immobilized CHL1-Fc and CHL1-ICD _{his6}	58
V.3. One-dimensional overlay of brain fractions using soluble CHL1-ICD _{his6} , L1-ICD _{his6} and NCAM 180-ICD _{his6}	60
V.4. Overlay approach of CHL1-ICD _{his6} after two-dimensional separation of a brain homogenate.....	62
V.5. Isolation and identification of the CHL1-ICD _{his6} -binding protein.....	64
V.6. Verification of the CHL1-hsc70 interaction by co-immunoprecipitation	65
V.7. Binding study of recombinant CHL1-ICD _{his6} and hsc70 _{his6} using an ELISA approach	66
V.8. Confirmation of hsc70 as CHL1-ICD _{his6} binding protein performing a two-dimensional overlay approach.....	68
V.9. Co-localization and co-capping of CHL1 and hsc70 in primary hippocampal cultures	71
V.10. Analysis of the hsc70 and CHL1 distribution in membrane subfractions	73
V.11. Co-immunoprecipitation of CHL1 and hsc70 from a crude brain fraction.....	75
V.12. Co-immunoprecipitation of CHL1 and hsc70 from brain membranes derived from mice of different ages	77

V.13.	Identification of a putative hsc70 binding motif in the intracellular domain of CHL1.....	79
V.14.	Site-directed mutagenesis of the putative hsc70 binding site in the intracellular domain of CHL1	80
V.15.	Co-precipitation of CHL1 and hsc70 from transfected CHO cells.....	82
V.16.	Co-precipitation of CHL1 and hsc70 from CHO cells after transfection of wildtype CHL1 and mutant CHL1	83
V.17.	Co-precipitation of CHL1 and hsc70 from N2A cells after transfection of wildtype CHL1 and mutant CHL1	84
V.18.	Functional analysis of the interaction between CHL1 and hsc70	85
V.18.1.	Determination of the specificity of the polyclonal anti CHL1 antibody	87
V.18.2.	Stimulation of neuritogenesis of primary hippocampal neurons by the anti CHL1 antibody	90
V.18.3.	CHL1-dependent stimulation of neurite outgrowth of CHL1 -/- hippocampal neurons after transfection of either wildtype CHL1 or mutant CHL1 deleted in the hsc70 binding site	92
VI.	DISCUSSION.....	97
VI.1.	The heat shock cognate 70	97
VI.2.	Characterization of the CHL1 – hsc70 interaction.....	101
VI.3.	Functional analysis of the CHL1 - hsc70 interaction	105
VII.	SUMMARY.....	108
VIII.	APPENDIX.....	112
VIII.1.	Oligonucleotides.....	112

VIII.2. Accessionnumbers	114
VIII.3. Plasmids	114
VIII.3.1. pQE30 constructs.....	114
VIII.3.2. pET28 construct.....	115
VIII.3.3. Site-directed mutagenesis	116
VIII.4. Abbreviations	119
IX. BIBLIOGRAPHY.....	122
Acknowledgement / Danksagung	141
Curriculum vitae	143

I. Introduction

In the developing and the adult nervous system, cells have to interact in a precise and regulated manner. Starting during early embryogenesis, cellular interactions are temporally and spatially modulated for generating neuronal induction, migration of neural progenitor cells and morphogenesis during the development of the nervous system. Formation of cellular polarity and the constitution of synaptic contacts establish a functional and ordered tissue. Even after termination of developmental processes, cellular contacts still implicate variability. Crucial stages of plasticity in adults including learning, memory consolidation and neuronal regeneration require structural flexibility of the nervous system. Synaptic plasticity and axonal outgrowth are generated by contact-mediated attraction or repulsion of nerve cells or nerve-glia-cell contacts. Neuronal and non-neuronal recognition molecules have been identified to be associated with the modulation of these regulated cell interactions. Several protein families are among these adhesion molecules like cadherins (Kemler and Ozawa, 1989; Takeichi, 1991), integrins (Hynes, 1992; Reichardt and Tomaselli, 1991), members of the extracellular matrix (ECM) (Sanes, 1989; Reichardt and Tomaselli, 1991) and proteins belonging to the immunoglobulin superfamily (IgSF) (Williams and Barclay, 1988; Brummendorf et al., 1993). Functionality of a recognition molecules is determined by several factors such as expression in different cell types, different developmental stages of the animal and the spatial distribution determine the function of a cell recognition molecule whether it can act as an attractive or a repellent modulator.

I.1. The immunoglobulin superfamily of cell adhesion molecules (CAMs)

This very prominent family of cell recognition molecules comprises immunoglobulin (Ig)-like domains in their extracellular portion. The presence of one or more copies of this highly conserved motif defines a large protein family of cell surface molecules which is involved in a diverse array of functions. They are expressed in a number of tissues during development and in the adult revealing importance in embryogenesis (Edelman and Crossin, 1991; Edelman, 1993; Sanes, 1989), control of hemostasis (Parise, 1989), circulation of lymphocytes (Dustin and Springer, 1991; Zimmerman et al., 1992) and in alterations of

invasive and metastatic behavior of malignant tumor cells (Zetter, 1990; Honn and Tang, 1992). The superfamily of Ig-like recognition molecules includes several subfamilies which have been categorized according to the number of Ig-like domains, the presence and number of fibronectin type III-like repeats, the mode of attachment to the cell membrane and the presence of catalytic domains (Figure 1). Cell recognition molecules containing Ig-like domains within their extracellular region are functionally subgrouped into primarily adhesion-related proteins as indicated in Figure 1 for the first subfamily of CAMs. IgSF molecules containing catalytical properties in their intracellular domain are grouped into subfamilies of receptor-type phosphotyrosine phosphatases (RPTPs) and receptor tyrosine kinases (RTKs).

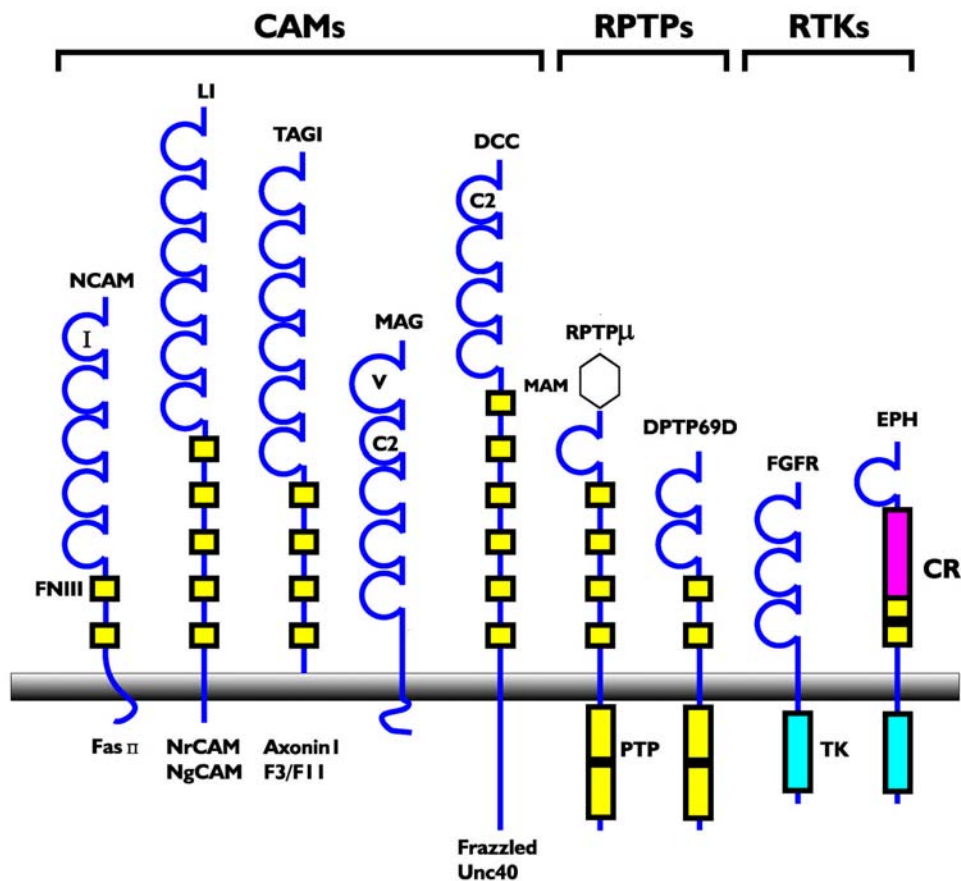


Figure 1: Subfamilies of several neuronal members of IgSF

Representatives of the three main subgroups, namely cell adhesion molecules (CAMs), receptor-type phosphotyrosine phosphatases (RPTPs) and receptor tyrosine kinases (RTKs) are shown. NCAM, L1, MAG and DCC are transmembrane members of the CAM subgroup, of which only TAG-1 is GPI-anchored. RPTP μ and DPTP69D represent the IgSF subgroup containing a catalytic phosphotyrosine phosphatase domain (PTP) in

their intracellular region. FGFR and EPH are molecules of the RTK subgroup containing an intracellular catalytic tyrosine kinase (TK) domain. Species homologues of IgSF members are given below. CR, cysteine-rich. (Walsh and Doherty, 1997).

Evolutionary relationship between CAMs and Igs. The prototypical examples of this family are antibodies (Edelman et al., 1969) and additional proteins, like the MHC-antigens, involved in the humoral and non-humoral immune defence in vertebrates (Orr et al., 1979). Many of these Ig-molecules in the immune system like the T-cell receptor (Kronenberg et al., 1986) are contributing to highly specific cell-cell recognition events (Springer, 1990). The first adhesion molecule that was fully characterized was the neural cell adhesion molecule NCAM that describes a prototypical representative of this protein superfamily (Brackenbury et al., 1977; Hoffman et al., 1982). Gene-cloning studies and subsequent protein sequencing revealed an evolutionary relationship between NCAM and immunoglobulins (Hemperly et al., 1986). Such observations supported the hypothesis that the duplication and diversification of genes for only a limited number of molecules has led to the generation of large families of recognition molecules playing key roles in the immune system, the development of nervous system and other tissues as well (Williams and Barclay, 1988). The completion of the human genome sequencing has provided the answer to the question by how many members the immunoglobulin superfamily is composited. Using criteria defined by the InterPro database (<http://www.ebi.ac.uk/interpro>), a final score has been estimated that 765 human genes contain Ig domains, which means that the immunoglobulin superfamily represents one of the largest protein superfamilies in the human genome (Lander et al., 2001). Furthermore, Ig domains show a high tendency to be presented in large modular multidomain proteins, which is illustrated by the observation that Ig domains occur along with more than 60 different other domains (as defined by Pfam database <http://www.sanger.ac.uk/Software/Pfam/index.shtml>) (Brümmendorf and Lemmon, 2001). The human genome encodes five times more IgSF members than the *Drosophila melanogaster* genome and twelve times more IgSF members than the *Caenorhabditis elegans* genome. This might be due to the fact that immunoglobulins are involved in the invention of the immune system and it can also be caused by the higher complexity of developmental processes in vertebrates in which IgSF members also participate (Venter et al., 2001).

I.2. Neuronal cell adhesion molecules of the immunoglobulin superfamily

Adhesive properties of cell-cell or cell-extracellular matrix (ECM) interactions can affect neuronal development including cell migration, proliferation and differentiation. In addition to adhesive or repellent functions, binding of CAMs can affect intracellular signalling. As mentioned before, the neural cell adhesion molecule (NCAM) was the first Ig-like cell adhesion molecule that was isolated and completely characterized (Brackenbury et al., 1977; Thiery et al., 1977). It demonstrates the prototypical representative of neural cell adhesion molecules of the Ig superfamily including a number of common functions also shared by other members of this protein family. The extracellular domain of NCAM is involved in various Ca^{2+} independent cell-cell and cell-extracellular matrix interactions, mediates cell migration (Rutishauser and Jessell, 1988), proliferation (Sporns et al., 1995), neurite outgrowth (Doherty et al., 1990) and axon fasciculation (Cremer et al., 1997). NCAM-dependent hippocampal remodeling (Itoh et al., 1995) and impaired long-term plasticity of hippocampal mossy fibers in NCAM-deficient mice (Joergensen, 1995) demonstrates further importance of NCAM-mediated cellular interactions. NCAM binding can alter second messenger signalling (Williams et al., 1994b) and influences kinase pathways implicating receptor tyrosine kinases and non-receptor kinases (Williams et al., 1994a; Beggs et al., 1994).

Structural features of neuronal IgSF molecules. Typical members of the neuronal Ig SF are depicted in Figure 2. The number of Ig-like domains varies from only one motif presented in P0 increasing to a module including six Ig-like domains arranged at the N-terminus of L1 and CHL1. Many, if not most cell adhesion molecules in the nervous system such as NCAM, L1 and CHL1 are composed not only by repetitive Ig-like domains, but combine these structures with other repeated motifs. One of these motifs is the fibronectin subtype III repeat (FN-III) that is present in NCAM, L1 and CHL1 as shown in Figure 2. Combination of repetitive domain structures is not only a common feature of immunoglobulin SF molecules. Typical members of extracellular matrix molecules such as Tenascin-C (Fischer et al., 1997), Tenascin-R (Fuss et al., 1993) and laminin (Mayer et al., 1993) contain a large number of EGF-like motifs combined with a varying number of FN-III domains of different subtypes. As

shown in Figure 2, neural IgSF molecules are attached to the cell surface via different ways including either a transmembrane domain or a glycosylphosphatidyl inositol (GPI-) anchor. In case of NCAM, three different major isoforms are generated via alternative splicing of a primary transcript from a single gene (Owens et al., 1987). Two transmembrane isoforms of 180 kDa and 140 kDa and a third isoform of 120 kDa that is GPI-linked are described. Several further isoforms result from alternative splicing in the extracellular domain which are specifically expressed in distinct tissues and/or at developmental stages (Cunningham et al., 1987; Owens et al., 1987; Small et al., 1988; Small and Akeson, 1990).

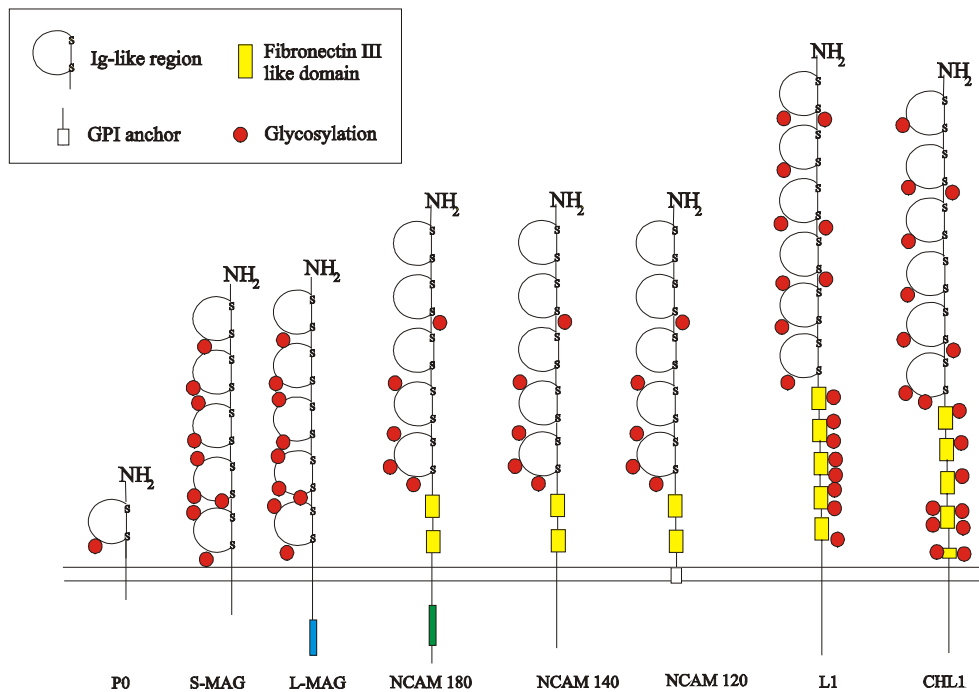


Figure 2: Members of neuronal CAMs belonging to the immunoglobulin superfamily

Typical representatives of cell adhesion molecules are shown as either transmembrane or GPI-linked molecules. The structural motif of one or more Ig-like domains is shared by all family members, other motifs are found only for distinct members such as the FN-III domain is not present in P0 or MAG isoforms. Glycosylation sites are present in all CAMs listed above.

A common feature that is shared by all members of Ig SF molecules is the high number of glycosylation sites which are present within the extracellular region. As many neural recognition molecules and adhesion molecules of the immune system, NCAM, L1 and CHL1 can carry the HNK-1 carbohydrate epitope which contains sulfated glucuronic acid. The α -2,

8-linked polysialic acid (PSA) is a carbohydrate not found to be associated with other proteins of vertebrate origin than the neural cell adhesion molecule. Developmentally regulated and functionally significant alterations in the amount and distribution of PSA attached to NCAM is of outstanding importance for NCAM function (Schachner and Martini, 1995). The PSA-carbohydrate epitope seems to decrease the adhesive cues of NCAM and to increase its neurite outgrowth promoting features (Rutishauser and Landmesser, 1996).

Common functional features of neuronal IgSF molecules. Neural cell adhesion molecules (CAMs) of the immunoglobulin superfamily modulate cell-cell-interactions at key sites during early development and in the adult. Additionally to solely adhesive or repellent functions, binding of CAMs can affect intracellular signalling and therefore influence developmental events, including cell migration, proliferation and differentiation. In general, three categories can be considered regarding CAM function (Crossin and Krushel, 2000). The first category describes phenotypic effects of CAMs and includes all developmental and morphological events like neurite outgrowth, axonal pathfinding and neurite fasciculation at early developmental stages (Kamiguchi and Lemmon, 1997; Brümmendorf et al., 1998). In adult, phenotypic CAM function comprises structural alterations after induction of long-term potentiation and is further contributed to morphological changes after learning and memory consolidation (Lüthi et al., 1994; Scholey et al., 1995). Implication of IgSF molecules in nerve regeneration presents a further important function of such cell adhesion molecules in adults. The second feature of IgSF molecules with regard to function is the effect on second messenger systems which are altered following CAM binding. Early studies on PC12 cells gave the first indication that IgSF binding can affect second messenger cascades (Schuch et al., 1989). Reduction of intracellular pH, elevated levels of intracellular calcium concentration and alterations in inositol phosphate metabolism were described for PC12 cells, primary cerebellar neurons, dorsal root ganglion neurons and for transformed Schwann cells (von Bohlen und Halbach et al., 1992; Frei et al., 1992; Schuch et al., 1989). Specific tyrosine kinases have further been implicated in the effects of CAMs on neurite outgrowth (Doherty and Walsh, 1994) suggesting that CAM binding promotes neuritogenesis by activation of tyrosine kinases as an upstream regulator of G proteins and calcium channels (Williams et al., 1994b). These findings led to the hypothesis that effects of Ig CAMs on neurite outgrowth could be mediated by stimulation of the fibroblast growth factor receptor (FGF-R) (Williams

et al., 1994a; Williams et al., 1994b; Williams et al., 1995). Furthermore, the role of non-receptor tyrosine kinases for the CAM-dependent stimulation of neurite outgrowth has received recent support. NCAM-dependent neurite outgrowth was impaired in neurons from pp59fyn knockout mice (Beggs et al., 1994). Immunoprecipitations revealed an functional complex between the 140-kDa isoform of NCAM and p59fyn. Another tyrosine kinase, FAK, became associated to the complex following crosslinking by secondary antibodies. Activation of this pathway has recently been shown to activate ras/MAPK signalling and subsequent phosphorylation of ERK1 and ERK2 kinases (Schmid et al., 1999). In contrast to this, L1-dependent neurite outgrowth was diminished in cells from pp60src mice, suggesting that this non-receptor tyrosine kinase may be a downstream mediator of L1-signalling (Beggs et al., 1994). Multiple phosphorylation sites within the intracellular domain of L1 (Sadoul et al., 1989) pronounce an association with kinases including p90rsk (Wong et al., 1996b), Raf-1, ERK-2 (Schaefer et al., 1999) and the casein kinase II (Wong et al., 1996a). Finally, the third category that summarizes functions of IgSF molecules addresses the alterations in gene expression followed by Ig CAM binding and IgSF-mediated activation of transcription factors. Binding of a particular IgSF molecule can alter not only the expression of other CAMs (Mauro et al., 1994), but also of other genes including hox and pax and further transcription factors as well as ribosomal and metabolic genes (Crossin et al., 1996; Crossin et al., 1997; Krushel et al., 1998). Several cell adhesion molecules of the IgSF, including NCAM, L1 and CHL1 are upregulated following neural injury (Daniloff et al., 1986; Rieger et al., 1985; Chaisuksunt et al., 2000; Zhang et al., 2000). These CAMs can promote neurite outgrowth, enhance neural regeneration and might have effects on processes such as astrocyte proliferation since that might also be important for regeneration. In fact, NCAM homophilic binding inhibits the proliferation of astrocytes cultured in vitro (Sporns et al., 1995) and can inhibit the proliferation of neural stem cells (Amoureux et al., 2000). Genes and intracellular pathways were determined to be involved in the NCAM-dependent suppression of astrocyte proliferation using subtractive hybridization analysis (Crossin et al., 1997). As observed in neurons, levels of NCAM mRNA are decreased following homophilic NCAM binding indicating a feedback loop in astrocytes. Additionally, levels of mRNA for glutamine synthetase and calreticulin are elevated following NCAM binding to astrocytes.

I.3. The cell adhesion molecule L1

The neural cell adhesion molecule L1 was originally identified in the early 1980s (Rathjen and Schachner, 1984). L1 is a phosphorylated, integral membrane glycoprotein that can be recovered from mouse brain tissue in a distinct set of polypeptides with apparent molecular masses of 200, 180, 140 and 80 kDa (Sadoul et al., 1988). It was originally recognized as a cell adhesion molecule being involved in granule neuron migration in the developing mouse cerebellar cortex (Lindner et al., 1983), fasciculation of neurites (Fischer et al., 1986) and neurite outgrowth on other neurites and Schwann cells (Chang et al., 1990; Seilheimer and Schachner, 1987). Recent studies on L1-knockout mice have confirmed that L1 is an important molecule for the development of the nervous system (Dahme et al., 1997). Its importance in human and mouse ontogenesis is underlined by the severity of neurological disorders associated with mutations in the L1 gene or a complete loss of L1 in the mouse model. These include hydrocephalus and mental retardation and have recently been summarized under the acronym CRASH syndrome (Fransen et al., 1995). This syndrome characterizes a neurological disorder with a clinical spectrum of corpus callosum hypoplasia, retardation, adducted thumbs, spastic paraparesis and hydrocephalus. L1 expression was also found on normal and transformed cells of hematopoietic origin in mouse and human (Kowitz et al., 1992; Kowitz et al., 1993) and on certain epithelial and endothelial cell types confirming L1 functionality in non-neuronal tissues (Thor et al., 1987; Pancook et al., 1997). Interaction studies demonstrated that L1 binding is mediated by several mechanisms including homophilic binding of L1 - L1 (Kadmon et al., 1990a; Kadmon et al., 1990b), assisted homophilic binding of L1 and L1/NCAM complexes on surfaces of adjacent cells (Kadmon et al., 1990a; Kadmon et al., 1990b) and finally a number of heterophilic interactions like L1-binding of axonin-1 (Kuhn et al., 1991) and the L1-interaction with the GPI-anchored molecule CD24 (Kadmon et al., 1995). L1 was also identified as a ligand for several RGD-binding integrins such as $\alpha 5\beta 1$, $\alpha_v\beta 1$, $\alpha_v\beta 3$ as well as the platelet integrin $\alpha_{IIb}\beta 3$ (Ruppert et al., 1995; Montgomery et al., 1996; Ebeling et al., 1996; Felding-Habermann et al., 1997; Blaess et al., 1998). Integrin-mediated cell binding and migration is supported by the RGD motif localized in the sixth Ig-like domain of L1 (Ruppert et al., 1995; Montgomery et al., 1996; Duczmal et al., 1997). Homophilic interaction of L1 induces neurite

outgrowth that requires activation of second messengers cascades in the stimulated cells (reviewed in Doherty et al., 1995). They have provided evidence suggesting that a G-protein-dependent activation of Ca^{2+} channels is involved in neurite outgrowth on L1-substrate such as on N-cadherin- and NCAM-substrate but not on laminin (Doherty et al., 1991; Saffell et al., 1992; Williams et al., 1992). A model has been proposed in which neurite outgrowth stimulated by these adhesion molecules requires a cis interaction with the FGF receptor (Doherty and Walsh, 1996; Green et al., 1996). Other signalling pathways might be activated following L1-binding since L1 associates with the serine/threonine kinases casein kinase II (Wong et al., 1996a) and the S6 kinase and is phosphorylated at serine residues serine¹¹⁸¹ and serine¹¹⁵² (Wong et al., 1996c). Tyrosine kinases have also been suggested to regulate L1 function including a partial role for pp60src in L1-mediated axonal outgrowth (Ignelzi, Jr. et al., 1994) and a putative role of the receptor-type phosphotyrosine phosphatase (RPTP) phosphacan/RPTP ζ / β has been proposed (Milev et al., 1994).

I.4. The L1 subfamily of neuronal IgSF molecules

L1 is a representative and the founder of a neural subfamily of immunoglobulin superfamily proteins (Brümmendorf and Rathjen, 1996; Hortsch, 1996) which is currently composed of four mammalian members – L1 (Moos et al., 1988), the recently described close homologue of L1 (CHL1) (Holm et al., 1996), the neuron-glia cell adhesion molecule (NgCAM)-related cell adhesion molecule (NrCAM) (Grumet et al., 1991) and neurofascin (Volkmer et al., 1992). Two invertebrate cell adhesion molecules such as *Drosophila* neuroglian and *leech* tractin are also belonging to the L1 subfamily (Bieber et al., 1989; Huang et al., 1997). Not listed are the rat homologue of L1 (NILE) (Prince et al., 1991), the human homologue of CHL1 (CALL) (Wei et al., 1998) and the zebrafish homologues of L1 (L1.1 and L1.2) (Tongiorgi et al., 1995). Only those L1-related proteins including a transmembrane domain are considered here. Besides the transmembrane L1-family members, several GPI-linked L1-related molecules exist such as F3/F11/contactin (Ranscht, 1988; Gennarini et al., 1989; Brümmendorf et al., 1989), the brain-derived immunoglobulin superfamily molecule (BIG-1)/plasmacytoma-associated glycoprotein (PANG) (Yoshihara et al., 1994; Connelly et al., 1994), BIG-2 (Yoshihara et al., 1995) and the transiently expressed axonal glycoprotein 1

(TAG-1)/TAX-1/axonin-1 (Furley et al., 1990; Zuellig et al., 1992; Hasler et al., 1993). Only transmembrane members contributing to the L1 subfamily of neuronal IgSF molecules are depicted in Figure 3.

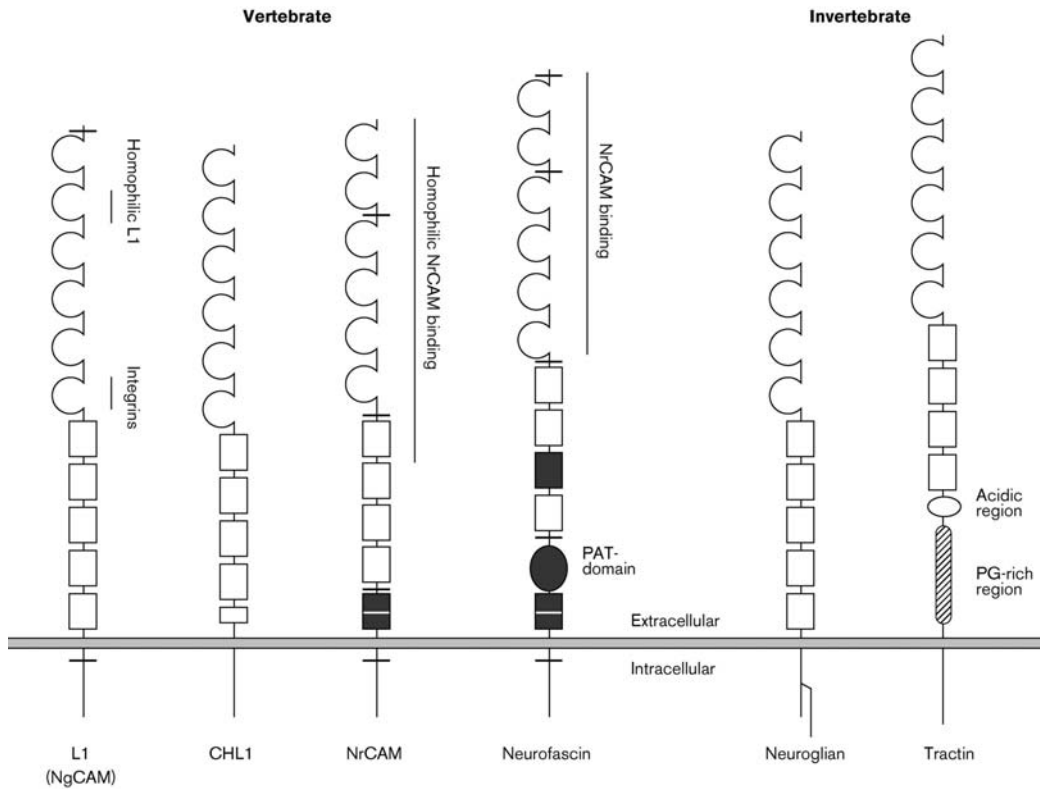


Figure 3: The L1-subfamily of neuronal cell adhesion molecules

Schematic representation of the L1-subfamily that is currently composed of four members identified in mouse (L1, CHL1, NrCAM and neurofascin) and two invertebrate members (neuroglian and tractin). Only the chicken L1-homologue NgCAM is depicted in brackets, other species homologues are mentioned in the text. The structure of six Ig-like domains is common among all family members and is combined with a varying number of FNIII-like domains. All members of the L1 subfamily shown here are transmembrane proteins with a highly conserved intracellular region of only approximately 110 kDa. Horizontal bars and dark boxes indicate alternatively spliced segments. PAT, proline/alanine/threonine-rich; PG, proline/glycine-rich. (Brümmendorf et al., 1998)

The structure of L1-like proteins. The structural hallmark of the L1 subfamily is the presence of six immunoglobulin (Ig)-like domains. The expression of four to five fibronectin type III (FNIII)-like domains, a single transmembrane stretch and a highly conserved

cytoplasmic portion of approximately 110 amino acids further defines the subgrouping of L1-like molecules. The number of FNIII-like domains is varying since L1, the chicken homologue NgCAM and *Drosophila* neuroglia contain five repeats, NrCAM, neurofascin and the invertebrate tractin comprise only four repetitive modules of FNIII-like domains. The CHL1 protein and its human homologue CALL – cell adhesion L1-like – (Wei et al., 1998) display only a half of the fifth FNIII-like repeat. This feature of only partially expression of a domain is still of unknown biological significance, but is shared by isoforms of neurofascin (Hassel et al., 1997) and NrCAM (Lane et al., 1996). Alternative splicing of the pre-mRNA is used to generate these variations in number and composition of domain arrangement in the L1 subfamily. Human L1 reveals only two short segments of alternative splicing which are evolutionary conserved in vertebrates (Jouet et al., 1995), whereas other family members such as neurofascin (Hassel et al., 1997) and NrCAM (Lane et al., 1996) are expressed in multiple isoforms. A systematic analysis of neurofascin gene expression reveals nine alternatively spliced exons generating more than fifty different protein isoforms which are developmentally and spatially regulated in their expression in the chicken brain.

Posttranslational modification of L1-subfamily members. Putative protease cleavage sites are described for L1, the homologue of L1 in chicken NgCAM, NrCAM and the invertebrate tractin (Faissner et al., 1985; Sadoul et al., 1988; Nybroe and Bock, 1990; Kayyem et al., 1992; Burgoon et al., 1995; Huang et al., 1997). They have been shown to be sensitive to posttranslational cleavage within a particular motif localized in the third FNIII-like domain. A potential cleavage site has also been observed between the Ig- and FNIII-like region in chicken neurofascin (Volkmer et al., 1992). Such cleavage of L1 results in an extracellular amino-terminal fragment of approximately 140 kDa and a transmembrane fragment of 80 kDa. Both fragments have been detected in developing and adult mouse brain since the functional significance of L1 cleavage still remains to be determined. Studies concerning the posttranslational modifications of L1 revealed a potential role of the plasminogen system being involved in the cleavage of L1. The addition of plasmin to cell lines results in a dose-dependent loss of surface L1 with simultaneous appearance of soluble L1 fragments. Addition of plasminogen to primary neurons leads to the generation of plasmin and the concomitant release of L1 fragments with an apparent molecular weight of approximately 140 kDa (Nayeem et al., 1999). More recently, studies regarding the ectodomain shedding of L1

underlined that a disintegrin and metalloproteinase (ADAM 10) is involved in the constitutive release of L1 from the cell surface by membrane-proximal cleavage (Beer et al., 1999; Mechtersheimer et al., 2001). Impaired migration of L1-transfected cells after inhibition of ADAM 10 was demonstrated indicating a functional role of L1 shedding for migration processes.

L1-related proteins interact with the actin-based cytoskeleton. L1 (NgCAM) has been demonstrated to co-localize with filamentous actin in filopodia and lamellipodia of growth cones of cultured chick DRG neurons (Letourneau and Shattuck, 1989). A linkage to the actin-based cytoskeleton has consistently been shown for several L1 subfamily members. The primary structure of the cytoplasmic portion of family members is highly conserved and contains a binding motif for ankyrin, a linker protein to the spectrin cytoskeleton (Davis and Bennett, 1994). A pentameric amino acid sequence (phe-ile-gly-gln-tyr [FIGQY]) that is conserved within the L1 subfamily except CHL1 has been mapped to be involved in ankyrin binding. Instead of FIGQY, the pentameric motif FIGA¹¹⁸⁵Y implicating an amino acid variation of glutamine to adenine is described for CHL1 (Holm et al., 1996). Thus, an interaction of CHL1 to the actin cytoskeleton via ankyrin-binding is of outstanding interest since CHL1 binding of ankyrin was not described so far. Interestingly, the linkage of L1-like proteins to ankyrin appears to be regulated by tyrosine phosphorylation (Garver et al., 1997). When neurofascin in rat neuroblastoma cells is tyrosine phosphorylated in the ankyrin-binding motif, neurofascin interaction with ankyrin is completely eliminated. Phosphorylation of the cytoplasmic portion at this particular tyrosine residue slightly increases the lateral mobility of neurofascin within the plasma membrane indicating a reduced interaction between membrane-spanning neurofascin and cytoskeleton-associated ankyrin (Garver et al., 1997). Phosphorylation of neurofascin was found highest during embryogenesis, suggesting that at later developmental stages the neurofascin-ankyrin interaction is stabilized to consolidate neuronal structures.

I.5. A new member of L1-related proteins: The close homologue of L1 (CHL1)

Screening of a λ gt11 expression library for cDNA clones encoding the cell adhesion molecule L1 with a polyclonal anti L1 antibody identified the clone 311 that revealed only 34.1 % homology to L1 (Lipman and Pearson, 1985). A particular DNA fragment derived from this clone was used for screening a different cDNA library and subsequently six independent clones were isolated. Two clones of 4.2 kb and 4.4 kb inserts contained the entire coding region of a close homologue of L1 (CHL1) (Holm et al., 1996). The 4.4 kb insert encodes a 5' untranslated region of 295 bp, an open reading frame of 3627 bp and a 3' untranslated region of 518 bp. Translation of the open reading frame leads to a protein of 1209 amino acids and a calculated molecular mass of 134.9 kDa. The putative extracellular portion is composed of 1081 amino acids containing 18 potential N-glycosylation sites and more than 60 possible sites for O-glycosylation. Hydropathy analysis according to Kyte and Doolittle (Kyte and Doolittle, 1982) identifies a single transmembrane segment of 23 amino acids followed by an intracellular portion that is composed of 105 amino acids. The extracellular domain comprises two structural motifs which are characteristic features of L1-subfamily: A stretch of 585 amino acids displays homology with Ig-like domains while a region composed of 472 amino acids shows homology with FNIII-like domains. Typical conserved amino acid residues assigned the Ig-like domains within the CHL1 sequence as Ig-subclass C2. Highly conserved tryptophan and tyrosine/phenylalanine residues define four FNIII-like domains. Since a fifth FNIII-like motif is only partially expressed in the CHL1 sequence, this new member of L1-subfamily introduces a new structural feature to the subclass of L1-related molecules. Further structural features are present in the extracellular region of CHL1 including an RGD motif in the second Ig-like domain that may contribute to integrin binding (Ruoslahti and Pierschbacher, 1987). CHL1 also contains a DGEA sequence in the β -strand C of the sixth Ig-like domain that is not found in other members of the L1-subfamily. This sequence was also described to be involved in integrin binding as $\alpha_2\beta_1$ integrin recognition of type I collagen contains this motif (Statz et al., 1991). Western blot analysis using antisera raised against an extracellular fragment of CHL1 revealed an expression pattern of CHL1 in three distinct fragments of 185, 165 and 125 kDa. The 185 kDa fragment was only weakly detectable in

non-detergent soluble brain fraction indicating that this might be the membrane-spanning form of CHL1 whereas the 165 kDa and 125 kDa fragments can be considered to be proteolytically released fragments (Holm et al., 1996). Deglycosylation analysis showed that N-linked carbohydrates contribute approximately 20 % to the molecular mass of CHL1. Furthermore, by immunoprecipitation of CHL1 the HNK-1 epitope was identified to be present in CHL1 as it has been described for other cell adhesion molecules (Keilhauer et al., 1985; Kunemund et al., 1988; Hall et al., 1993; Hall et al., 1995). Evaluation of structural homologies of CHL1 with other L1-related molecules revealed that CHL1 is most similar to chicken NgCAM in the extracellular domain (37% identity) and to mouse NrCAM in the intracellular domain (64% identity). The degree of identity is not sufficient to consider these proteins as species homologues, therefore CHL1 was defined as a new, the fourth member of the L1 family in mouse with L1, NrCAM and neurofascin (Moscoso and Sanes, 1995).

Expression of CHL1 in primary cell cultures and in the nervous system. The systematic analysis of CHL1 expression in certain neuronal cell types reveals a distinct but also overlapping expression pattern compared to L1 expression. Both molecules are detectable in subpopulations of primary cultures of hippocampal neurons, cortical neurons, mesencephalic neurons and neurons derived from the dorsal root ganglion. In spinal cord neurons, both proteins are expressed but CHL1 is only weakly detectable compared to the strong L1 expression while small cerebellar neurons express L1 but not CHL1. Remarkable differences in CHL1 expression exist in glial cells since astrocytes only express CHL1 but not L1. Non-mature oligodendrocytes also show CHL1 expression that becomes down-regulated during development to mature oligodendrocytes (Hillenbrand et al., 1999). Differences in protein expression on glial cells suggest distinct functions of CHL1 and L1 with regard to regeneration processes since gliosis is a functional feature during nerve regeneration (reviewed in McGraw et al., 2001). Localization analysis of CHL1 using *in situ* hybridization of cerebellar cortex and hippocampal cortex partially confirmed an overlapping expression pattern of CHL1 and L1. Only in few subpopulations a distinct distribution of CHL1 was observable since CHL1 was not detected in granule cells of the dentate gyrus where L1 is weakly expressed. Furthermore, CHL1 mRNA appears to be less abundant in hippocampal pyramidal cells in the CA2 and CA4 regions while L1 was evenly detectable throughout this area. In the cerebellar cortex, CHL1 and L1 transcripts are distributed in a more similar

pattern with the only exception that hardly any CHL1 labelling is visible in the inner molecular layer, where L1 mRNA is strongly expressed (Holm et al., 1996; Hillenbrand et al., 1999).

Functional features of CHL1. The question was addressed whether CHL1 can interact in a homophilic manner as it was described for several cell adhesion molecules like L1, neuroglian or TAG-1 (Kadmon and Altevogt, 1997; Hortsch et al., 1995; Malhotra et al., 1998). However, cell aggregation assays could neither demonstrate a homophilic interaction between CHL1-CHL1 molecules nor a heterophilic interaction between CHL1 and L1 (Hillenbrand et al., 1999). The identification of an extracellular receptor of CHL1 is still of current interest since no extracellular binding partner of CHL1 has been isolated so far. When CHL1 is given as a substrate for neurite outgrowth, it stimulates neuritogenesis of cultured hippocampal and cerebellar neurons suggesting the presence an unknown receptor of CHL1 involved in CHL1-dependent neurite outgrowth (Hillenbrand et al., 1999). A recent study investigated the effect of CHL1-Fc fusion protein on the survival of cultured murine cerebellar granule and hippocampal neurons of rat embryos. Serum deprivation induces apoptosis that can be prevented by either soluble or substrate-coated CHL1 fusion protein. Addition of CHL1 increased the number of surviving neurons by about 45 % (Chen et al., 1999). Several studies also focused on the CHL1 expression in neurons and glial cells following nerve injury in the peripheral and the central nervous system. Crush or cut and subsequent ligation of the sciatic nerve provokes a strong upregulation of CHL1 mRNA levels in the injured motor neurons and in small to medium sized sensory neurons. Interestingly, no CHL1 upregulation was observed in large primary sensory neurons of DRG after sciatic nerve crush. After dorsal root injury a modest and transient increase in CHL1 mRNA expression was detectable in DRG neurons and a remarkable upregulation of CHL1 was seen in satellite cells around the DRG neurons after sciatic nerve or dorsal root injury. CHL1 upregulation was also observed in putative Schwann cells and astrocytes following dorsal root injury (Zhang et al., 2000). Recent studies demonstrated on the one hand a CHL1 upregulation in thalamic neurons following implantation of a living graft and on the other hand an enhanced CHL1 mRNA expression levels in regenerating neurons of the thalamic reticular nuclei (TRN). Furthermore, many glial cells display upregulated CHL1 mRNA levels at the brain/graft interface at early survival times up to two weeks after operation underscoring once more the importance of CHL1 in

nerve regeneration (Chaisuksunt et al., 2000). The cloning and chromosomal localization of the human CHL1 homologue CALL (Wei et al., 1998) suggests an important role of CHL1 in neurological disorders since the CALL gene was mapped to the chromosome 3p26 locus, a region that is associated with mental retardation in 3p⁻ patients (Asai et al., 1992).

II. Aim of the study

The new member of the L1-subfamily of immunoglobulin superfamily proteins, the close homologue of L1 (CHL1) is a recently described neuronal cell adhesion molecule that possesses typical structural and functional features assigning CHL1 to this important family of cell recognition molecules. Functional properties including promotion of neurite outgrowth, prevention of neuronal cell death and the upregulation of CHL1 expression during regeneration events after peripheral and central nerve injury suggest an important role of CHL1 for cellular processes during nervous system development. Recent studies have confirmed the involvement of CHL1 during development of the nervous system, since the human homologue of CHL1 (CALL) has been implicated in neurological disorders of the 3p⁻ and the ring chromosome 3 syndrome leading to mental retardation. Although several studies addressed the question of the extracellular binding mechanisms of CHL1, the identification of a CHL1 receptor still failed. Binding studies using only the extracellular portion of this cell adhesion molecule could demonstrate that homophilic binding activity of CHL1 as well as a heterophilic interaction between CHL1 and L1 can be excluded. Intracellular interactions of CHL1 have not been described so far, although putative binding sites for ankyrin and for the binding of integrins have been identified in the intracellular domain of CHL1. The identification of a receptor/ligand binding to CHL1 could give insights in the mechanisms by which this cell adhesion molecule mediates cell-cell interactions and by which CHL1 is involved in the formation of an intracellular network composed of transmembrane cell adhesion molecules and the cytoskeleton. Finally, the identification of an intracellular binding partner would help to understand how CHL1 can affect intracellular signalling cascades.

In this study, binding analyses using recombinant CHL1 fusion proteins were performed with the aim to isolate a putative binding partner. For this purpose, the extracellular domain of CHL1 was produced in eucaryotic CHO cells whereas the intracellular portion of CHL1 was prepared from a bacterial expression system. The recombinant fusion proteins were purified according to their fusion tags and subjected to a number of biochemical *in vitro* binding studies including an affinity-chromatography analysis with the immobilized CHL1 fragments and an overlay binding approach using the soluble intracellular domain of CHL1 as a probe

for binding to separated brain fractions. After isolation and identification of a putative CHL1 binding protein, the interaction should be confirmed using alternative binding assays while for the functional analysis of the CHL1 interaction the binding site either within the intracellular domain of CHL1 or within the sequence of the binding partner should be identified. For the further understanding of this important feature of CHL1, mutants which are deleted in the putative binding site should be investigated to characterize the functional role of this interaction.

III. Material

III.1. Chemicals

All chemicals were purchased from the following companies in p.a. quality: GibcoBRL (Life Technologies, Karlsruhe, Germany), Macherey-Nagel (Düren, Germany), Merck (Darmstadt, Germany), Serva (Heidelberg, Germany) and Sigma-Aldrich (Deisenhofen, Germany). Restriction enzymes were obtained from New England Biolabs (Frankfurt am Main, Germany) and MBI Fermentas (St. Leon-Rot, Germany), molecular weight standards were obtained from GibcoBRL (Life Technologies). DNA purification kits were purchased from Life Technologies, Pharmacia Biotech (Freiburg, Germany), Macherey & Nagel and Qiagen (Hilden, Germany). Plasmids and molecular cloning reagents were obtained from Clontech (Heidelberg, Germany), Invitrogen (Groningen, The Netherlands), Pharmacia Biotech, Promega (Mannheim, Germany), Qiagen and Stratagene (La Jolla, California, USA). Oligonucleotides were ordered from Metabion (Munich, Germany). All oligonucleotides used were listed in the appendix. Cell culture material was ordered from Nunc (Roskilde, Denmark), Life Technologies and PAA Laboratories GmbH (Cölbe, Germany).

III.2. Solutions and buffers

(in alphabetical order)

Antibody dilution buffer <i>(immunocyto-/histo-chemistry)</i>	0.1	% (w/v) BSA in TBS
Antibody dilution buffer <i>(Western blotting)</i>	3	% (w/v) BSA in TBS
	0.1	% (v/v) Tween-20
BCA-Reagent A <i>(BCA kit)</i>	1	% (w/v) Bicinchoninacid disodium salt
	1,7	% (w/v) Na ₂ CO ₃ × H ₂ O

III. Material

	0,16	% (w/v)	Natriumtartrat
	0,4	% (w/v)	NaOH
	0,95	% (w/v)	NaHCO ₃ pH 11.25
BCA-Reagent B (<i>BCA kit</i>)	4	% (w/v)	CuSO ₄ × 5 H ₂ O
Blocking buffer (<i>immunocyto-/histo-chemistry</i>)	1	% (w/v)	BSA in TBS
Blocking buffer (<i>Western blotting</i>)	3	% (w/v)	BSA in TBS
Blocking buffer (<i>CNBr activated sepharose</i>)	0,2	M	Glycine pH 8.0
Blotting buffer (<i>Western blotting</i>)	25	mM	Tris
	192	mM	Glycine
	0.01	%	SDS
	10	%	Methanol
Coupling buffer (<i>CNBr activated sepharose</i>)	0,1	M	NaHCO ₃ pH 8.3
	0,5	M	NaCl
Developer solution (<i>silver stain</i>)	7,5	g	Na ₂ CO ₃
	30	μl	Formaldehyde*
			up to 250 ml H ₂ O (* freshly added)
DNA-sample buffer (5x) (<i>DNA-gels</i>)	20	%(w/v)	Glycerol in TAE buffer
	0,025	%(w/v)	Orange G

III. Material

dNTP-stock solutions (PCR)	20	mM	each dATP, dCTP, dGTP, dTTP
Ethidiumbromide solution (staining solution DNA gels)	10	µg/ml	Ethidiumbromide in 1xTAE
Elution buffer (fusion protein production)	0,1	M	Acetate pH 4.0
Elution buffer (affinity chromatography/ immunoprecipitation)	0,1 0,5	M M	Glycine pH 2.7 NaCl
Fixation solution (silver stain)	75 25	% %	Ethanol Acetate acid
Homogenisation buffer (raft preparation)	0.32 1 1 1 5	M mM mM mM mM	Sucrose CaCl ₂ MgCl ₂ NaHCO ₃ Tris-HCl pH 7.4
Incubation buffer (silver stain)	75 17 1,25 0,5	ml g ml g	Ethanol Sodium acetat Glutaraldehyde (25 % w/v)* Na ₂ S ₂ O ₃ x H ₂ O* up to 250 ml (* freshly added)
IPTG (protein expression)	1	M	238 mg/ml results in 1000x stock

III. Material

Ligation buffer (10x)	200	mM	Tris-HCl pH 7.9
	100	mM	MgCl ₂
	100	mM	Dithiothreitol (DTT)
	6	mM	ATP
Lysis buffer (cells for co-immunoprecipitation)	20	mM	Na ₃ PO ₄ pH 7.4
	150	mM	NaCl
	0,2	mM	CaCl ₂
	1	mM	MgCl ₂
	1	mM	ADP
	1	%	Triton X-100
Native lysis buffer (bacterial lysis)	50	mM	NaH ₂ PO ₄ pH 8.0
	300	mM	NaCl
	10	mM	Imidazole
Denaturing lysis buffer (bacterial lysis)	8	M	Urea
	0,1	M	NaH ₂ PO ₄
	0,01	M	Tris-HCl pH 8.0
Phosphate buffered saline (PBS)	150	mM	NaCl
	20	mM	Na ₃ PO ₄ pH 7.4
Phosphate buffered saline with Ca ²⁺ and Mg ²⁺ (PBS+Ca/Mg)	20	mM	Na ₃ PO ₄ pH 7.4
	150	mM	NaCl
	0.2	mM	CaCl ₂
	1	mM	MgCl ₂
Protease inhibitors (COMPLETE™)	1 tablet COMPLETE™ resuspended in 2 ml PBS results in a 25 x stock solution		

III. Material

RIPA-buffer (<i>cell lysis</i>)	50	mM	Tris-HCl pH 7.4
	150	mM	NaCl
	1	mM	EGTA
	10	mM	NaF
	2	mM	Na ₃ VO ₄
	1	% (w/v)	Triton X-100
	1	x	complete™ protease inhibitor mix
Running gel 10% (<i>protein gels</i>)	3.92	ml	deionized water
	5.26	ml	1 M Tris pH 8.8
	0.14	ml	10% SDS
	4.70	ml	30% Acrylamide – Bis 37:1
	70.0	μl	10% APS
	7.00	μl	TEMED
	Sample buffer (5x) (<i>protein-gels</i>)	0.312	M
10		% (w/v)	SDS
5		% (w/v)	β-Mercaptoethanol
50		% (v/v)	Glycerol
0.13		% (w/v)	Bromphenol Blue
SDS running buffer (10x) (<i>protein-gels</i>)	0.25	M	Tris-HCl pH 8.3
	1.92	M	Glycine
	1	M	SDS
Silvering buffer (<i>silver stain</i>)	0,5	g	AgNO ₃
	50	μl	Formaldehyde (37 % w/v)* up to 250 ml H ₂ O (* freshly added)
Stacking gel 5% (<i>protein gels</i>)	3.77	ml	deionized water
	0.32	ml	1 M Tris pH 6.8

III. Material

	0.05	ml	10% SDS
	0.83	ml	30% Acrylamide – Bis 37:1
	25.0	μl	10% APS
	7.00	μl	TEMED
Staining solution <i>(protein gels)</i>	40	% (v/v)	Ethanol
	10	% (v/v)	Acetic acid
	0,1	% (w/v)	Serva Blue R250
Stopping solution <i>(silver stain)</i>	1	% (w/v)	Glycine in H ₂ O
Stripping buffer <i>(Western blots)</i>	0.5	M	NaCl
	0.5	M	Acetic acid
TAE (50x) <i>(DNA gels)</i>	2	M	Tris-Acetate pH 8.0
	100	mM	EDTA
TBF1 <i>(competent E.coli)</i>	100	mM	RbCl
	50	mM	MnCl ₂
	30	mM	potassium acetate
	10	mM	CaCl ₂
	15	% (v/v)	Glycerol
			adjust pH 5.8
TBF2 <i>(competent E.coli)</i>	10	mM	MOPS
	10	mM	RbCl
	75	mM	CaCl ₂
	15	% (v/v)	Glycerol
			adjust pH 8.0 with KOH

III. Material

Tris plus buffer	5	mM	Tris-HCl pH 7.4
<i>(lipid raft isolation)</i>	1	mM	CaCl ₂
	1	mM	MgCl ₂
	1	mM	NaHCO ₃
TNE buffer	20	mM	Tris pH 7.5
<i>(brain homogenisation</i>	150	mM	NaCl
<i>for affinity chromatography)</i>	1	mM	EDTA
	1	mM	EGTA
	1	% (v/v)	Triton X-100
	1	x	complete™ protease inhibitor mix
Tris buffered saline (TBS)	10	mM	Tris HCl pH 8.0
	150	mM	NaCl
Washing buffer 1	0,1	M	Tris pH 8.0
<i>(fusion protein production)</i>	0,5	M	NaCl
Washing buffer 2	25	mM	Tris pH 6.8
<i>(fusion protein production)</i>			
Washing buffer	0,1	M	Acetate pH 4.0
<i>(CNBr activated sepharose)</i>	0,5	M	NaCl

III.3. Bacterial media

(Media were autoclaved and antibiotics were supplemented prior to use)

LB-medium	10 g/l	bacto-tryptone pH 7.4
	10 g/l	NaCl
	5 g/l	yeast extract
LB/Amp-medium	100 mg/l	ampicillin in LB-Medium
LB/Amp-plates	20 g/l	agar in LB-Medium
	100 mg/l	ampicillin
LB/Kan-medium	25 mg/l	kanamycin in LB-Medium
LB/Kan-plates	20 g/l	agar in LB-Medium
	25 mg/l	kanamycin

III.4. Cell culture media

Media were prepared from a 10X stock solution purchased from Gibco GBL

CHO cell Medium	Glasgow MEM (GMEM) (with nucleotides)	
	supplemented with	
	10 % (v/v)	fetal calf serum (FCS)
	50 U/ml	penicillin/streptomycin
	4 mM	L-glutamine
N2A cell Medium	Dulbecco MEM (DMEM)	
	supplemented with	
	10 % (v/v)	fetal calf serum (FCS)
	50 U/ml	penicillin/streptomycin

	1 mM	pyruvate
Versene	Gibco GBL	
HBSS	Gibco GBL	

III.5. Bacterial strains and cell lines

<i>Escherichia coli</i> DH5 α	Clontech
	<i>deoR</i> , <i>endA1</i> , <i>gyrA96</i> , <i>hsdR17</i> ($r_k^-m_k^+$), <i>recA1</i> , <i>relA1</i> , <i>supE44</i> , <i>thi-1</i> , Δ (<i>lacZYA-argFV169</i>), Φ 80 <i>lacZ</i> Δ M15, F ⁻
<i>Escherichia coli</i> M15[pREP4]	QIAGEN
	<i>Nal</i> ^S , <i>Str</i> ^S , <i>Rif</i> ^S , <i>Lac</i> ⁻ , <i>Ara</i> ⁻ , <i>Gal</i> ⁻ , <i>Mtl</i> ⁻ , F ⁻ , <i>RecA</i> ⁺ , <i>Uvr</i> ⁺ , <i>Lon</i> ⁺
<i>Escherichia coli</i> BL21(DE3)	Novagene
	F ⁻ , <i>ompT</i> , <i>hsdS_B</i> ($r_B^-m_B^-$), <i>gal</i> , <i>dcm</i> (DE3)
<i>Escherichia coli</i> XL1-Blue	Stratagene
	<i>recA1</i> , <i>endA1</i> , <i>gyrA96</i> , <i>thi-1</i> , <i>hsdR17</i> , <i>supE44</i> , <i>relA1</i> , <i>lac</i> [F [']], <i>proAB</i> , <i>lac</i> ^q Z Δ M15, <i>Tn10</i> (<i>Tet</i> ^r)
CHO-K1	<u>C</u> hinese <u>H</u> amster <u>O</u> vary
	dehydrofolatereductase deficient hamster cell line
N2A	Mouse neuroblastoma cell line
	established from the spontaneous tumor of a strain A

III.6. Molecular weight standards

1kb DNA ladder 14 bands within the range from 200-10000 bp
(Gibco)

BenchMark Protein Ladder™ 6 µl of the *BenchMark Protein Ladder* (Life
Technologies) were loaded on the SDS-PAGE gel

Band No.	apparent molecular weight (kDa)
1	220
2	160
3	120
4	100
5	90
6	80
7	70
8	60
9	50*
10	40
11	30
12	25
13	20*
14	15
15	10

*20kDa and 50 kDa proteins are more prominent for proper identification

III. Material

BenchMark Prestained Protein Ladder[™] 6 μ l of the *BenchMark Prestained Protein Ladder* (Life Technologies) were loaded on the SDS-PAGE gel

Band No.	apparent molecular weight (kDa)
1	173
2	121
3	80
4	62*
5	49
6	36
7	25
8	21
9	15
10	9.0

*Orientation band (pink in color)

III.7. Plasmids

pBluescript SK⁺ plasmid used for cloning and blue/white selection on X-gal containing plates. Amp-resistance (Stratagene)

pQE30 prokaryotic expression plasmid for recombinant expression of proteins, carrying a RGS-motif followed by a hexahistidine-domain (6xHis) at the 5' end of the multiple cloning site for purification. Amp-resistance (Qiagen)

pET28 prokaryotic expression plasmid for recombinant expression of proteins, carrying a pentahistidine motif at each side of the

multiple cloning site and a thrombin protease site between multiple cloning site and his-tag. Kan-resistance (Novagen)

pcDNA3 mammalian expression vector for transfection of eucaryotic cells. Amp-resistance (Invitrogen)

EGFP Mammalian expression plasmid encoding for the enhanced green fluorescent protein. Kan-resistance (Clontech)

III.8. Antibodies

anti-CHL1 rabbit polyclonal antibody raised against the extracellular domain of mouse CHL1-Fc (produced in the lab of M. Schachner)

Immunoblotting (IB): 1:10000 (crude serum)

Immunocytochemistry: 1:500 (ProteinA-purified fraction)

Immunohistochemistry: 1:10 (affinity-purified fraction)

anti-L1 rabbit polyclonal antibody raised against the extracellular domain of mouse L1-Fc (produced in the lab of M. Schachner)

IB: 1:5000

anti-hsc70 affinity-purified goat polyclonal antibody (Santa Cruz, clone sc-1059), raised against a peptide mapping the carboxy terminus of human hsc70 (identical to mouse sequence)

IB: 1:2500

anti-hsp70 mouse monoclonal antibody (Santa Cruz, clone sc-24), derived by fusion of immunized BALB/c spleen cells with NS-1 mouse myeloma cells (Santa Cruz)

IB: 1:4000

III. Material

anti-RGS HisTM mouse monoclonal antibody, recognizes RGS(H)₄ epitope encoded by pQE30 vector (Qiagen)

IB: 1:2500

anti-Penta HisTM mouse monoclonal antibody, recognizes five consecutive histidine residues (Qiagen)

IB: 1:2000

IV. Methods

IV.1. Cell culture of cell lines

IV.1.1. Stable transfected CHO cells

CHO cells were stably transfected with pEE 14 expression vector (Bebbington, 1991) containing the portion of the CHL1 gene encoding the extracellular part of CHL1 (Chen et al., 1999). For purification, the human Fc portion was fused to the C-terminus of the protein. The stably transfected clones were kindly provided by Dr. Suzhen Chen.

IV.1.2. Cell culture of stable transfected CHO cells

CHO cells were cultured in GMEM with 10 % FCS (fetal calf serum) and 2% penicillin/streptomycin (P/S) at 37°C, 5 % CO₂ and 90 % relative humidity in 75 cm² flasks (Nunc) with 15 ml medium. Cells were passaged when they were confluent (usually after 3-4 days). Medium was removed and cells were detached by incubation with 4 ml Versene for 5 min at 37°C. Cells were centrifuged (200xg, 5 min, RT) and the pellet was resuspended in 10 ml fresh medium. For production of CHL1-Fc, cells were seeded in 175 cm² flasks and medium was exchanged against GMEM containing 2 % ultra low IgG FCS with gentamycin (*f.c.* 0.015 mg/ml) and l-glutamine (*f.c.* 2mM).

IV.1.3. Transient transfection of cells

For transient transfection of CHO or N2A cells (Hawley-Nelson et al., 1993), the Lipofectamine Plus kit (Life Technologies) was used. One day before transfection, 2 x 10⁵ cells were seeded per 35 mm dish. When cells had grown to 80-90% confluency (usually after 18-24 h), they were washed with HBSS and medium was exchanged against GMEM without FCS and antibiotics. Cells were transfected with 2 µg total DNA per 35 mm well. 6 µl Plus reagent and 4 µl Lipofectamine were used per transfection assay. Transfection was performed

as described in the manufacturers protocol according to the literature (Shih et al., 1997). Transfection was terminated after 4 h by addition of an equal volume of GMEM, 10 % FCS, 2% P/S. Twentyfour h after transfection, cells were detached with 250 µl Versene per well and split either 1:2 for biochemical analysis or 1:6 for immunocytochemistry on coverslips.

IV.1.4. Lysis of transfected cells

Fortyeight hours after transfection of CHO or N2A cells, the medium was removed and cells were washed once with ice-cold HBSS. Cells were lysed in 250 µl RIPA buffer containing 1 % Triton X-100 or in PBS containing 1 % Triton X-100 and 1mM ADP per 35 mm well. Cells were scraped off the wells and transferred into a 1.5 ml Eppendorf tube. Debris was removed by centrifugation (15.000 x g, 4°C, 10 min) and the protein concentration of the supernatant was determined by using the BCA kit (Pierce). The supernatant was stored at –20°C.

IV.1.5. Co-immunoprecipitation from transiently transfected CHO or N2A cells

Cells were transfected with the plasmids coding for wildtype CHL1 or one of the mutated CHL1 constructs. For immunoprecipitation, cells from three confluent 35 mm dishes were used. 48 h after transfection, cells were lysed in 750 µl PBS containing 1 % Triton X-100 and 1 mM ADP. Debris was removed by centrifugation (15.000 x g, 4°C, 10 min) and the supernatant was transferred to a 1.5 ml Eppendorf tube. The supernatant was diluted with PBS without Triton X-100 to give a final concentration of 0.5 %. For co-precipitation experiments, the cell lysate was pre-cleared with 25 µl ProteinA dynabeads for 1 hour at 4°C with constant agitation. The beads were removed by centrifugation and 20 µl of polyclonal anti CHL1 antiserum was added to the cell lysate supernatant and incubated at 4°C overnight with agitation. On the second day, 25 µl ProteinA dynabeads were added to the samples and incubated for further 2 hours at 4°C with agitation. Beads were collected after this time period by using a Dynal magnet. Cell lysate was removed completely and beads were washed 5 x for 5 min with PBS containing 0.1 % of Triton X-100 and 1 mM ADP. The immunocomplex was eluted from the beads with 45 µl glycine buffer pH 2.7 and neutralized with 5µl 1 M Tris pH

8.0. Precipitates were subjected to SDS-PAGE and Western blotting and analyzed for the presence of hsc70.

IV.2. Cell culture of primary hippocampal neurons

IV.2.1. Preparation of dissociated hippocampal cultures

For preparation of dissociated hippocampal cultures, mice of postnatal day 1 – 4 were used. Hippocampi were prepared by Galina Dityateva. Preparations were performed as described (Brewer et al., 1993; Lochter et al., 1991).

In brief, the procedure was performed as followed:

1) Dissection

Mice were decapitated and brains removed from skull. Brains were cut along the midline, hippocampi were prepared and split into 1 mm thick pieces.

2) Digestion

Hippocampi were washed twice with dissection solution and treated with trypsin and DNaseI for 5 min at RT. Digestion solution was removed, hippocampi were washed twice and the reaction was stopped by adding trypsin inhibitor

3) Dissociation

Hippocampi were resolved in dissection solution containing DNaseI. Tituration with pasteur pipettes having successively smaller diameters dissociated hippocampi to homogeneous suspensions.

4) Removal of cell debris and plating of cells

By subsequent centrifugation (80 x g, 15 min, 4°C) and resuspension in dissection buffer, cell debris was removed. Cells were counted in a Neubauer cell chamber and plated to provide a density of 1.000 cells/mm².

IV.2.2. Neuritogenesis of hippocampal neurons

Hippocampi were prepared as described before and plated on 96-well-plates. The wells were pre-coated with 0.01% poly-L-lysine (Sigma) overnight at 4°C and washed three times with cold HBSS. Antiserum, ProteinA-purified IgG fraction or protein was coated in different dilutions overnight at 4°C. As a positive control, laminin was coated and as a negative control only poly-L-lysine was given as substrate for neurite outgrowth. The solutions were removed and the wells were washed and dried under the hood. Dissociated hippocampal neurons were plated in 100 µl with densities of 5.000 – 7.500 cells per well. Cells were allowed to grow for 24 hours at 37°C and 5% CO₂. After this time period, cells were fixed by adding 10 µl 25% glutaraldehyde (*f.c.* 2.5%) and stained with 1% toluidine blue in 1% borate buffer for 2 hours at RT. Cells were washed twice with H₂O and dried at RT. Cells were imaged with a Kontron microscope (Zeiss) and analysed with Carl Zeiss Vision KS 400 V2.2 software. For each experimental value, neurites of at least 50 cells with neurites longer than the cell body diameter were measured (Lochter et al., 1991; Müller-Husmann et al., 1993).

IV.2.3. Transfection of hippocampal neurons

For transfection of hippocampal neurons, cells were plated on coverslips (diameter 12 mm) which were placed in 24 well plates and pre-coated with either poly-L-lysine or anti CHL1 IgG fraction obtained from polyclonal antiserum. Cells were allowed to attach for at least 4 hours. For transfection of primary cells, CaPO₄ transfection was carried out using the Stratagene Mammalian Transfection Kit. Six hours before the transfection was started, the temperature of the CO₂ incubator was reduced to 35°C and CO₂ concentration was changed to 3%. 10 – 20 µg of total DNA was used per approach. In case of co-transfection with EGFP, CHL1-DNA was applied in 5-fold excess. Transfections were performed according to the instruction manual (Stratagene). Twentyfour hours after the first transfection, cell were re-transfected. Finally, cells were kept in culture for additional 6 hours before they were fixed as described below. All images of hippocampal neurons were obtained with a Zeiss LSM510 argon-crypton confocal laser-scanning microscope equipped with a 63x oil-immersion

objective lens. Images were quantified using the image processing software *Scion Image* (Scion Corporation).

IV.3. Immunocytochemistry

IV.3.1. Immunocytochemistry of living cells

Coverslips with the attached cells were washed with PBS+Ca/Mg and placed on Parafilm in a humid chamber. Cells were blocked with TBS/BSA 1% for 30 min at RT. 100 µl TBS/BSA 1% containing the primary antibody in the appropriate dilution were added on the coverslips and incubated at RT for 20 min. Afterwards, coverslips were placed into 12-well dishes and washed for three times with TBST. Then coverslips were covered with 100 µl TBS/BSA 1% containing the fluorescent dye-coupled secondary antibody in a 1:250 dilution and incubated for 20 min at RT in the dark. Finally, coverslips were washed three times again with TBS, fixed as described below and embedded on slides with Aqua Poly/Mount medium (Polysciences Inc).

IV.3.2. Fixation of cells

The medium was removed from the coverslips and cells were fixed with 1 ml 4% paraformaldehyde in PBS for 10 min at RT. Cells were washed twice with PBS and stored in PBS at 4°C.

IV.3.3. Immunocytochemistry of fixed CHO cells and hippocampal neurons

Coverslips were placed on Parafilm in a humid chamber and incubated with 100 µl blocking buffer for 1 hour at RT. The blocking buffer was removed by aspiration and the coverslips were covered with 100 µl antibody solution containing the appropriate primary antibody and incubated overnight for 1 hour at RT in a humid chamber. Coverslips were washed three times with TBS/BSA 1% and incubated with 100 µl antibody solution containing the fluorescent dye-labeled secondary antibody (Cy3, Cy5, FITC) for 1 – 2 hours at RT in the

dark. Finally, cells were washed three times with TBS and mounted on objectives with Aqua Poly/Mount medium (Polysciences Inc.). Coverslips were stored in the dark at 4°C.

IV.4. Immunohistochemistry

All immunohistochemical experiments were performed by Bettina Rolf and Dr. Udo Bartsch. Four- to six-week-old CHL1 deficient mice (Montag et al., 1997) and wild-type littermates were deeply anesthetized and perfused through the left ventricle with 4% paraformaldehyde in PBS pH 7.4. Brains were removed and post-fixed in the same fixative overnight at 4°C. Indirect immunofluorescence was performed as described (Weber, 1999). In brief, 40µm thick slices were blocked in PBS containing 1% BSA for 2 hours at RT followed by incubation with affinity-purified antibody against CHL1 (III.6.4) in 1:10 dilution with PBS/0.1% BSA overnight at RT. After washing three times for 10 min at RT with PBS/0.1% BSA, sections were incubated with Cy3-conjugated antibodies against rabbit IgG (1:250 in PBS/0.1% BSA) for 1 hour at RT washed and mounted with Aqua-Poly/Mount (Polysciences, Warrington, PA). Indirect immunofluorescence for the detection of CHL1 was also performed on cryostat sections as described (Bartsch et al., 1992b). Briefly, cryostat sections were prepared from fresh frozen brains in 12 µm thin slides, placed onto poly-L-lysine coated coverslips and air-dried for 1 hour at RT. Afterwards, sections were fixed in methanol at -20°C and blocked in PBS/0.1% BSA. Primary antibodies against CHL1 (1:10 in PBS/0.1% BSA) were incubated overnight at 4°C. Sections were washed and incubated with Cy3-conjugated antibodies against rabbit IgG (1:250 in PBS/0.1% BSA), washed again and mounted onto slides. Imaging and analysis of tissue was performed with an Axiophot fluorescence microscope (Zeiss, Oberkochen, Germany)

IV.5. Generation of polyclonal antiserum from rabbit

IV.5.1. Immunization

In presence of Complete Freund's Adjuvant (CFA, Sigma), two rabbits were injected intramuscularly with 5 mg of E.coli cell lysate of transformed bacteria expressing CHL1 as priming immunization. Four weeks after the priming immunization, booster immunizations were started and continued at 2 – 3 weeks intervals. For each booster immunization, 2 mg of purified CHL1-Fc mixed with 2 ml of Incomplete Freund's adjuvants (IFA, Sigma) per rabbit were applied. After the fifth booster immunization, the animals were bled.

IV.5.2. Preparation of serum from blood

Immediately after bleeding, a wooden stick was applied to each blood sample. Samples were allowed to incubate for 4 hours at RT to form a clot. Afterwards, they were placed overnight at 4°C to retract the clot. It was removed carefully by the wooden stick after complete aggregation and serum was transferred to a 50-ml centrifugation tube. Remaining blood cells and debris were pelleted by centrifugation (2700 x g, 10 min, 4°C) and the supernatant was stored in aliquots at -20°C.

IV.5.3. Preparation of IgG fraction from crude serum

Preparation of IgG fraction with saturated ammonium sulfate (SAS)

One volume of saturated ammonium sulfate solution was added dropwise to two volumes of antiserum with constant stirring at 4°C. A precipitate was allowed to form at 4°C for 4 hours under constant stirring. Afterwards, the sample was centrifuged (12.000 x g, 20 min, 4°C) and the pellet was washed twice by subsequently resuspending in 33 % SAS and centrifugation. After the last centrifugation step, the pellet was resolved in PBS. A convenient volume for

resuspension was 5 – 10 % of the original antiserum volume. The IgG fraction was finally dialyzed against three changes of PBS to fully remove the ammonium sulfate.

Preparation of IgG fraction with ProteinA sepharose

Freeze-dried ProteinA sepharose was reswollen and prepared as described in the manufacturer's protocol. 10 ml of crude antiserum were applied with 1 – 2 ml of reswollen ProteinA sepharose and incubated overnight at 4°C with constant agitation. Serum was removed by centrifugation (200 x g, 5 min, 4°C) and beads were washed four times for 5 min at 4°C. Bound immunoglobulins were eluted with acidic glycine buffer and neutralized with 1 M Tris pH 8.0. Buffer was exchanged against PBS by using a Amicon ultrafiltration unit and the protein concentration was determined using the BCA kit (Pierce).

IV.5.4. Affinity purification of IgG fraction

Coupling of mouse CHL1-Fc and human IgG to CNBr-activated sepharose

Coupling of recombinant proteins to activated sepharose was performed as described (affinity chromatography, III.5.18) according to the manufacturer's instructions. 2 mg of ProteinA-purified recombinant CHL1-Fc and 2 mg of commercially available human IgG fraction was conjugated covalently to sepharose. Suspensions were transferred into empty glass columns and beads were allowed to settle under slow buffer flow to build up a homogeneously packed column bed.

Affinity purification

5 ml of a ProteinA-purified IgG fraction obtained from anti CHL1 polyclonal serum was initially loaded onto a sepharose 4B pre-column to remove components binding unspecifically to the matrix. Successively, the flow through was applied first to the human IgG column and finally to the CHL1-Fc column. By the human IgG column, those immunoglobulins were extracted which recognize the human Fc tag of the CHL1 fusion protein. Thus, the flow

through of the human IgG column solely contains immunoglobulins which specifically bind to the CHL1 portion of the fusion protein. Both columns were washed with approximately the 10-fold volume of column bed volume and were eluted with acidic glycine buffer pH 2.7. Only the eluate of the CHL1 column was neutralized and used for immunohistochemistry (see IV.4).

IV.6. Molecular biology

IV.6.1. Bacterial expression system (pQE 30, Qiagen)

For recombinant expression of proteins in *E. coli* (Ausubel, 1996; Sambrook et al., 1989), the corresponding cDNA of a protein was inserted in frame with a ATG start codon and a purification tag of the convenient expression plasmid. The appropriate *E. coli* strain was transformed with the expression construct and streaked on LB plates supplemented with the indicated antibiotic. 20 ml of LB pre-culture containing the appropriate antibiotic were inoculated by a single colony and incubated overnight at 37°C with constant agitation. Afterwards, the 20 ml were transferred into a 400 ml LB culture and incubated at 37°C under constant agitation until the culture had reached an optical density of 0.6. Protein expression was induced by adding IPTG (*f.c* 1 mM.) to the culture with further incubation for 2-6 h at 37°C. Bacteria were collected by centrifugation (4000 x g, 10 min, 4°C) and stored at -20°C. Protein expression was monitored by removing 1 ml aliquots of the culture every hour after IPTG induction. Bacteria were pelleted, lysed in sample buffer and applied on an SDS gel for Coomassie staining.

IV.6.2. Production of competent bacteria

DH5 α , M15[REP4] or XL1-Blue bacteria were streaked on LB-plates containing the appropriate antibiotics and incubated overnight at 37°C. Single colonies were picked and used for inoculation of 10 ml of an overnight culture. 1 ml of the overnight culture was added to 100 ml of pre-warmed LB broth containing antibiotics and shaken until an optical density of OD₆₀₀ of 0.5 was reached (approximately 90 – 120 min). The culture was cooled down on ice,

transferred to sterile round-bottom tubes and centrifuged at low speed (4000 x g, 5 min, 4°C). The supernatants were discarded and the cells were resuspended in cold TBF1 buffer (30 ml for a 100 ml culture). The suspension was kept on ice for additional 90 min. Then the cells were collected by centrifugation (4000 x g, 5 min, 4°C), the supernatant was discarded again and the cells resuspended in 4 ml ice-cold TBF2 buffer. Aliquots of 100 µl were prepared, frozen in dry ice-ethanol mix and stored at -80°C.

IV.6.3. Transformation of bacteria

To 100 µl of competent DH5α or M15[pREP4], either 50-100 ng of plasmid DNA or 20 µl of ligation mixture were added and incubated for 30 min on ice. After a heat shock (2 min, 42°C) and successive incubation on ice (3 min), 800 µl LB-medium were added to the bacteria and incubated at 37°C for 30 min. The cells were then centrifuged (10000 x g, 1 min, RT) and the supernatant removed. Cells were resuspended 100 µl LB medium and plated on LB plates containing the appropriate antibiotics. Plates were incubated overnight at 37°C.

IV.6.4. Plasmid isolation of E.coli

Small scale plasmid isolation of E. coli (Miniprep)

3 ml LB/Amp-Medium (100 µg/ml ampicillin) was inoculated with a single colony and incubated overnight at 37°C with constant agitation. Cultures were transferred into 2 ml Eppendorf tubes and cells were pelleted by centrifugation (12,000 rpm, 1min, RT). Plasmids were isolated from the bacteria according to the manufacturers protocol. The DNA was eluted from the columns by addition of 50 µl 10 mM Tris-HCl pH 8.0 with subsequent centrifugation (12,000 rpm, 2 min, RT).

Large scale plasmid isolation of E. coli (Maxiprep)

For preparation of large quantities of DNA, the Qiagen Maxiprep kit was used. A single colony was inoculated in 2 ml LB/amp (100 µg/ml ampicillin) medium and grown at 37°C for 8 h with constant agitation. Afterwards, this culture was added to 500 ml LB/amp medium supplemented with 100 µg/ml ampicillin and the culture was incubated overnight at 37°C with constant agitation. Cells were pelleted in a Beckmann centrifuge (6,000g, 15 min, 4°C) and DNA was isolated as described in the manufacturers protocol. Finally, the DNA pellet was eluted in 600 µl of prewarmed (70°C) 10 mM Tris-HCl pH 8.0 and the DNA concentration was determined.

IV.6.5. Enzymatic modification of DNA

Digestion of DNA

For restriction, the DNA was incubated with twice the recommended amount of appropriate enzymes in the recommended buffer for 2 h. Restriction was terminated by addition of sample buffer and the sample was applied on a agarose gel. If two enzymes were incompatible with each other, the DNA was digested successively with the enzymes. The DNA was purified between the two digestions using the rapid purification kit (Life Technologies).

Dephosphorylation of plasmid DNA

After restriction, the plasmid DNA was purified and SAP buffer (Boehringer Ingelheim) and 1 U SAP (shrimps alkaline phosphatase) per 100 ng plasmid DNA were added. The reaction was incubated at 37°C for 2 h and terminated by incubation at 70°C for 10 min. The plasmid DNA was used for ligation without further purification.

Ligation of DNA fragments

Ligation of DNA fragments was performed by mixing 50 ng vector DNA with the fivefold molar excess of insert DNA. 1 μ l of T4-Ligase and 2 μ l of ligation buffer were added and the reaction mix was brought to a final volume of 20 μ l. The reaction was incubated either for 2 h at RT or overnight at 16°C. The reaction mixture was used directly for transformation without any further purification.

IV.6.6. Polymerase chain reaction (PCR)

Amplification of DNA fragments was performed in a 50 μ l reaction mix with thin-walled PCR tubes in MWG-PCR cyclers. *Turbo-Pfu*-Polymerase and the appropriate reaction buffer were obtained from Stratagene. The following reaction mixture was used:

Template	2-10 ng
Primer 1 (10pM)	1 μ l
Primer 2 (10pM)	1 μ l
Nucleotides (dNTPs) (20 mM)	1 μ l
PCR-buffer (10 x)	5 μ l
<i>Turbo-pfu</i> - Polymerase	2,5 U
ddH ₂ O	ad 50 μ l

The PCR was performed with the following step gradient:

1) Initial denaturing	94°C	1 min
2) Denaturing	94°C	1 min
3) Annealing	T _m -4°C	1 min
4) Synthesis	72°C	1 min/ 1kb DNA
5) Termination	72°C	10 min
6) Cooling	4°C	

The amplification procedure (steps 2-4) was repeated 30 times.

The melting temperature of the primers depends on the GC content and was calculated by the following formula:

$$T_m = 4 \times (G+C) + 2 \times (A+T)$$

If the two primers had different melting temperatures, the lower of both was used. Afterwards, the quality of the PCR product was monitored by gel electrophoresis and the PCR product was purified with the rapid PCR purification kit.

IV.6.7. DNA gel electrophoresis

DNA fragments were separated by horizontal electrophoresis chambers (BioRad) using agarose gels. Agarose gels were prepared by heating 1-2 % (w/v) agarose (Gibco) in 1xTAE buffer, depending on the size of DNA fragments. The gel was covered with 1xTAE buffer and the DNA samples were pipetted into the sample pockets. DNA sample buffer was added to the probes and the gel was run at constant voltage (10V/cm gel length) until the orange G dye had reached the end of the gel. Afterwards, the gel was stained in an ethidiumbromide staining solution for 20 min. Finally, gels were documented using the E.A.S.Y. UV-light documentation system (Herolab, Wiesloh, Germany).

IV.6.8. Extraction of DNA fragments from agarose gels

For isolation and purification of DNA fragments from agarose gels, ethidiumbromide-stained gels were illuminated with UV-light and the appropriate DNA band was excised from the gel with a clean scalpel and transferred into an Eppendorf tube. The fragment was isolated following the manufacturer's protocol. The fragment was eluted from the column by addition of 50 µl prewarmed (70°C) Tris-HCl (10 mM, pH 8.0). The DNA-concentration was determined using the undiluted eluate.

IV.6.9. Purification of DNA fragments

For purification of DNA fragments, the Rapid PCR Purification kit was used according to the manufacturer's protocol. The DNA was eluted from the column by addition of 50 μ l prewarmed (70°C) Tris-HCl (10 mM, pH 8.0). The DNA-concentration was determined using the undiluted eluate.

IV.6.10. Determination of DNA concentrations

DNA concentrations were determined spectroscopically using an Amersham-Pharmacia spectrometer. The absolute volume necessary for measurement was 50 μ l. For determining the concentration of DNA preparations (III 1.2), the eluate was diluted 1:50 with water and the solution was pipetted into a 50 μ l cuvette. Concentration was determined by measuring the absorbance at 260 nm, 280 nm and 320 nm. Absorbance at 260 nm had to be higher than 0.1 but less than 0.6 for reliable determinations. A ratio of A_{260}/A_{280} between 1,8 and 2 indicated a sufficient purity of the DNA preparation.

IV.6.11. DNA sequencing

DNA sequencing was performed by the sequencing facility of the ZMNH using Step-by-Step protocols for DNA-sequencing with Sequenase-Version 2.0, 5th ed., USB, 1990. For preparation, 1 μ g of DNA was diluted in 7 μ l ddH₂O and 1 μ l of the appropriate sequencing primer (10 pM) was added.

IV.6.12. Site-directed mutagenesis

As template DNA for site-directed mutagenesis, full length CHL1 cloned in pcDNA3 was provided by Dr. Birthe Schnegelsberg. For mutation of single amino acids within a DNA fragment, the Quickchange Site-directed mutagenesis kit (Stratagene) was used. For detailed information, see the manufacturer's instructions. For vector cards, primer design and location of mutated amino acids, see appendix.

In brief, primers were designed such that:

- 1) they contained the desired mutation and annealed to the same sequence on opposite strands of the plasmid.
- 2) the primers had a length between 25 and 45 bases and the melting temperature was greater than 78°C.
- 3) the desired mutation (deletion or insertion) was in the middle of the primer with 10~15 bases of correct sequence on both sites.

During PCR reaction, it was important to keep primer concentrations in excess. Therefore, the amount of template was varied while primer concentrations were kept constant. The reaction mixture was prepared as followed with 3 different template concentrations:

Template	10, 20, 50 ng	
Mutation-Primer 1	(10 pM)	1 µl
Mutation-Primer 2	(10 pM)	1 µl
Nucleotides (dNTPs)	(20 mM)	1 µl
PCR-buffer (10 x)		5 µl
<i>Turbo-pfu</i> - Polymerase		1 µl (2,5 U)
ddH ₂ O		ad 50 µl

The following step gradient was applied for mutagenesis:

1) Initial denaturing	94°C	30 sec
2) Denaturing	94°C	30 sec
3) Annealing	55°C	1 min
4) Synthesis	72°C	2 min/ 1kb DNA
5) Cooling	4°C	

The number of cycles (steps 2-4) was set to 18 to minimize undesired mutations. For determining the length of step 4, the sizes of the insert and the plasmid have to be taken into account. After PCR reaction, 5 μ l of the mixtures were applied on an agarose gel to check for sufficient amplification. The template DNA (e.g. non mutated DNA) in the amplification reaction was digested by adding 1 μ l of Dpn I restriction enzyme directly into the amplification reaction with subsequent incubation for 1h at 37°C. Afterwards, the amplification reaction was transformed into competent XL1-Blue bacteria as described. Single colonies were picked from the plate and inoculated into 3 ml cultures. Plasmid DNA was prepared and the mutation was verified by sequencing.

IV.7. Proteinbiochemistry

IV.7.1. One-dimensional SDS-polyacrylamide gel electrophoresis

Separation of proteins was performed by means of the discontinuous SDS-polyacrylamide gel electrophoresis (SDS-PAGE) using the Mini-Protean III system (BioRad). The size of the running and stacking gel was as followed:

Running gel: height 4.5 cm, thickness 1 mm
 10 % - 12 % acrylamide solution

Stacking gel: height 0.8 cm, thickness 1 mm
 4 % - 5% (v/v) acrylamide solution
 15-well combs or without combs for preparative gels

After complete polymerization of the gel, the chamber was assembled as described in the manufacturer's protocol. Up to 35 μ l sample were loaded in the pockets and the gel was run at constant voltage of 80 V for 10 min and then at 140 V until the bromphenol blue line had reached the end of the gel. Gels were then either stained or subjected to Western blotting.

IV.7.2. Two-dimensional SDS-polyacrylamide gel electrophoresis

The option of two-dimensional gel electrophoresis was recommended in case of preparative gels, since resolution of protein mixtures is highly increased by the use of this method. In the first dimension, brain homogenates were separated by isoelectric focussing on an immobilized pH gradient (IPG). The principles of isoelectric focusing on IPGs are described in detail elsewhere (Westermeyer, 1993). Briefly, due to the net charge, amphoteric molecules like proteins can migrate in an electric field. Proteins focus at a specific pH value, where all negative and positive charges are compensated and the molecule is not charged anymore (isoelectric point). Afterwards, pH gradient stripes were equilibrated in SDS sample buffer and applied to vertical SDS gel electrophoresis. In the second dimension, proteins were separated due to their molecular weight. For separation of proteins in the first dimension, commercially available IPG stripes with varying pH ranges and different stripe lengths were used. Initially, IPG stripes with wide pH range (pH 3 – 10) were used to determine the approximate isoelectric point of the protein of interest. Finally, for the isolation of a protein, a narrow pH range (pH 4 – 7) on large 18 cm-stripes was used. All IPG stripes were purchased by Amersham Pharmacia Biotech. After separation in the second dimension, gels were subjected to Western blotting for either an overlay assay, an immunological detection of a particular protein or for silver staining.

IV.7.3. Coomassie staining of polyacrylamide gels

After SDS-PAGE, the gels were stained in staining solution (1h, RT) with constant agitation. The gels were then incubated in destaining solution until the background of the gel appeared nearly transparent.

IV.7.4. Silver staining of polyacrylamide gels

After SDS-PAGE, gels were fixed and incubated with freshly prepared glutaraldehyde and thiosulphite in acetate/ethanol solution for 30 min at RT with constant agitation. Gels were washed intensively for at least three times for 5 min and subsequently silvered for 20 min.

Afterwards, gels were developed with sodium carbonate and reaction was stopped with glycine buffer.

IV.7.5. Electrophoretic transfer of proteins on nitrocellulose membranes (Western blotting)

Proteins were transferred from the SDS-gel onto a nitrocellulose membrane (Protran Nitrocellulose, Schleicher & Schüll) using either a MINI TRANSBLOT-apparatus or a ProteanII apparatus for blotting of 18 cm gels after 2-dimensional separation (both BioRad). After equilibration of the SDS-gel in blot buffer for 5 min, the blotting sandwich was assembled as described in the manufacturer's protocol. Proteins were transferred electrophoretically in blot buffer at constant voltage (85 V for 120 min or 35 V overnight at 4°C). The prestained marker BenchMark™ (Gibco BRL) was used as a molecular weight marker and to control the efficiency of the electrophoretic transfer.

IV.7.6. Immunological detection of proteins on nitrocellulose membranes

After electrophoretic transfer, the membranes were removed from the sandwiches and placed protein-binding site up in glass vessels. Membranes were washed once in TBS and incubated in blocking buffer for 1 h at room temperature. Afterwards, the primary antibody was added in the appropriate dilution either for 2 h at RT or overnight at 4°C. The primary antibody was removed and membranes were washed five times for 5 min with TBST. The appropriate secondary antibody was applied for 2 h at RT. Membranes were washed again five times for 5 min with TBST and immunoreactive bands were visualized using the enhanced chemiluminescence detection system (ECL).

IV.7.7. Overlay approach

Instead of incubation with a primary antibody, nitrocellulose membranes were incubated with recombinantly expressed proteins in an appropriate dilution. Proteins were allowed to interact with a putative binding partner that was separated in gel electrophoresis and transferred to

nitrocellulose membrane. Protein-protein interaction was detected with primary antibodies against the fusion tag of the recombinant molecule and visualized with HRP-conjugated secondary antibody by ECL detection system.

IV.7.8. Immunological detection using enhanced chemiluminescence (ECL)

The immunocomplex composed of nitrocellulose membrane bound protein, primary antibody and secondary antibody coupled with horse-raddish peroxidase (HRP) was detected using the enhanced chemiluminescence detection system (Pierce). The membrane was soaked for 1 min in detection solution (1:1 mixture of solutions I and II). The solution was removed and the blot was placed between two Saran wrap foils. The membrane was exposed to X-ray film (Biomax-MR, Kodak) for varying time periods.

IV.7.9. Enzyme-linked Immunosorbent assay (ELISA)

Several antigens were immobilized on polyvinylchloride surface in 96-well microtiter plate in a wide range of dilutions (1 ng/ μ l to 0.2 μ g/ μ l) overnight at 4°C under constant agitation. Non-absorbed proteins were removed and the wells were washed five times for 5 min at RT. The wells were blocked for one hour at RT with 1 % BSA in TBS and subsequently incubated with the putative binding protein for a further hour at RT. Non-bound proteins were removed and the wells were washed five times for 5 min at RT to remove unspecifically bound proteins. Specifically bound proteins were detected with certain primary antibodies and the appropriate HRP-linked secondary antibodies. Protein binding was visualized by the detection reaction of HRP with ABTS reagent that resulted into a coloured product that was quantified using an ELISA reader at 562 nm.

IV.7.10. Expression of recombinant proteins in *Escherichia coli*

In general, expression of recombinant proteins in *E. coli* can be obtained by introduction of desired cDNA coding for a protein of interest into an appropriate expression vector (Sambrook et al., 1989). The choice of the vector depends on the desired position of a fusion tag, on the presence of a reporter protein function, whether internal protease sites are required and how DNA fragments will be inserted in the correct reading frame. The expression construct is created by ligation of digested vector and insert and then transformed into the appropriate host cells carrying a repressor plasmid. Transformed host cells were streaked out on LB plates supplemented with antibiotics. A 20 ml LB pre-culture with the appropriate antibiotic was inoculated with a single colony and incubated overnight at 37°C with constant agitation. Afterwards, the pre-culture was transferred into a 400 ml expression culture and incubated at 37°C under constant agitation until the culture had reached an optical density of OD₆₀₀ of 0.6. Protein expression was induced by adding IPTG (*f.c.* 1 mM) to the culture with further incubation for 2-6 h at 37°C. Bacteria were collected by centrifugation and stored at –20°C. Protein expression was monitored by removing small aliquots of the culture every hour after IPTG induction. Bacteria were pelleted, lysed in sample buffer and applied on a SDS gel.

IV.7.11. Expression in *E. coli* using the pQE-system

The cDNAs encoding for several proteins (intracellular domain of CHL1, intracellular domain of NCAM 180 and NCAM 140 (both provided by Dr. Markus Delling) and hsc 70 (provided by Dr. Christine Knuehl, Charité, Berlin) were cloned into the pQE expression vector and transformed into *E. coli* M15 [pREP4] host cells. All proteins were expressed with an N-terminal 6xHis affinity tag for purification and detection. Induction of protein expression, production and purification of the proteins via Ni-NTA column was performed according to the *QIAexpressionist* handbook.

IV.7.12. Expression in *E. coli* using the pET-system

The cDNA encoding the intracellular domain of L1 was cloned into the pET28 expression vector. pET28/L1-ICD constructs were transformed into the host strain BL21 (λ DE3 lysogen), in which the T7 RNA polymerase is under control of IPTG-inducible *lacUV5* promoter. Therefore, the target gene is under control of T7 promoter. L1-ICD was constructed with the his-tag located N-terminal. Production and purification were performed as described in the *QIAexpressionist* handbook.

IV.7.13. Lysis of bacteria

Sonification

Small scale bacterial cultures were centrifuged (8000 x g, 4°C, 10 min) and the pellet was resuspended in 2x SDS sample buffer. The suspension was lysed using a sonicator (Branson Sonifier B15, level 6, 50% pulse, 5 x 20 s, on ice) and the debris was removed by centrifugation (10000 x g, 4°C, 10 min). The supernatant was subjected to SDS-PAGE and the gel was subsequently stained with Coomassie blue.

French press

Bacteria cultured for expression in large scale were pelleted (8000 x g, 4°C, 10 min) and resuspended in native lysis buffer (20 ml lysis buffer per 400 ml culture). The suspension was transferred into a precooled *French-Pressure-20K*-chamber (capacity: 40 ml). Bacteria were compressed (Spectronic Instruments/SLM Aminco, 10000 psi, 5 min) and lysed by opening the valve carefully. The procedure was repeated 3 times and then the suspension was centrifuged (15.000xg, 10 min, 4°C) in a Beckman centrifuge.

IV.7.14. Expression of recombinant proteins in stable transfected CHO cells

The expression vector pEE 14 coding the extracellular part of mouse CHL1 fused to human Fc tag was constructed and provided by Dr. Suzhen Chen. The isolation of stable transfected clones was under control of the glutamine synthetase selection system (CELLTECH Ltd., UK, 1990). Further culturing of cells under selection conditions were performed according to the instruction manual. Stably transfected cells secreted the Fc-tagged fusion proteins into the cell supernatant which was harvested after 4 – 5 days in culture before medium became yellow. The supernatant was centrifuged (500 x g, 15 min, 4°C) to remove detached cells and subsequently centrifuged (10.000 x g, 15 min, 4°C) to remove cell debris or other particles. The supernatant was loaded onto a ProteinA sepharose column with a loading velocity of 0.25 ml/min. The column was washed with at least the 20-fold volume of the column bed with two different washing buffers. Specifically bound fusion protein was eluted with acetate buffer pH 4.0, collected and neutralized with 1 M Tris pH 8.0. The buffer was exchanged against PBS using an Amicon ultrafiltration unit and protein concentration was determined using the BCA protein concentration determination kit (Pierce)

IV.7.15. Determination of protein concentration (BCA)

The protein concentration of cell lysates was determined using the BCA kit (Pierce). Solution A and B were mixed in a ratio of 1:50 to give the BCA solution. 10 µl of the cell lysate was applied to 200 µl BCA solution in microtiter plates and incubated for 30 min at 37°C. BSA standards ranging from 100 µg/ml to 2 mg/ml were co-incubated. The extinction of the samples was determined at 562 nm in a microtiter plate by an ELISA reader.

IV.7.16. Brain homogenisation

Brains were prepared from C57BL/6J mice of different ages varying from 3 – 4 postnatal day up to 3 weeks after birth. Mice were decapitated, brains were removed from skulls and immediately transferred into a Dounce homogenizer (Weaton, Teflon pestle, 0.1 µm). Brains were homogenized in TNE buffer containing 1 % Triton X-100 and protease inhibitor diluted

to the appropriate concentration and subjected to affinity chromatography or immunoprecipitation. For application of brain homogenates to sucrose gradients, brains were homogenized in HEPES buffer containing sucrose without detergent or protease inhibitors. Depending on the further experiments, brains were either ultracentrifuged subsequently with 100.000 x g, 1 hour, 4°C to obtain fractions (non-detergent soluble, detergent-soluble or Triton insoluble fraction) or were applied as crude homogenates to the experiment without any further centrifugation step.

IV.7.17. Preparation of membrane subfractions

The preparation of raft subfractions was performed by Dr. Ralf Kleene. Brains were removed from 7-day old or adult mice. All following steps were carried out at 4°C. Brains were homogenized in 3 ml homogenisation buffer applying 12 up-and-down. The homogenate was centrifuged (1.000 x g, 10 min, 4°C) and supernatant was further centrifuged at 17.500 x g for 15 min. The resulting pellet was resuspended in homogenisation buffer and was applied on top of a sucrose step gradient (1.2 M, 1.0 M, 0.85 M and 0.65 M). The 1.000 x g-pellet was resuspended in homogenisation buffer and the sucrose concentration was adjusted to 1 M using 2.34 M sucrose stock solution. This solution was laid on 1.2 M sucrose and was overlaid with homogenisation buffer. The sucrose gradients were ultracentrifuged at 100.000 x g for 2 hours using a SW28 rotor. The bands at the 1.0/1.2 M interfaces which contained synaptosomes were collected, diluted at least two times with Tris plus buffer and subsequently centrifuged at 100.000 x g for 30 min. The pellet was resuspended in Tris plus buffer and incubated for 30 min in ice in order to osmotically shock the synaptosomes. Membranes were isolated by centrifugation at 100.000 x g for 30 min, resuspended in Tris plus buffer, pooled and applied to a sucrose step gradient (1.2 M, 1.0 M, 0.85 M and 0.65 M) and centrifuged as described. The band at the 1.0/1.2 M interface which contained synaptosomal membranes was collected, diluted at least two times with Tris plus buffer and centrifuged at 100.000 x g for 30 min. The membranes were resuspended in Tris plus buffer and incubated for 30 min on ice in the absence or presence of 0.15 M NaHCO₃, pH 11. Mock-treated and alkali-treated membranes were re-isolated by ultracentrifugation, resuspended in Tris plus buffer and incubated for 30 min on ice after addition of Triton X-100 (*f.c.* 1%). The samples

were centrifuged at 120.000 x g for 1 hour using a SW55Ti rotor. The resulting supernatant was subjected to a methanol-chloroform protein precipitation performed as described (Wessel and Flugge, 1984) while the pellets were resuspended in Tris plus buffer. Parts of these suspensions were used to isolate low density Triton-insoluble membrane subdomains (rafts). The sucrose concentration was adjusted to 1.2 M and the suspensions were overlaid with 1.1 M sucrose and 0.3 M sucrose. The gradient was centrifuged at 120.000 x g for 1 hour. The protein layer from the 0.3/1.1M interface which contained the lipid rafts and from the 1.1/1.2 M interface which represented the non-raft fraction were collected, diluted at least three times and centrifuged at 120,000 g for 20 min. The resulting pellets were used for further analysis.

IV.7.18. Affinity chromatography

Coupling gels for ligand immobilization

For affinity chromatography, recombinant CHL1-Fc or CHL1-ICD_{his6} was immobilized on activated CNBr sepharose 4B by covalent conjugation via primary amino groups of the proteins. The coupling procedure was carried out according to the instruction manual.

In brief, the coupling was performed as followed:

- 1) The required amount of freeze-dried powder was suspended in 1mM HCl and the active CNBr-sepharose 4B was allowed to swell completely
- 2) Protein buffer was exchanged against sodium carbonate buffer pH 8.3.
Protein : gel ratio was 2 : 1
- 3) Protein-gel suspension was incubated overnight at 4°C with constant agitation
- 4) Remaining active groups of the gel were blocked by addition of glycine buffer
- 5) Coupling was finished by alternate washing with basic carbonate buffer or acidic acetate buffer to remove an excess of absorbed protein

For affinity chromatography, coupled sepharose gel was transferred into an empty glass column and placed at 4°C. For immunoprecipitations, beads were stored in Falcon-tubes at 4°C and applied in aliquots to the experiment.

Affinity chromatography

Brain homogenates were applied to the affinity columns either containing CHL1-Fc- or CHL1-ICD_{his6}-conjugated beads. In case of CHL1-Fc affinity chromatography, membrane fractions were loaded after dilution with detergent-free homogenisation buffer to obtain a final concentration of 0.2 % Triton X-100. The total amount of brain protein varied between 20 – 40 mg of membrane fraction. The CHL1-ICD_{his6} column was loaded with non-detergent soluble fraction with comparable amounts of protein. The application of brain homogenate was performed with low loading velocities (0.1 ml/min), whereas washing and elution was under faster buffer flow (0.5 ml/min). For washing, two different buffers with high salt/high pH-content and non salt/low pH, respectively, were used. The elution was achieved by acidic glycine buffer pH 2.7 and eluates were collected in fractions of small volume and neutralized immediately. All acidic fractions were subjected to SDS-PAGE and visualized by silver staining.

IV.7.19. Immunoprecipitation

For immunoprecipitations, either activated sepharose beads covalently coupled with anti CHL1 IgG fraction or ProteinA beads with pre-absorbed anti CHL1 antiserum were used. The incubation of brain homogenates with antibody-conjugated beads was performed overnight at 4°C with constant agitation. Beads were pelleted at 200 x g at 4°C, supernatant was removed quantitatively and the beads were subsequently washed five times for 5 min at RT with ice-cold homogenisation buffer containing 0.1 % Triton X-100 without protease inhibitors. Only in case of immunoprecipitations with crude homogenates or crude membrane fractions, antibodies were absorbed to magnetic ProteinA Dynabeads (Dynal). Purification was obtained by placing the gel suspension into the magnetic tube holder to collect dynabeads on one side of the Eppendorf tube. The supernatant was carefully removed without disturbing the bead clot and washing was performed analogously to the immunoprecipitation with sepharose beads. Bound protein was eluted with 45 µl of acidic glycine buffer pH 2.7, neutralized with 5 µl 1 M Tris pH 8.0 and applied to SDS-PAGE.

V. Results

V.1. Production of recombinant CHL1-Fc and CHL1-ICD_{his6}

The extracellular portion of CHL1 and the intracellular domain of CHL1 were produced in order to obtain an *in vitro* binding assay. For this purpose, stably transfected CHO cells were cultured to express recombinant CHL1-Fc that was secreted into the cell supernatant. Cell culture supernatants were harvested successively and collected in four independent pools (Figure 1A, lanes 1 – 4). The extracellular portion of CHL1 was isolated from these supernatants via the human Fc-tag using a ProteinA column. After purification of the fusion protein a single band of approximately 200 kDa was seen in the Coomassie stained gels (Figure 1A, lane 5). M15 *E.coli* bacteria were transformed with a procaryotic expression vector coding for CHL1-ICD_{his6}. Protein expression was induced by application of IPTG to the bacterial suspension. IPTG-induction led to the production of a his-tagged fusion protein that comprised the intracellular domain of CHL1 revealing a molecular mass of approximately 18 kDa (Figure 1B, lanes 1,2). For the purification of CHL1-ICD_{his6}, proteins which were soluble after lysis of bacteria under native conditions (Figure 1B, lane 3) were applied to a Ni-NTA column. Purification of the CHL1-ICD_{his6} fusion protein using the hexa histidine tag was quantitative since the flow through of the Ni-NTA column was completely lacking the fusion protein (Figure 1B, lane 4). After competitive elution of CHL1-ICD_{his6} with high concentrations of imidazole, the purified intracellular domain of CHL1 was isolated as a predominant band. The purified CHL1-ICD_{his6} showed an apparent molecular weight of approximately 18 kDa in the Coomassie stained gels (Figure 1B, lanes 7,8). This protein emerged previously in whole bacteria lysates after induction of protein expression (Figure 1B, lanes 2,3).

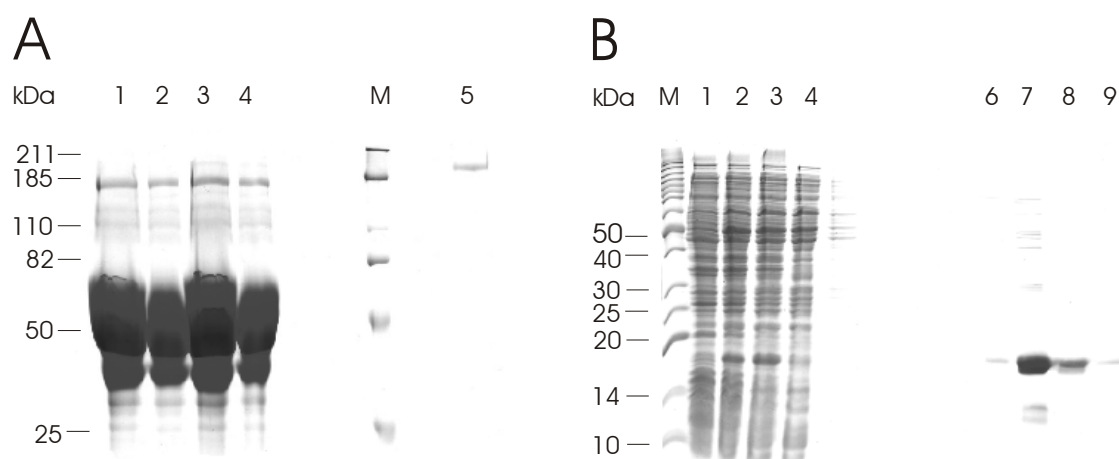


Figure 1: Purification of CHL1-Fc and CHL1-ICD_{his6}

(A): Cell culture supernatants of stably transfected CHO cells producing CHL1-Fc were harvested and collected in four independent pools (lanes 1 – 4). For isolation of the extracellular portion of CHL1, they were successively applied to a ProteinA sepharose column. After washing, specifically bound CHL1-Fc was eluted using an acidic acetate buffer (lane 5). All samples were subjected to SDS-PAGE and stained with Coomassie-Blue. M: Molecular weight marker. Molecular weights are indicated on the left. Note, that the purification revealed a single protein of approximately 200 kDa (lane 5).

(B): M15 bacteria transformed with the pQE30 expression vector encoding CHL1-ICD_{his6} were lysed before (lane 1) and after induction (lane 2) of protein expression and analyzed by SDS-PAGE. After IPTG-induction, a protein appeared with an apparent molecular mass of approximately 18 kDa (lane 2). Proteins which were soluble after lysis under native conditions were applied to a Ni-NTA column (lane 3). The flow through of the Ni-NTA column was collected (lane 4) and specifically bound fusion protein was eluted using high imidazole concentrations (lanes 6 – 9). A predominant band of approximately 18 kDa was isolated by Ni-NTA column purification (lanes 7,8). The soluble protein fraction, the flow through and the elution fractions were applied to SDS-PAGE. Gels were stained with Coomassie-Blue after separation. M: Molecular weight marker. Molecular weights are indicated on the left.

V.2. Affinity chromatography of brain homogenates using immobilized CHL1-Fc and CHL1-ICD_{his6}

For isolation of putative binding partners of CHL1, the recombinant proteins CHL1-Fc and CHL1-ICD_{his6} were immobilized. CHL1-Fc was conjugated to CNBr-activated sepharose while the intracellular portion was linked to NHS-activated sepharose containing a (CH₂)₁₂-

spacer arm. Homogeneously packed columns were generated and brain homogenates were applied with the intention to segregate proteins which have bound specifically either to the extracellular portion or the intracellular domain of CHL1. Detergent extracts of brain membranes were applied to the CHL1-Fc column. After extensive washing, proteins were eluted using an acidic acetate buffer (Figure 2A). A non-detergent soluble fraction of a brain homogenate containing proteins which were soluble under native conditions was allowed to bind to the CHL1-ICD_{his6} column. Non-specifically bound proteins were removed by extensive washing and proteins bound to CHL1-ICD_{his6} were eluted using an acetate buffer at pH 2.7 (Figure 2B). Representative elution profiles of either CHL1-Fc or CHL1-ICD_{his6} column are presented below. Obviously, in non of these binding approaches specifically bound proteins were isolated, neither from the CHL1-Fc column (Figure 2A, lanes 2 – 11) nor from the CHL1-ICD_{his6} column (Figure 2B, lanes 2 – 11). In both affinity chromatography assays a quite even elution pattern was observed without a remarkable enrichment of one or more distinct bands indicating that no putative binding partner was isolated by this approach.

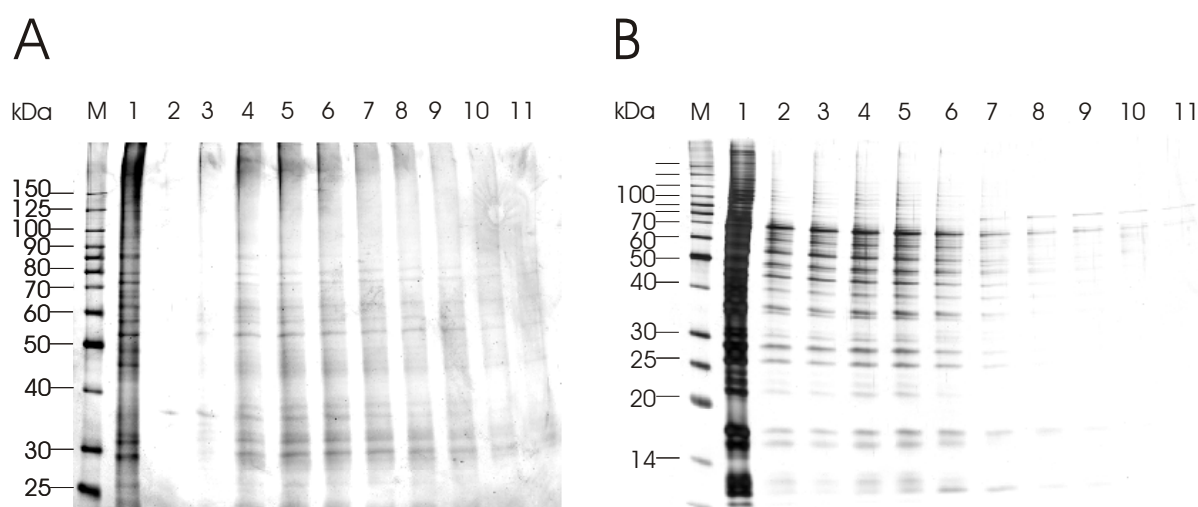


Figure 2: Affinity chromatography of brain homogenates using CHL1-Fc or CHL1-ICD_{his6} conjugated sepharose columns

(A): Detergent-solubilized brain membranes were prepared for the isolation of putative CHL1-Fc binding proteins. The extract was applied to the CHL1-Fc column (approximately 20 mg per approach). The flow through (lane 1) contained non-bound proteins and was discarded after the binding assay. Following extensive washing, bound proteins were eluted using an acetate buffer and collected in fractions (lanes 2 – 11). The flow through and the elution fractions were subjected to SDS-PAGE and silver staining was performed after separation. M: Molecular weight marker. Molecular weights are indicated at the left margin.

(B): 20 mg of a non-detergent soluble fraction from a brain homogenate was applied to the CHL1-ICD_{his6} affinity column. Proteins were allowed to interact with the immobilized fusion protein, afterwards the column was washed and bound proteins were eluted using an acidic acetate buffer. The flow through (lane 1) and the elution fractions (lanes 2 – 11) were subjected to SDS-PAGE and gels were silver stained after separation. M: Molecular weight marker. Molecular weights are indicated on the left.

V.3. One-dimensional overlay of brain fractions using soluble CHL1-ICD_{his6}, L1-ICD_{his6} and NCAM 180-ICD_{his6}

The affinity chromatography using immobilized CHL1-ICD_{his6} was repeated in a modified manner. CHL1-ICD_{his6} was conjugated non-covalently to Ni-NTA beads and a brain homogenate was allowed to bind to the fusion protein in a fluid phase (“batch approach”). Consistent with the elution profiles which were received from the column affinity chromatography, no protein that specifically bound to CHL1-ICD_{his6} was isolated using the batch approach (data not shown). The elution fractions of the batch affinity chromatography were further subjected to SDS-PAGE and transferred to nitrocellulose membrane. Immobilized proteins were then incubated with soluble CHL1-ICD_{his6} in an overlay approach. Non of the proteins which were isolated using CHL1-ICD_{his6} beads in a batch chromatography, showed binding to the soluble fusion protein in an overlay approach. Thus, non of the proteins which were slightly enriched by the batch approach were confirmed to bind to CHL1-ICD_{his6} using an alternative method. Additionally to the elution fractions isolated from the batch approach, brain homogenate fractions were subjected to the same SDS-PAGE as a positive control. In those particular lanes, a remarkable interaction of CHL1-ICD_{his6} to a protein of approximately 60 – 70 kDa appeared (data not shown). To verify the specificity of the binding of CHL1-ICD_{his6} to this protein, the same approach was used with two further cell adhesion molecules, namely with the intracellular domain of L1 (L1-ICD_{his6}) and the intracellular portion of the 180 kDa-isoform of NCAM (NCAM180-ICD_{his6}). Both proteins were also applied as hexa histidine tagged fusion proteins. Only following CHL1-ICD_{his6} incubation, a signal appeared that was predominantly observed in the non-detergent soluble fraction (Figure 3A, lane 1, indicated by an arrow). Neither after incubation using L1-ICD_{his6} (Figure 3B) nor after incubation using NCAM180-ICD_{his6} (Figure 3C) this signal was detectable indicating that it was specific for CHL1-ICD_{his6}. A further strong signal of

approximately 40 kDa was present in the Triton X-100 insoluble fraction after all incubations (Figure 3, A – C, lane 3). Using the anti RGS his6 antibody alone without prior incubation of a fusion protein demonstrated that this signal was due to unspecific binding of the anti RGS his6 antibody (Figure 3D, lane 3).

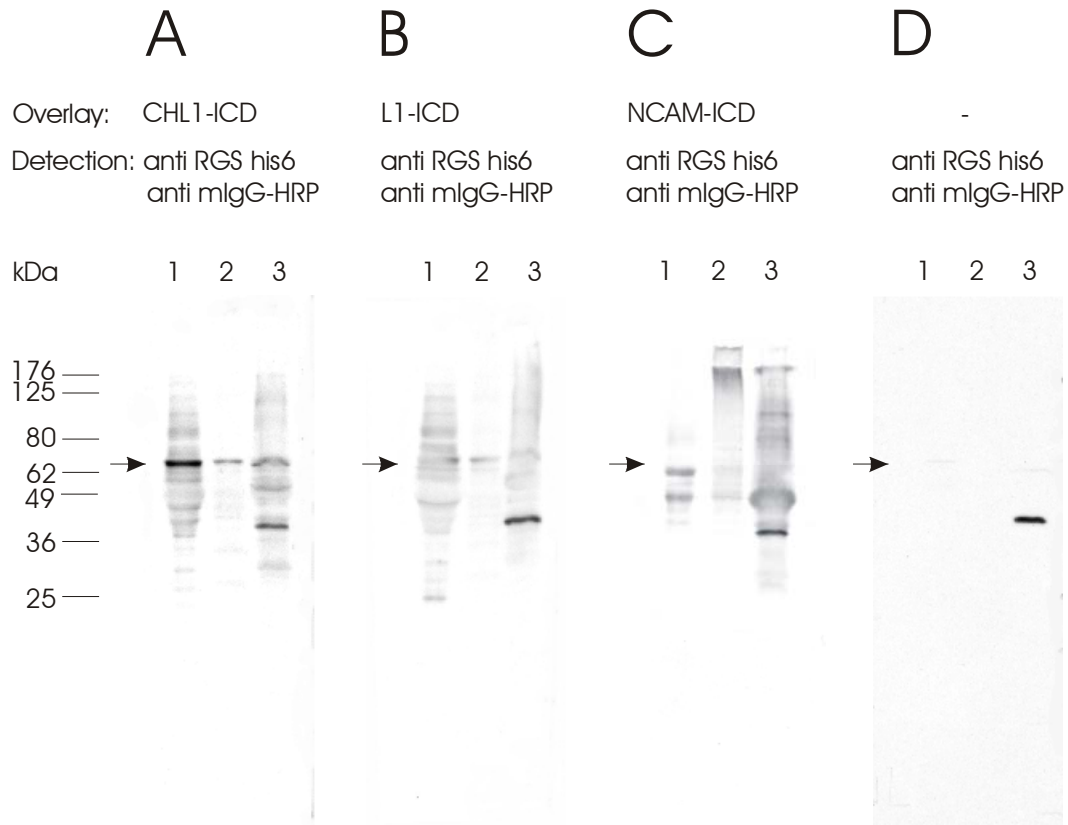


Figure 3: Overlay analysis of fractions from a brain homogenates using the intracellular domains of different cell adhesion molecules

Fractions of a brain homogenate including the non-detergent soluble fraction (lane 1), the Triton X-100 soluble membrane fraction (lane 2) and the Triton X-100 insoluble membrane fraction (lane 3) were subjected to SDS-PAGE (20 µg/lane) and transferred to nitrocellulose membrane after separation.

(A): Brain fractions were incubated with CHL1-ICD_{his6} (*f. c.* 0.02 mg/ml). As negative controls, the same fractions were incubated with L1-ICD_{his6} (*f.c.* 0.02 mg/ml) (B) and with NCAM 180-ICD_{his6} (*f.c.* 0.02 mg/ml) (C). Bound fusion protein was detected with the anti RGS his6 antibody (1/1000) and the anti mouse IgG-HRP secondary antibody (1/10000). The anti RGS his6 antibody was used without previous incubation of fusion protein (D) to demonstrate unspecific binding of the detection antibody to a protein of approximately 40 kDa. Arrows indicate bound protein (A) and non bound proteins (B – D). Molecular weights are presented on the left.

V.4. Overlay approach of CHL1-ICD_{his6} after two-dimensional separation of a brain homogenate

In order to isolate the protein that binds to soluble CHL1-ICD_{his6}, it was necessary to improve the separation of the brain homogenate. Therefore, proteins of a brain homogenate which were soluble under native conditions in a non-detergent lysis buffer were acetone-precipitated and subjected to an isoelectric focusing which allows the separation of proteins according to their isoelectric point. Subsequently, focused proteins were further separated in the second dimension on a SDS-PAGE according to their molecular weights and transferred to nitrocellulose membrane. The immobilized proteins were then incubated with soluble CHL1-ICD_{his6} and the detection of bound fusion protein was performed as described for the one-dimensional overlay approach using the anti RGS his6 antibody. As seen in that binding assay, the protein that specifically bound CHL1-ICD_{his6} was also detectable in the two-dimensional overlay approach. The molecular weight of the CHL1-ICD_{his6} binding protein was confirmed to be approximately 70 kDa and a slightly acidic isoelectric point of approximately 5.5 – 6.0 could be assigned to the signal (Figure 4A). Negative controls were carried out using L1-ICD_{his6} and NCAM180-ICD_{his6} (data not shown) showing no specific binding to that particular protein or any other protein. Because of the high number of proteins with a molecular weight of approximately 70 kDa and a slightly acidic isoelectric points (Figure 4B), a further separation was recommended for the isolation of the CHL1-ICD_{his6} binding protein.

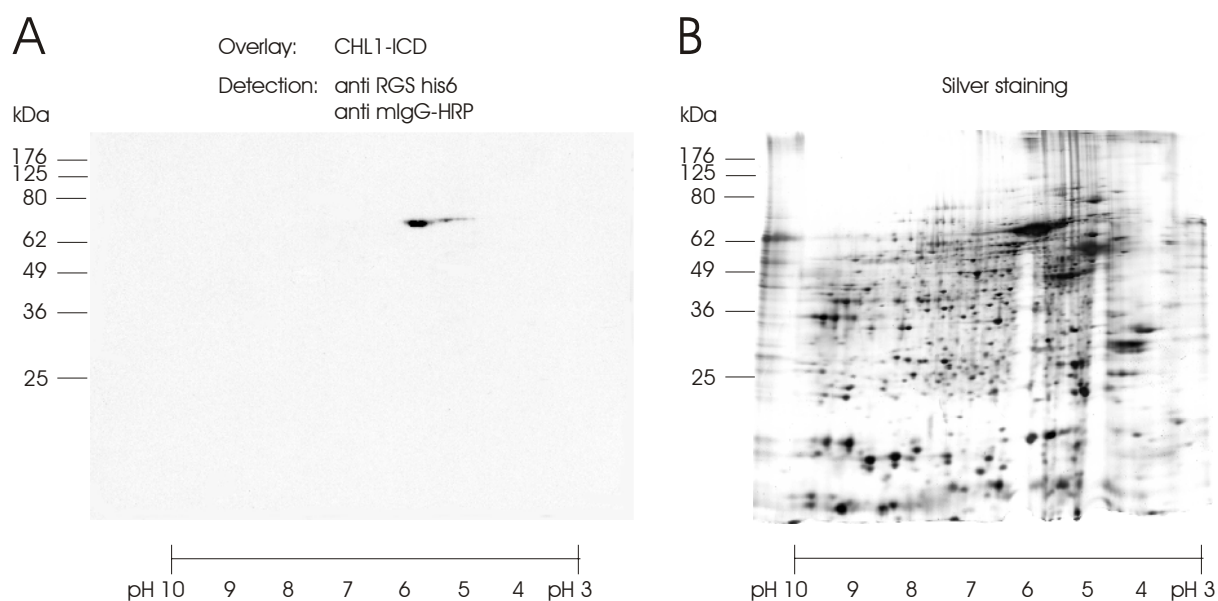


Figure 4: Overlay analysis of separated soluble brain proteins after two-dimensional gel electrophoresis using CHL1-ICD_{his6}

The non-detergent soluble proteins from a brain homogenate (200 μ g protein per approach) were acetone-precipitated and subjected to an isoelectric focusing on an IPG stripe of 7cm and a pH-gradient of 3 – 10. Afterwards, the IPG stripes were subjected to SDS-PAGE for separation of proteins in the second dimension according to the molecular weight. Molecular weights are indicated on the left. The pH values are indicated below the figures.

(A): After separation, proteins were transferred to nitrocellulose membrane and incubated with CHL1-ICD_{his6} (*f.c.* 0.02 mg/ml). Detection of bound fusion protein was performed using the anti RGS his6 antibody (1/1000) and the secondary anti mouse IgG-HRP antibody (1/10000).

(B): After SDS-PAGE, gels were silver stained in order to assign a distinct protein spot to the signal that was observed in the overlay approach.

To further advance the separation of the soluble brain proteins for isolation of the CHL1-ICD_{his6} binding protein, the two-dimensional gel electrophoresis was carried out on longer IPG stripes within a pH range of pH 4 – 7. By this enhancement of separation, a distinct single spot in the silver stained gel was identified to correspond to the signal that was observed in the overlay approach. The particular protein that was assigned to the signal is indicated by a red circle in the silver stained gel (Figure 5B).

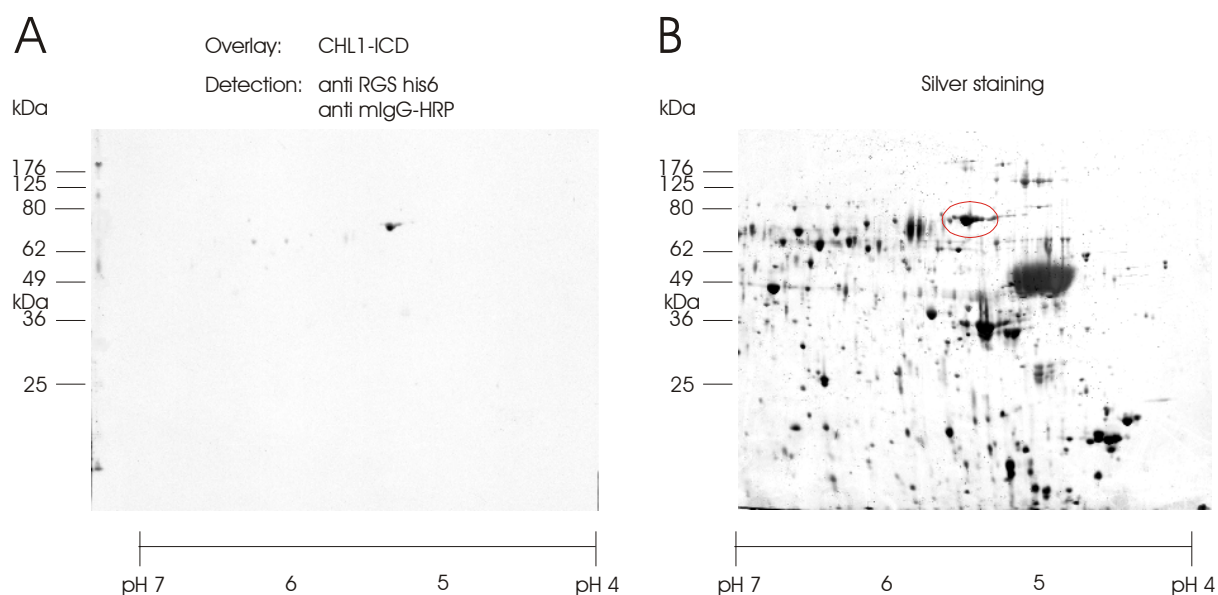


Figure 5: Overlay analysis of separated soluble brain proteins after enhanced two-dimensional gel electrophoresis using CHL1-ICD_{his6}

The non-detergent soluble fraction of a brain homogenate was acetone-precipitated using 400 µg per precipitation and separated on IPG stripes with 18cm in length and a more limited pH gradient ranging from pH 4 – 7. After isoelectric focusing, proteins were further separated in the second dimension on large SDS-PAGE. Molecular weights are indicated on the left. The pH values are indicated below the figures.

(A): Afterwards, proteins were transferred to nitrocellulose membrane and incubated with soluble CHL1-ICD_{his6} (*f.c.* 0.02 mg/ml). For analysis of bound fusion protein, the anti RGS his6 antibody was applied (1/1000) and detected with an anti mouse IgG-HRP secondary antibody (1/10000).

(B): After separation, gels were silver stained. The protein that corresponds to the CHL1 binding protein in an overlay approach is indicated by a red circle.

V.5. Isolation and identification of the CHL1-ICD_{his6} -binding protein

The two-dimensional gel electrophoresis of a brain homogenate was repeated and the silver staining was performed according to Shevchenko (Shevchenko et al., 1996) in order to isolate and identify the 70 kDa protein that showed binding to the intracellular domain of CHL1. The silver stained protein spot that correlated to the signal that was observed in the two-dimensional overlay approach was cut out and the protein was sequenced using the matrix-assisted laser desorption/ionization – mass spectroscopy (MALDI-MS) (Jensen et al., 1997; Mortz et al., 1994). The protein sequencing was carried out by Dr. Bernhard Kuster in the

laboratory of Prof. Matthias Mann, Odense, DK. The protein that bound to CHL1-ICD_{his6} in the overlay binding assay was identified as the murine heat shock cognate 70, further abbreviated as hsc70 (GenBankTM accession number M19141) (Giebel et al., 1988). The molecular weight of 70 kDa and the isoelectric point of 5.5 that are described for hsc70 (Pelham, 1986) correspond to those of the protein which were determined here for the CHL1-ICD_{his6} binding protein.

V.6. Verification of the CHL1-hsc70 interaction by co-immunoprecipitation

Since the interaction of CHL1 and hsc70 was identified under denaturing conditions of an overlay approach, CHL1 binding of hsc70 was analyzed in a more native system. The detergent extract of a brain homogenate containing CHL1 (Figure 6A, lane 1) as well as hsc70 (Figure 6C, lane 1) was incubated with either an anti CHL1 antibody or an anti hsc70 antibody for immunoprecipitation. Immunocomplexes were isolated using ProteinA beads. Bound proteins were eluted using an acidic acetate buffer and analyzed for co-precipitation of hsc70 or CHL1, respectively. As negative control, a polyclonal antibody against L1 was applied for precipitation. The analysis of the immunoprecipitates revealed that neither after precipitation of CHL1 a co-precipitation of hsc70 was detectable (Figure 6A, lane 4) nor after precipitation of hsc70 a co-precipitation of CHL1 occurred (Figure 6C, lane 3). Thus, in this particular binding study using a co-immunoprecipitation approach the interaction between CHL1 and hsc70 could not be confirmed. In the negative control using the anti L1 antibody for immunoprecipitation, no co-precipitation of hsc70 was detected (Figure 6B, lane 4). In principle, the immunoprecipitation worked since CHL1 and L1 were present in the immunocomplexes that were eluted from ProteinA sepharose beads after precipitation of CHL1 or L1 (Figure 6 A/B, lane 3). Hsc70 was detectable in the brain fraction utilized for immunoprecipitation (Figure 6 A/B, lane 6) as well as in the supernatant after precipitation (Figure 6 A/B, lane 5). CHL1 was also present in the homogenate before and after precipitation of hsc70 (Figure 6C, lane 5 and lane 4).

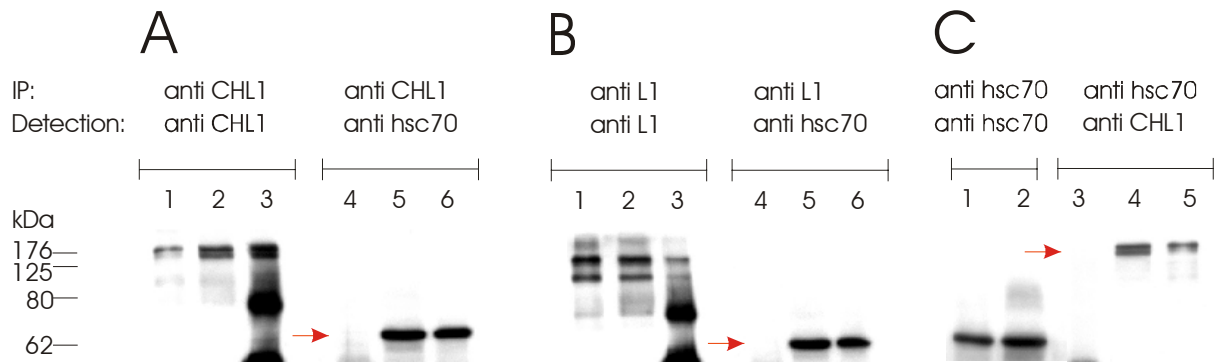


Figure 6: Immunoprecipitation of CHL1, L1 and hsc70 and analysis of co-precipitation of hsc70 and CHL1

A detergent extract of a brain homogenate was incubated with a polyclonal anti CHL1 antibody (A), a polyclonal anti L1 antibody (B) and a polyclonal anti hsc70 antibody (C) for immunoprecipitations. Immunocomplexes were purified using ProteinA sepharose and analysis of a putative co-precipitation was carried out using anti hsc70 antibody (A/B, lane 4) and anti CHL1 antibody (C, lane 3), respectively. Brain fractions which were used for the immunoprecipitation (A/B, lanes 1,6 and C, lanes 1,5), supernatants of ProteinA sepharose after immunoprecipitation (A/B, lanes 2,5 and C, lanes 2,4) and the eluates from ProteinA sepharose (A/B, lanes 3,4 and C, lane 3) were subjected to SDS-PAGE and further transferred to nitrocellulose membrane.

(A): Detection of CHL1 was carried out using a polyclonal rabbit antibody against the extracellular domain of CHL1 (A, lanes 1 – 3), hsc70 presence was analyzed by the use of a polyclonal goat anti hsc70 antibody (A, lanes 4 – 6). (B): Detection of L1 was performed using a polyclonal rabbit anti L1 antibody (B, lanes 1 – 3) while hsc70 detection (B, lanes 4 – 6) was carried out as described in (A). (C): Hsc70 was detected using a polyclonal goat anti hsc70 antibody (C, lanes 1,2) while CHL1 presence was analyzed using the polyclonal rabbit anti CHL1 antibody (C, lanes 3 – 5). The ProteinA eluates are indicated by an arrow where a putative co-precipitation was expected (A/B, lane 4 and C, lane 3).

V.7. Binding study of recombinant CHL1-ICD_{his6} and hsc70_{his6} using an ELISA approach

To prove a direct binding of CHL1 and hsc70, recombinant proteins were produced in a procaryotic expression system. Recombinant BAG-1 that is known to bind to hsc70 (Kanelakis et al., 1999; Luders et al., 2000) was used as a positive control. CHL1-ICD_{his6}, BAG-1_{his6} and hsc70_{his6} were coated on absorbent plastic surfaces and incubated with the respective putative binding partner. The immobilization of the fusion proteins was previously controlled by incubation of coated proteins with anti RGS his6 antibody or penta his antibody,

respectively, without preceded incubation of the putative binding protein. Detection of the potential interaction partner was carried out using specific antibodies against hsc70, the intracellular domain of CHL1 and BAG-1. The immobilization on a plastic surface worked well for all analyzed fusion proteins since they were detected following coating to plastic surface using antibodies against the fusion tag (Figure 7, pink square, green square and blue square indicating the detection of coated CHL1-ICD_{his6}, BAG-1_{his6} or hsc70_{his6}, respectively). The interaction of CHL1 and hsc70 could not be confirmed in the ELISA assay since binding of hsc70_{his6} to immobilized CHL1-ICD_{his6} was not observed (Figure 7, pink diamonds). Vica versa, binding of soluble CHL1-ICD_{his6} to immobilized hsc70_{his6} was also not detectable (Figure 7, blue diamonds). In contrast to this, the interaction between the previously known binding partners BAG-1_{his6} and hsc70_{his6} was confirmed in the ELISA assay. Interestingly, the binding of BAG-1 and hsc70 was only detectable after immobilization of hsc70_{his6} (Figure 7, blue triangles) and application of soluble BAG-1_{his6} while in the reciprocal approach, when BAG-1_{his6} was coated and subsequently incubated with soluble hsc70_{his6}, no interaction was observed (Figure 7, green triangles).

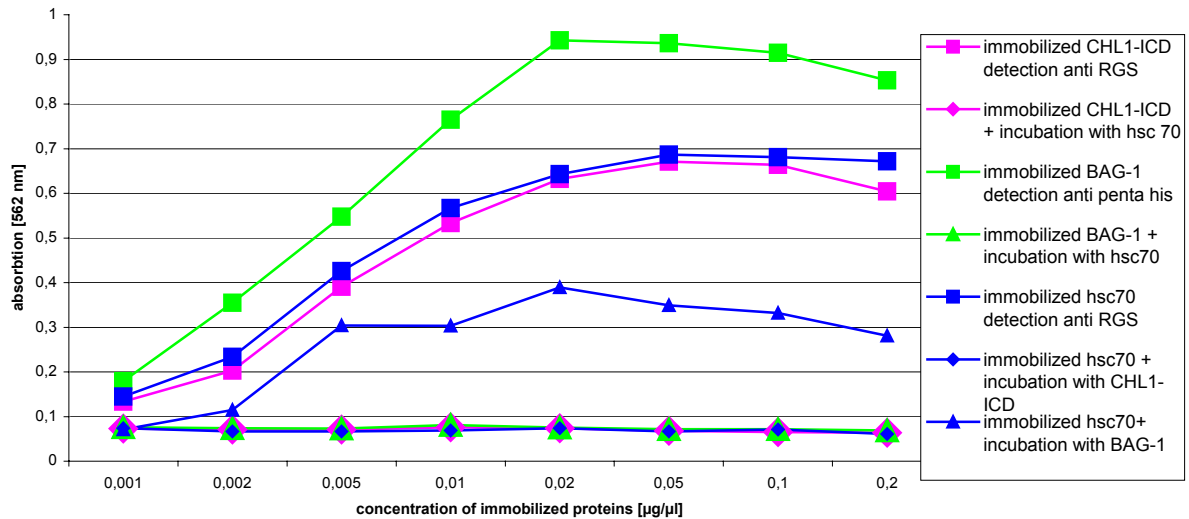


Figure 7: ELISA binding assay for the evaluation of CHL1– hsc70 interaction

CHL1-ICD_{his6} was immobilized (1 ng/µl to 0.2 µg/µl) to a plastic surface and coating was controlled using the anti RGS his6 antibody (pink squares). Immobilized CHL1-ICD_{his6} was incubated with hsc70_{his6} (0,2 mg/ml) and binding to hsc70_{his6} was analyzed with polyclonal anti hsc70 antibody (pink diamonds).

BAG-1_{his6} was coated in the same range of dilutions as described for CHL1-ICD_{his6} and the immobilization was controlled using the anti penta his antibody (green squares). Coated BAG-1_{his6} was incubated with hsc70_{his6} (concentration as above) and bound hsc70_{his6} was detected with a polyclonal anti hsc70 antibody (green triangles).

Hsc70_{his6} was immobilized in the same dilutions as CHL1-ICD_{his6} and BAG-1_{his6} were coated. Hsc70_{his6} was detected with anti RGS his6 antibody for control of immobilization (blue squares). Coated hsc70_{his6} was incubated with CHL1-ICD_{his6} (blue diamonds) and BAG-1_{his6} (blue triangles). Detection of bound proteins was carried out using the monoclonal antibody 2C2 against the intracellular domain of CHL1 (kindly provided by Dr. M. Grumet) and a polyclonal antibody against BAG-1 (provided by Dr. F. Hartl, Munich).

V.8. Confirmation of hsc70 as CHL1-ICD_{his6} binding protein performing a two-dimensional overlay approach

Three different binding approaches namely the immunoprecipitation, the ELISA assay and a BIAcore™ SPR analysis (data not shown) failed to confirm the interaction between CHL1 and hsc70. Thus, a confirmation of the CHL1-hsc70 binding in the overlay approach was strongly recommended. It was also intended to verify that the correct protein spot in the silver-stained gel was correlated to the signal observed in the overlay and that the accurate protein was isolated for MALDI-MS analysis. For this purpose, a non-detergent soluble brain fraction was separated in a two-dimensional gel electrophoresis and transferred to nitrocellulose membrane. This was done three times in parallel. One membrane was subjected to an overlay approach using soluble CHL1-ICD_{his6} (Figure 8A). The other membranes were analyzed with either the anti hsc70 antibody (Figure 8B) or the anti hsp70 antibody that was used as a negative control (Figure 8C). The signal of the protein that bound to soluble CHL1-ICD_{his6} was reproducible in the two-dimensional overlay approach (Figure 8A). Soluble CHL1-ICD_{his6} bound to a protein of 70 kDa and the isoelectric point of 5.5. The hsc70 antibody recognized a protein with an identical molecular weight and isoelectric point whereas the hsp70 antibody detected a protein with a comparable molecular weight but a slightly more basic isoelectric point of approximately 5.8 (Figure 8C). These different isoelectric points coincide with isoelectric points of hsc70 and hsp70 described in the literature (Pelham, 1986). These experiments supported the MALDI-MS analysis which identified hsc70 as a CHL1 binding protein. In a further approach, purified recombinant hsc70 expressed in bacteria was separated in a two-dimensional gel electrophoresis and transferred

to nitrocellulose membrane. The assay was carried out in two independent approaches for a CHL1-ICD_{his6} overlay (Figure 8D) and for detection of hsc70 by the specific antibody (data not shown). Consistent with the CHL1-ICD_{his6} overlay of brain homogenate, this approach also confirmed the binding of CHL1-ICD_{his6} to hsc70 since the soluble fusion protein bound to recombinant hsc70 (Figure 8D). Due to the fact that CHL1 binds to hsc70 only in an overlay approach and not in an ELISA assay (Figure 7), the question did arise whether the interaction of CHL1 and hsc70 was only an artefact due to the quite denaturing conditions of an overlay approach or whether hsc70 must be presented in a distinct conformation that allows an interaction to CHL1. This status could be mimicked under conditions prevailing during electrophoresis. Within the cell, a specific conformation of a particular protein can be supported by assistant proteins. These proteins could modify the folding of nearby proteins and mediate interactions to other binding proteins by the conformational alteration.

V. Results

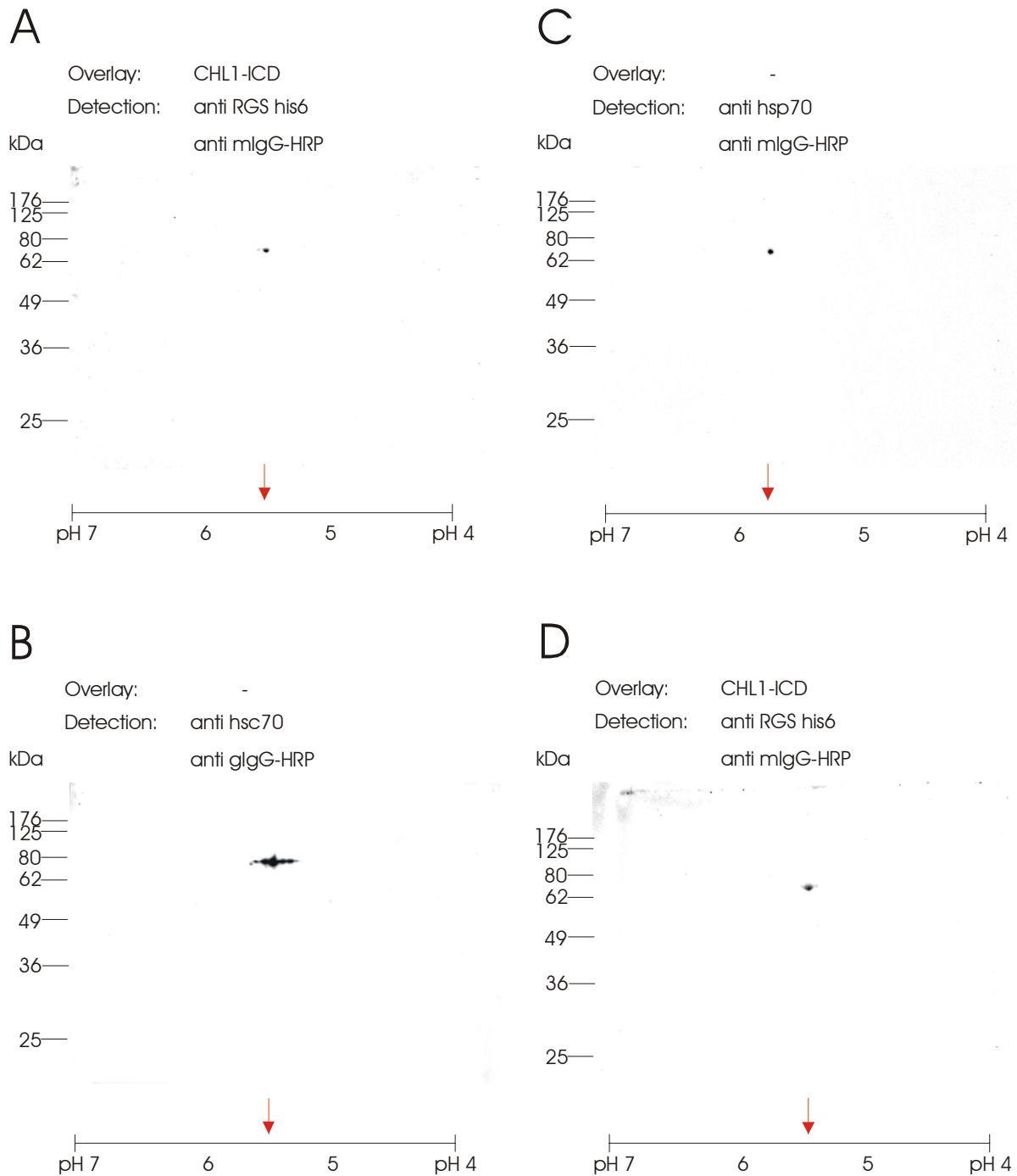


Figure 8: Confirmation of hsc70 - CHL1-ICD_{his6} binding in a two-dimensional overlay approach

(A – C): Non-detergent soluble brain proteins were acetone-precipitated (200 µg per precipitation) and separated in a two-dimensional gel electrophoresis including first an isoelectric focusing on IPG stripes (7cm / pH 4 – 7) and afterwards separation in a SDS-PAGE. After separation, proteins were transferred to a nitrocellulose membrane and incubated with soluble CHL1-ICD_{his6} (*f.c.* 0.02 mg/ml) in an overlay approach (A). Detection of bound fusion protein was carried out using the anti RGS his6 antibody (1/1000) and anti mouse IgG-HRP

secondary antibody (1/10000). (B): Analysis of hsc70 was performed using a specific goat anti hsc70 and an anti goat IgG-HRP secondary antibody (1/10000). (C): Hsp70 was detected using a specific mouse anti hsp 70 antibody and a secondary anti mouse IgG antibody that was HRP-conjugated (1/10000).

(D): Recombinant hsc70 was separated using the same conditions as described for (A – C) and transferred to a nitrocellulose membrane. Afterwards, the immobilized protein was incubated with CHL1-ICD_{his6} (*f.c.* 0.02 mg/ml) in an overlay approach. Detection of bound fusion protein was performed as described in (A).

Molecular weights are indicated on the left. The pH values are indicated below the figures. Arrows emphasize the pH of detected proteins.

V.9. Co-localization and co-capping of CHL1 and hsc70 in primary hippocampal cultures

Since none of the biochemical approaches showed an interaction between CHL1 and hsc70 under native conditions, a cellular system was used to confirm the CHL1 – hsc70 binding. A co-localization of both proteins could be indicative for an interaction. Thus, the localization of CHL1 and hsc70 in primary cell cultures was analyzed. Hippocampi of new born or postnatal 4-day old mice were prepared, dissociated and cultured for three days. Afterwards, cells were stained either with a polyclonal antibody against hsc70 (Figure 9A) or with a purified polyclonal antibody against CHL1 (Figure 9B). The overlay of both stainings displayed an obvious co-localization of CHL1 and hsc70 that was indicated by a yellow staining (Figure 9C). Interestingly, this co-localization was distributed in a very distinct pattern over the whole length of neurites (Figure 9C, indicated by arrows). In a further approach, hippocampi from newborn mice were prepared and cultured for only one day. In these younger cultures, the co-localization of CHL1 and hsc70 was less pronounced and also the distinct distribution pattern of hsc70 that was seen in older cultures was not observed (Figure 10A). For co-capping of CHL1 and hsc70, the cells from newborn mice were pre-incubated with a polyclonal rabbit anti CHL1 antibody. Primary antibodies were clustered with a secondary anti rabbit antibody and afterwards cells were stained with a polyclonal anti hsc70 antibody. Initiated by the pre-clustering of CHL1, hsc70 accumulated in defined areas (Figure 10, B/C). A yellow staining was revealed that indicated a co-localization of CHL1 and hsc70 (Figure 10B).

Although hsc70 is described to be a cytosolic protein (Pelham, 1986; Hartl, 1996) and a widespread expression of the protein all over the cell was expected, only a very restricted

distribution pattern was observed in older cultures or after co-capping of younger cultures indicating a localization of this protein in particular cellular subdomains (Figure 9A). The distinct distribution of CHL1 and hsc70 suggests that the interaction takes place in a strongly regulated manner and only under particular conditions which were probably occurring under the denaturing conditions prevailing during and after electrophoretic separation. Both experiments together, namely the overlay assay showing a direct binding and the immunocytochemistry of primary hippocampal neurons demonstrating a co-localization of CHL1 and hsc70 in certain subdomains, may indicate that a specific conformation which might be a crucial factor for the interaction between CHL1 and hsc70 is probably only received in distinct membrane subcompartments. To verify this assumption, further biochemical analyses were carried out to define the localization of CHL1 – hsc70 interaction and to identify conditions that facilitate the binding of CHL1 and hsc70.

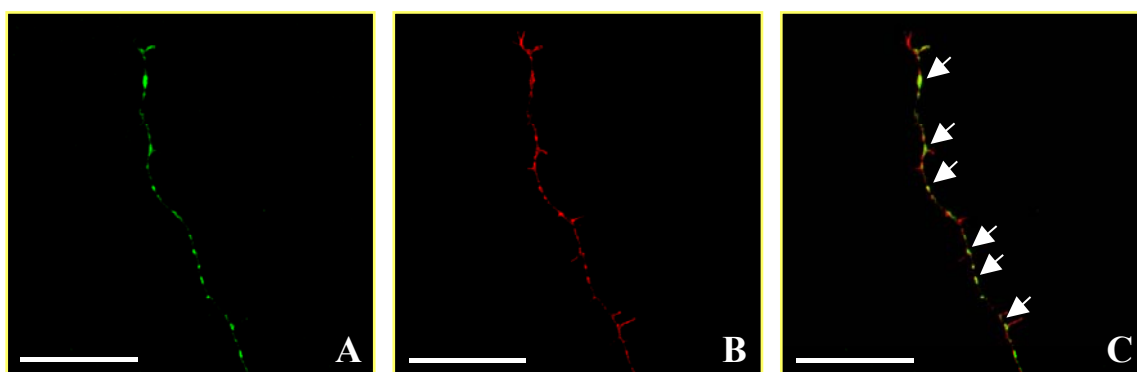


Figure 9: Co-localization of CHL1 and hsc70 in primary hippocampal neurons

Hippocampal neurons from 4-day old mice (3 days in culture) were stained either with anti hsc70 antibody (green, A) or with anti CHL1 antibody (red, B). Double labeling with anti hsc70 antibody and anti CHL1 antibody resulted in an overlay image (C). Yellow staining indicates co-localization of CHL1 and hsc70 (arrows). Scale bar represents 20 μm .

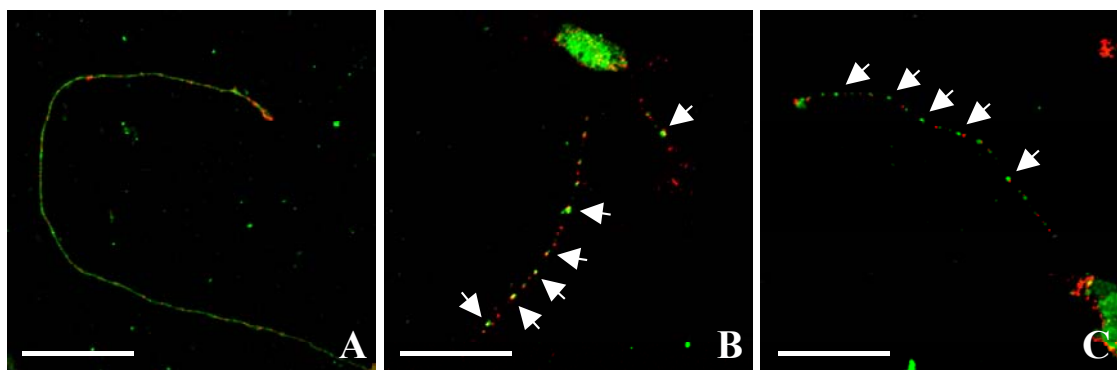


Figure 10: Co-capping of CHL1 and hsc70 in primary hippocampal neurons

(A): Dissociated hippocampal neurons from newborn mice (1 days in culture) were double-labeled with anti hsc70 antibody (green) and with anti CHL1 antibody (red).

(B/C): For co-capping, cells were pre-incubated with the polyclonal rabbit anti CHL1 antibody and primary antibodies were clustered with a secondary anti rabbit antibody. Afterwards, cells were stained with polyclonal anti hsc70 antibody. Co-localization of CHL1 and hsc70 is indicated by yellow staining (arrows). Scale bar represents 20 μm .

V.10. Analysis of the hsc70 and CHL1 distribution in membrane subfractions

The results of the immunocytochemistry of primary hippocampal neurons suggest that CHL1 and hsc70 may interact only in distinct membrane subdomains indicated by a co-localization of both proteins in restrictive areas. This putative co-distribution of CHL1 and hsc70 in particular cellular subfractions was addressed by biochemical analyses and it turned out that CHL1 and hsc70 were only co-distributed in fractions of enriched synaptosomes (data not shown, personal communication Dr. Ralf Kleene). The immunocytochemical study further indicated that the age of the cells influences the localization between CHL1 and hsc70 and probably also the interaction between both proteins. Cells prepared from newborn mice showed a quite widespread distribution of hsc70 and the co-localization of CHL1 and hsc70 was only detectable after co-capping of CHL1 while in neurons prepared from 4-day old animals, the hsc70 distribution was observed in a distinct pattern and co-localization was seen without preceded co-capping. This observation may indicate that the localization of CHL1 and hsc70 to certain subdomains and thereby the interaction is dependent or regulated during developmental stages in mice. Thus, a biochemical analysis of CHL1 and hsc70 distribution

in subdomains from 7-day old mice compared to adult mice were carried out. Enriched synaptosomes were prepared by subsequent sucrose gradient centrifugation steps. Further ultracentrifugation procedures allowed to separate synaptosomal membranes which were either mock-treated or alkali treated. Afterwards, the membranes were solubilized in Triton X-100 containing buffer in the cold and separated in Triton X-100 soluble and insoluble material. The Triton X-100 insoluble fraction was further separated in a so-called raft fraction and a non-raft fraction. A typical property of rafts is the floating to low density fractions within a sucrose gradient. It has been shown that a preceding alkaline treatment of the membranes increases the yield of rafts (personal communication, Dr. Ralf Kleene). This alkali treatment presumably removes extracellular matrix (ECM) proteins and proteins of intracellular structures such as cytoskeleton components from proteins of the raft fraction. The loss of the interactions to ECM or cytoskeletal proteins confers a lower density to the rafts that allows the floating within a sucrose gradient to a layer of lower density. Without alkali treatment, typical raft proteins are detectable in the non-raft fraction that is sedimented within the sucrose gradient.

Hsc70 and CHL1 were detectable in the total synaptosomal membrane fraction that was used as the starting material (Figure 11, A – D, lanes 1,6). Both proteins were observed in the Triton X-100 soluble fraction (Figure A – D, lanes 5,10) as well as in the Triton X-100 insoluble fraction (Figure 11, A – D, lanes 2,7). In the case of 7-day old animals, both proteins were only present in the non-raft fraction when membranes were mock-treated (Figure 11, A/C, lane 4) but in the raft fraction neither hsc70 nor CHL1 were detectable (Figure 11, A/C, lane 3). After alkali treatment, hsc70 and CHL1 appeared exclusively in the raft fraction that showed floating to the sucrose layer of low density (Figure 11, A/C, lane 8) whereas expression of hsc70 or CHL1 was completely diminished in the non-raft fraction in young animals (Figure 11, A/C, lane 9). In adults, hsc70 and CHL1 were detectable in the non-raft fraction as well as in the raft fraction without alkali treatment (Figure 11, B/D, lanes 3,4) whereas floating within the sucrose gradient to a layer of low density (“raft fraction”) was observed after alkali treatment (Figure 11, B/D, lane 8). As it was seen for younger animals, hsc70 and CHL1 were no more detectable in the non-raft fraction following alkaline treatment (Figure 11, B/D, lane 9). These results suggest that CHL1 and hsc70 are localized in raft subdomains with or without binding to extracellular matrix proteins and/or to cytoskeletal elements.

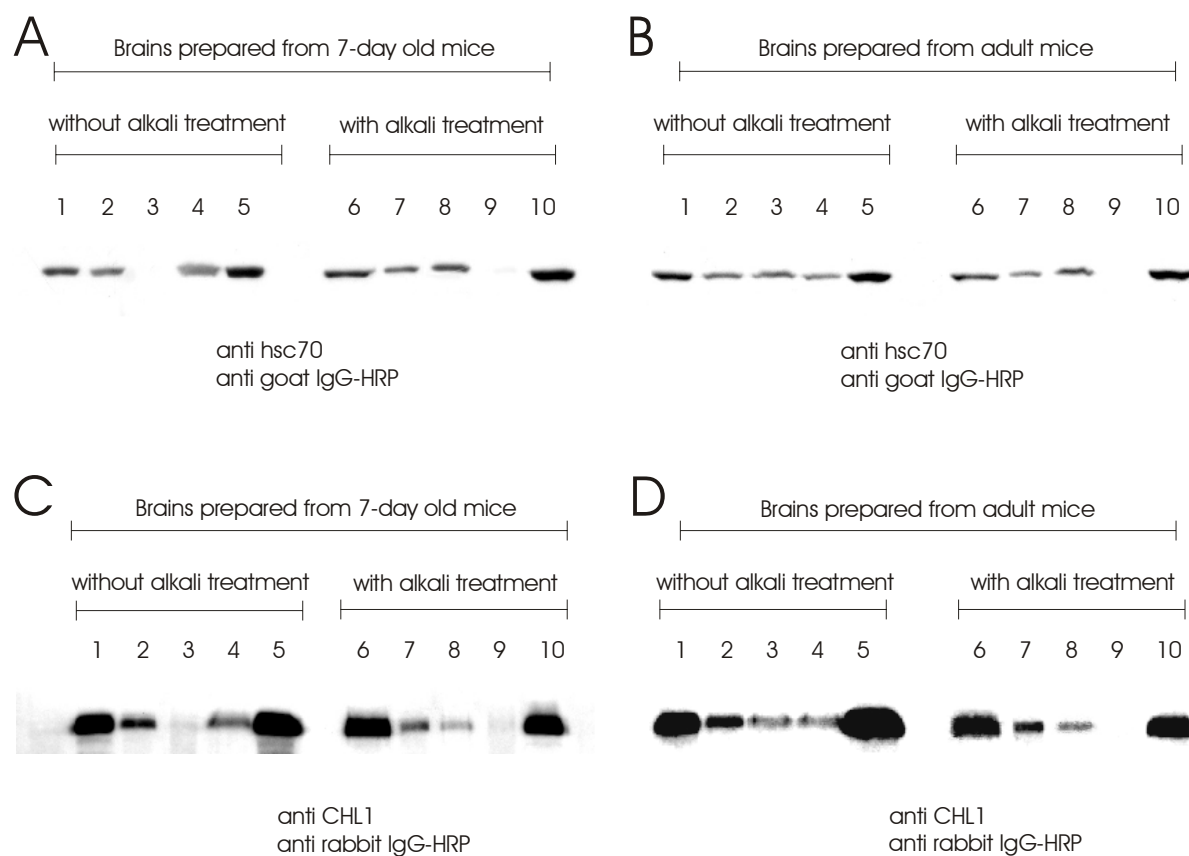


Figure 11: Distribution of hsc70 and CHL1 in membrane subfractions

For the analysis of hsc70 and CHL1 distribution in particular membrane subdomains, a fraction of total synaptosomal membranes was prepared from 7-day old mice (A/C) and adult mice (B/D). Fractions were isolated without pre-treatment (A – D, lanes 1 – 5) or with pre-treatment of 0.15 M bicarbonate, pH 11 (A – D, lanes 6 – 10). The synaptosomal membrane fraction (lanes 1,6) was further separated to Triton X-100 insoluble material (lanes 2, 7) and Triton X-100 soluble material (lanes 5, 10). The Triton X-100 insoluble material was separated in a raft (lanes 3, 8) and non-raft fraction (lanes 4, 9) using a sucrose gradient. All fractions were subjected to SDS-PAGE and transferred to nitrocellulose membrane for detection of either hsc70 (A/B) using a polyclonal goat anti hsc70 antibody or CHL1 detection (C/D) using a polyclonal rabbit anti CHL1 antibody.

V.11. Co-immunoprecipitation of CHL1 and hsc70 from a crude brain fraction

The co-localization analysis of CHL1 and hsc70 in hippocampal neurons indicated that an interaction between both proteins may occur only in membrane subdomains. The co-distribution of CHL1 and hsc70 in the Triton X-100 insoluble fraction and in the so-called raft

and non-raft fraction supported the assumption drawn from the co-localization assay that the interaction between the putative binding partners may be restricted to detergent-insoluble membrane subdomains. Taking these results in account and since a precededly performed co-immunoprecipitation failed to confirm the interaction between CHL1 and hsc70, an immunoprecipitation of CHL1 was repeated, but the conditions for the precipitation were modified. This time, brain homogenates were prepared in the presence of 1 % Triton X-100 and applied to the immunoprecipitation without any further centrifugation step in order not to remove Triton X-100 insoluble material. To avoid sedimentation of detergent-insoluble material during ProteinA sepharose centrifugation, magnetic ProteinA Dynabeads were used for purification of immunocomplexes from these crude detergent extracts. A further modification was the addition of ADP as a co-factor since other hsc70 interactions were previously described to be ADP-dependent (Frydman and Höhfeld, 1997). A co-immunoprecipitation of hsc70 using the polyclonal anti CHL1 antibody was only detectable in the presence of ADP (Figure 12, lanes 3,4) but not in the presence of ATP (Figure 12, lanes 1,2). In the negative control using brain extracts which were derived from CHL1 knock-out animals, no co-precipitation of hsc70 occurred at all, not in the presence of ATP (Figure 12, lane 9) and not even in the presence of ADP (Figure 12, lane 10). In a further control using a polyclonal antibody against L1 for immunoprecipitation, only a very weak background staining of hsc70 appeared in the immunoprecipitate in the presence of ADP (Figure 12, lanes 6,8) whereas no detection of hsc70 was seen after precipitation of L1 in the presence of ATP (Figure 12, lanes 5,7). The background staining was possibly due to contaminations of Triton X-100 insoluble material in the precipitate.

hsc70 was detectable in the CHL1-immunocomplex when a crude homogenate was used for immunoprecipitation. As already mentioned, the co-distribution of CHL1 and hsc70 in primary hippocampal neurons further indicated that the age of the animal might be a crucial factor for the interaction between CHL1 and hsc70. Since the co-localization in restricted subdomains was only observed in neurons derived from older animals, a preceding pre-clustering of CHL1 was required to show the co-localization of CHL1 and hsc70 in neurons derived from younger animals. Thus, a co-immunoprecipitation approach was carried out regarding the developmental stage of the animals that is proposed to influence the distribution of CHL1 and hsc70 in detergent-insoluble subdomains and thereby to influence the facilitation of an interaction between both binding proteins. A non-detergent soluble fraction and a crude membrane fraction containing Triton X-100 were prepared from 5-day old mice and from 3-weeks old mice. The crude fraction was further separated to Triton X-100 soluble and insoluble material. An immunoprecipitation of CHL1 was carried out in the presence of ADP and immunocomplexes were purified using magnetic ProteinA Dynabeads. The eluates were analyzed for co-precipitation of hsc70. In case of 5-day old animals, a co-immunoprecipitation of hsc70 from the crude membrane fraction was only weakly detectable (Figure 13A, lane 2). In older animals, a more pronounced co-precipitation of hsc70 was obtained from the crude membrane fraction (Figure 13A, lane 6) and was additionally detectable when the Triton X-100 insoluble fraction was used for precipitation (Figure 13A, lane 8). CHL1 and hsc70 expression levels were controlled in all fractions which were applied to the precipitation (Figure 13, B/C). Although the CHL1 expression was remarkably higher in the crude membrane fraction prepared from 5-day old animals when compared to 3-weeks old animals (Figure 13B, lanes 2,6), a co-immunoprecipitation of hsc70 was much stronger seen in older animals (Figure 13A, lanes 2,6). No co-immunoprecipitation of CHL1 and hsc70 was detectable in the Triton X-100 insoluble fraction in younger animals (Figure 13A, lane 4) whereas in older animals hsc70 was visible in the immunoprecipitate isolated from this particular fraction (Figure 13A, lane 8). Although, the expression level of CHL1 was definitively lower in the detergent-insoluble fraction prepared from older animals when compared to 5-day old animals (Figure 13B, lanes 4,8) the co-immunoprecipitation was remarkably intensive indicating that the developmental stage of the animal facilitates the interaction between CHL1 and hsc70. Furthermore, the results suggest that the localization of the CHL1 – hsc70 interaction is more restricted to detergent-insoluble subdomains with older

age of the animals since in younger mice no interaction at all was seen in the Triton X-100 insoluble fraction.

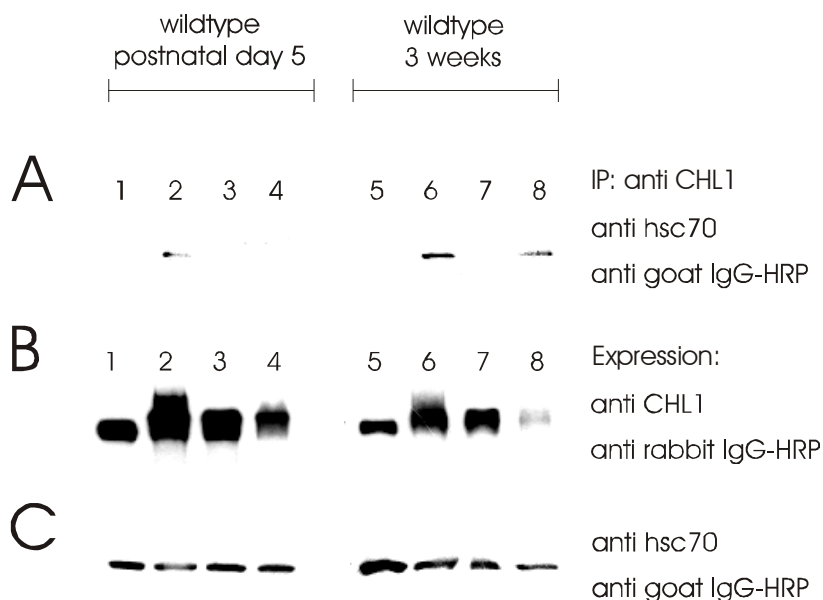


Figure 13: Co-immunoprecipitation of CHL1 and hsc70 from several membrane fractions of brain homogenates derived from 5-day old or 3-weeks old mice

Brains were prepared from 5-day old mice (lanes 1 – 4) and 3-weeks old mice (lanes 5 – 8) and a non-detergent soluble fraction (lanes 1,5) as well as a crude membrane fraction containing Triton X-100 (lanes 2,6) was isolated. The crude membranes were further separated to Triton X-100 soluble (lanes 3,7) and Triton X-100 insoluble material (lanes 4,8). All fractions were incubated with a polyclonal antiserum against CHL1 for immunoprecipitation in the presence of ADP. The immunocomplexes were purified using ProteinA Dynabeads and the eluates were analyzed for co-precipitation of hsc70 (A). Fractions were also subjected to SDS-PAGE for analysis of either CHL1 expression (B) or hsc70 expression (C).

V.13. Identification of a putative hsc70 binding motif in the intracellular domain of CHL1

To address the question whether a putative binding site for hsc70 within the intracellular domain of CHL1 exist, published sequences of previously known hsc70 binding motifs were compared with the sequence of the intracellular portion of CHL1. The information of three conserved motifs described for the binding of hsc70 was considered. In detail, the tetratricopeptide repeat motif (Van Der et al., 2000; Liu et al., 1999), the tetrameric sequence

[EEX(4)], namely EEVD (Schneikert et al., 1999; Liu et al., 1999) and the well established J-domain (Hennessy et al., 2000; Chamberlain and Burgoyne, 1997a; Cheetham et al., 1994) have been determined to be a hsc70 binding motif. The highly conserved tripeptide HPD of the J-domain was of particular interest since this short sequence was sufficient for hsc70 binding and point mutations within this sequence caused a complete loss of hsc70 binding (Chamberlain and Burgoyne, 1997b). In fact, this tripeptide was identified in the intracellular domain of CHL1 (Figure 14, indicated by an arrow). Consistent with the observation that L1 failed to bind to hsc70, this tripeptide was not present in the intracellular domain of L1 within a region of 5 amino acid residues (position 16 – 20) that is rather non-conserved comparing L1 and CHL1 (Kelley and Georgopoulos, 1997).

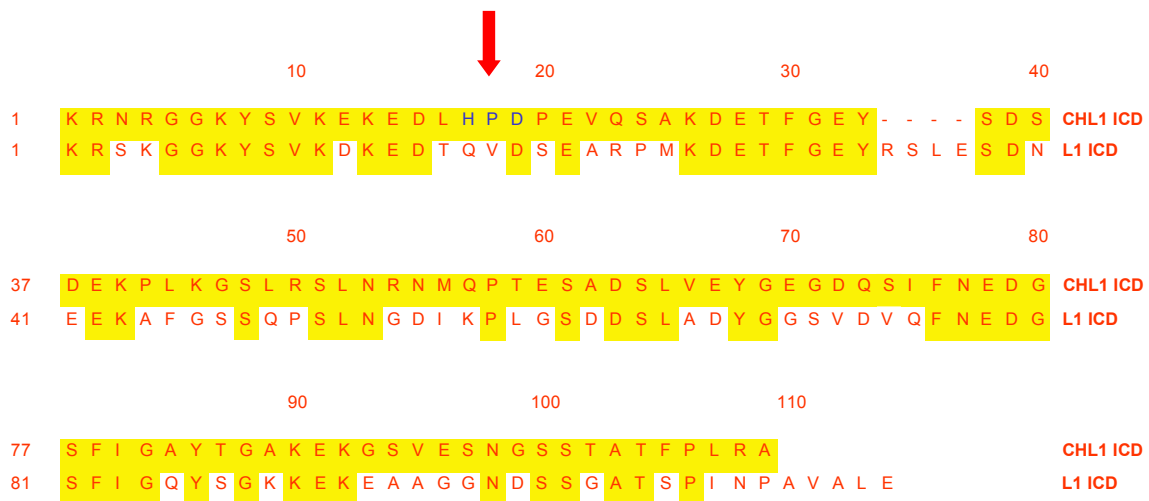


Figure 14: Alignment of the intracellular domain of CHL1 and L1 and identification of the HPD tripeptide only in the intracellular domain of CHL1 and not in the intracellular domain of L1.

V.14. Site-directed mutagenesis of the putative hsc70 binding site in the intracellular domain of CHL1

The highly conserved tripeptide HPD was previously described to be the most important sequence within the J-domain that can mediate hsc70 binding alone (Chamberlain and Burgoyne, 1997b). Analogous to the described point mutations that causes total loss of hsc70

binding (Chamberlain and Burgoyne, 1997a; Zhang et al., 1999), the HPD tripeptide in the intracellular domain of CHL1 was mutated using a site-directed mutagenesis. Four mutations were generated of which only two mutations affected the putative hsc70 binding site. In the first mutation, a single basepair exchange was generated resulting in an amino acid exchange of histidine to glutamine. The second mutation of the HPD tripeptide was a single basepair exchange of aspartate to adenine. A further mutation was generated possibly affecting the CHL1 distribution in Triton X-100 insoluble raft fraction. In this mutation, a putative palmitoylation site (Ren and Bennett, 1998) was deleted by a single basepair exchange that led to the amino acid exchange of a cysteine residue to serine which cannot be palmitoylated. Palmitoylation was previously described to be involved in the localization of proteins to raft subdomains (Kabouridis et al., 1997; Zhang et al., 1998). By deletion of this particular cysteine residue, the distribution of CHL1 into rafts might be diminished including that this also could impair the interaction of CHL1 and hsc70. Finally, the same triplet was mutated in a fourth mutagenesis, that generated a stop codon instead of the transmembrane cysteine. Using this mutation, a CHL1 construct was generated lacking the entire intracellular domain that offers a convenient tool as a negative control.

Mutation	Amino acid exchange	Affected basepairs	Basepair exchange
H 1121 Q	histidine → glutamine	3361 - 3363	CAC → CAA
D 1123 A	aspartate → adenine	3367 - 3369	GAT → GCT
C 1102 S	cysteine → serine	3304 - 3306	TGC → TCC
Δ ICD	cysteine → stop	3304 - 3306	TGC → TGA

For detailed information of mutagenesis and vector design see Methods, IV.6.12 and Appendix, VIII.3.3.

V.15. Co-precipitation of CHL1 and hsc70 from transfected CHO cells

In order to establish a cellular system for the analysis of the CHL1 mutations, transfected CHO cells were tested to be an appropriate cell system for co-precipitation of CHL1 and hsc70. First, cells were transfected with the expression vector pcDNA3 encoding wildtype CHL1. Crude cell lysate as well as Triton X-100 soluble and insoluble fractions were analyzed either for co-precipitation and for co-distribution of CHL1 and hsc70 (Figure 15). Only in the crude cell lysate and the Triton X-100 soluble fraction, a co-precipitation of CHL1 and hsc70 was detectable (Figure 15A, lanes 1,2). A co-precipitation was not seen in the Triton X-100 insoluble fraction (Figure 15A, lane 3) and in non-transfected CHO cells (Figure 15A, lane 4). In contrast to brain homogenates, where CHL1 expression was remarkably high in the Triton X-100 insoluble fraction, only weak expression of CHL1 was found in that particular fraction of CHO cell lysates (Figure 15B, lane 3). Consistent with this observation, co-precipitation of CHL1 and hsc70 was only observed in the Triton X-100 soluble fraction (Figure 15A, lane 2), but not in the Triton X-100 insoluble fraction of CHO cell lysates (Figure 15A, lane 3). In summary, CHO cells are considered to be an appropriate cell system for analysis of the CHL1 mutants for co-immunoprecipitation of hsc70.

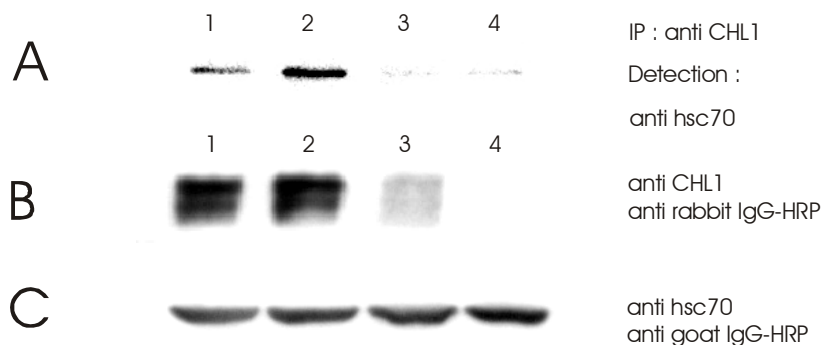


Figure 15: Co-precipitation of CHL1 and hsc70 from CHL1-transfected CHO cells

CHO cells were transiently transfected with the pcDNA3 expression vector coding for wildtype CHL1. After two days in culture, cells were harvested and lysed in a 1% Triton X-100 containing buffer. The crude cell lysate (lane 1), the Triton X-100 soluble (lane 2) and Triton X-100 insoluble fraction (lane 3) as well as a crude lysate of non-transfected CHO cells (lane 4) were incubated with a polyclonal anti CHL1 antiserum for

immunoprecipitation. The precipitation was carried out in the presence of ADP and the immunocomplexes were purified using magnetic Protein A Dynabeads. The eluates were analyzed for co-precipitation of hsc70 (A). Furthermore, all fractions were subjected to SDS-PAGE and transferred to nitrocellulose for detection of either CHL1 (B) using a rabbit polyclonal anti CHL1 antiserum or hsc70 (C) using a goat polyclonal anti hsc70 antibody.

V.16. Co-precipitation of CHL1 and hsc70 from CHO cells after transfection of wildtype CHL1 and mutant CHL1

To demonstrate that the HPD tripeptide is the hsc70 binding domain within the intracellular portion of CHL1, wildtype CHL1 and mutant CHL1 deleted in the putative hsc70 binding site were transfected into CHO cells. Additionally, the mutants containing an amino acid exchange in the transmembrane cysteine residue at position 1102 were transfected. After two days in culture, cells were harvested and prepared for the immunoprecipitation of CHL1 (Figure 16). To control that all constructs are equally expressed after transfection, cell lysates were also analyzed with regard to CHL1 presence using the polyclonal anti CHL1 antibody (Figure 16B). For control of endogenous hsc70 levels, cell lysates were analyzed using a polyclonal anti hsc70 antibody (Figure 16C). Only in cells expressing wildtype CHL1 and in cells transfected with CHL1 that was mutated in the putative palmitoylation site, a remarkable co-precipitation of hsc70 was revealed (Figure 16A, lanes 1,4). Cells which were transfected with CHL1 constructs containing a deletion in the putative hsc70 binding site completely failed to co-precipitate with hsc70 (Figure 16A, lanes 2,3). Furthermore, both the CHL1 construct lacking the entire intracellular domain and the non-transfected cells did not show any co-precipitation of CHL1 and hsc70 (Figure 16A, lanes 5,6). Interestingly, only CHL1- Δ ICD showed an expression as a single isoform since all other CHL1 mutants displayed expression of full length and processed isoforms (Figure 16B, lanes 1 – 4). The mutant lacking the complete intracellular domain was detectable as one predominant fragment with a molecular mass of approximately 140 kDa (Figure 16B, lane 5).

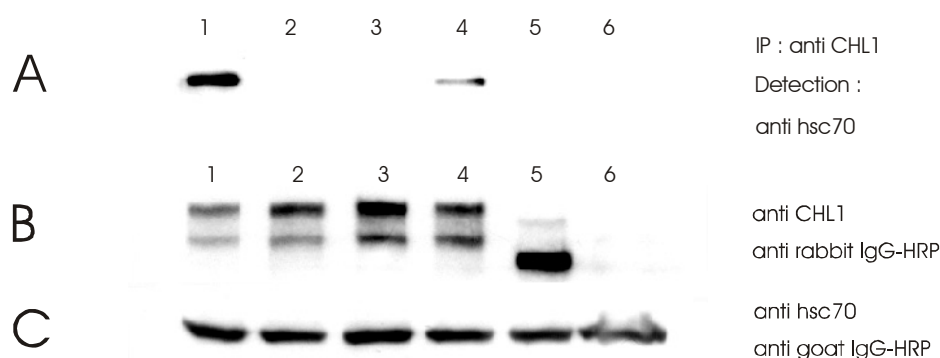


Figure 16: Co-precipitation of CHL1 and hsc70 from wildtype CHL1-transfected and mutant CHL1-transfected CHO cells

CHO cells were transiently transfected with pcDNA3 expression vector encoding wildtype CHL1 or mutant CHL1 constructs. After two days in culture, cells were harvested and lysed. A crude lysate was used for immunoprecipitations of CHL1 (A) and for detection of either CHL1 (B) or hsc70 expression (C). CHO cells were transfected with wildtype CHL1 (lane 1), H1121Q (lane 2), D1123A (lane 3), C1102S (lane 4) or C1102Stop (lane 5). Non-transfected cells were used as a negative control (lane 6). For immunoprecipitation of CHL1 from transfected CHO cell lysates, 25 μ l of a polyclonal anti CHL1 antiserum was applied and immunocomplexes were purified using ProteinA Dynabeads. Eluates were subjected to SDS-PAGE and co-precipitation of hsc70 determined using a polyclonal goat anti hsc70 antibody. Cell lysates were also subjected to SDS-PAGE in the same order as given in (A) and transferred to nitrocellulose membrane. Detection of CHL1 (B) was carried out by the use of a polyclonal rabbit anti CHL1 antiserum. Hsc70 detection (C) was performed using a polyclonal goat anti hsc70 antibody.

V.17. Co-precipitation of CHL1 and hsc70 from N2A cells after transfection of wildtype CHL1 and mutant CHL1

For verification of the co-precipitation results obtained from transfected CHO cells, a further cell line was used for co-precipitation of wildtype versus mutated CHL1. N2A cells which did not express CHL1 endogenously were transfected with either wildtype or mutant CHL1 constructs and were allowed to express the transfected protein for two days in culture. Cell lysates were utilized for precipitation of CHL1. Consistent with the precipitation from transfected CHO cells, a co-precipitation of hsc70 was only detectable in cell lysates derived from wildtype transfected (Figure 17A, lane 1) and C1102S transfected N2A cells (Figure 17A, lane 4). Cells which were transfected with CHL1 constructs mutated in the putative

hsc70 binding site showed no remarkable co-precipitation of CHL1 and hsc70 (Figure 17A, lanes 2,3) indicating that the HPD tripeptide is a prerequisite for CHL1 binding of hsc70. Neither the Δ ICD mutant nor the non-transfected N2A cells which were applied for negative control showed any co-precipitation of hsc70 (Figure 17A, lanes 5,6).

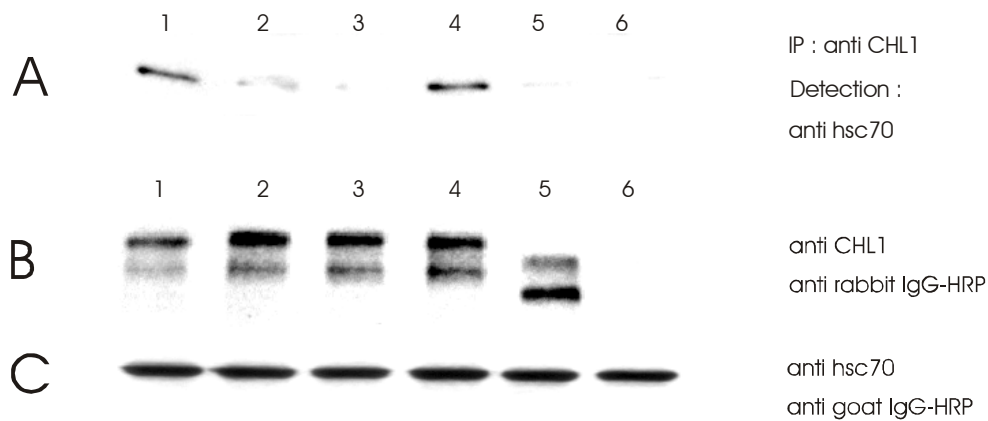


Figure 17: Co-precipitation of CHL1 and hsc70 from wildtype CHL1- and mutant CHL1-transfected N2A cells

N2A cells were transiently transfected with pcDNA3 expression vector encoding either wildtype or mutant CHL1. After two days in culture, cells were harvested and lysed in the presence of 1% Triton X-100 and 1 mM ADP. Crude lysates were used for immunoprecipitations of CHL1 (A) and for detection of either CHL1 (B) or hsc70 expression (C). Lysates of wildtype transfected N2A cells (lane 1), H1121Q mutant (lane 2), D1123A mutant (lane 3), C1102S mutant (lane 4), C1102Stop (lane 5) and non-transfected N2A were subjected to an immunoprecipitation of CHL1. Immunocomplexes were purified by ProteinA Dynabeads and eluates were subjected to SDS-PAGE and transferred to nitrocellulose membranes. Co-precipitation was analyzed using a polyclonal goat hsc70 antibody. Expression control of transfected CHL1 (B) and endogenous hsc70 (C) in N2A cell lysates was performed using a polyclonal rabbit anti CHL1 antiserum or the polyclonal goat anti hsc70 antibody.

V.18. Functional analysis of the interaction between CHL1 and hsc70

For functional analysis of the CHL1 – hsc70 binding, the question was addressed whether the intracellular interaction between CHL1 and hsc70 is involved in neurite outgrowth after extracellular stimulation of CHL1. It was hypothesized that stimulation of CHL1 promotes neurite outgrowth that requires structural alterations of the cytoskeleton. This cascade starts

with an extracellular stimulus of CHL1 that is transduced via the transmembrane cell adhesion molecule into the cell. Intracellularly, proteins must be activated downstream of the transmembraneous CHL1 which initiate modulations in composition and structure of the cytoskeleton. The heat shock cognate 70 is considered to be a good candidate to transfer the extracellular stimulus into the inside of the cell resulting in reorganization processes of the intermediate filament, microtubuli assembly or the actin-based cytoskeleton (Napolitano et al., 1985; Whatley et al., 1986; Haus et al., 1993). For functional analysis of the CHL1 – hsc70 interaction, hippocampal neurons derived from CHL1 deficient mice were cultured and subsequently transfected either with wildtype CHL1 or with CHL1 mutants deleted in the hsc70 binding motif. Since no extracellular binding partner of CHL1 has been identified so far, a polyclonal antiserum raised against the extracellular domain of CHL1 was used for stimulation assumingly mimicking the interaction with a binding partner. CHL1-dependent stimulation of neurite outgrowth of CHL1 knock-out hippocampal neurons is only expected after transfection of wildtype CHL1. On the other hand, an impaired promotion of CHL1-dependent neuritogenesis could be assumed following transfection of CHL1 mutants suggesting that the extracellular stimulus of CHL1 can only alter cytoskeletal structures when a functional interaction between CHL1 and hsc70 is present. As mentioned before, the heat shock cognate70 is regarded to be involved in the modification of filamentous components of the cytoskeleton which are required for morphological changes during neuritogenesis. Our hypothesis proposes that in neurons where the binding of CHL1 and hsc70 cannot take place the extracellular stimulus will not trigger structural changes of the cytoskeletal organization resulting in an impaired CHL1-dependent stimulation of neurite outgrowth.

In preliminary studies, the specificity of the polyclonal anti CHL1 antibody for binding to CHL1 was investigated. First, the immunohistochemical detection of CHL1 in cerebellar sections was carried out and then cultured primary hippocampal neurons derived from wildtype versus CHL1 deficient mice were stained using the polyclonal anti CHL1 antibody. A further preliminary assay considered the question whether the polyclonal antibody raised against the extracellular domain of CHL1 has the potential to stimulate neurite outgrowth as it has been previously described for stimulation of neuritogenesis using antibodies in case of L1-dependent stimulation using the monoclonal antibody 557 (Appel et al., 1995). Finally, if the polyclonal anti CHL1 antibody stimulates neuritogenesis of hippocampal neurons, it should be used in neurons derived from CHL1 deficient mice after transfection of either

wildtype CHL1 or CHL1 mutants which were deleted in the hsc70 binding motif to investigate CHL1-dependent promotion of neurite outgrowth.

V.18.1. Determination of the specificity of the polyclonal anti CHL1 antibody

Specific binding of the polyclonal anti CHL1 antibody was analyzed using cerebellar cortex sections derived from wildtype mice and from CHL1 deficient mice. For the immunohistochemical analysis, the polyclonal anti CHL1 antiserum was affinity-purified. The purification was performed using first a human IgG pre-column and followed by an affinity chromatography column with immobilized CHL1-Fc fusion protein. A highly specific staining of CHL1 was detectable following incubation of cerebellar sections with the affinity-purified anti CHL1 antibody. CHL1 expression was observed on distinct cells in the molecular layer which were probably basket and stellate cells (Figure 18, A/B, *mol*). The remarkable dense CHL1 staining in this particular layer on the other hand suggested an expression of CHL1 on dendrites of Golgi and granule cells which were present in the internal granular layer (Figure 18, A/B, *igl*). These certain cells showed high levels of CHL1 in their somata confirming previous results showing CHL1 mRNA expression in these particular cells by an *in situ* analysis (Holm et al., 1996). Golgi and granule cells develop extensive dendritic trees which were intensively stained for CHL1. Purkinje cells were negative for CHL1 expression. These conspicuous cells showed no CHL1 expression in their somata (Figure 18, A/B, indicated by arrowheads) and no staining on dendrites (Figure 18, A/B, indicated by arrowheads labeled with a star). The immunohistochemical localization of the CHL1 protein was confirmed by an *in-situ* hybridization that revealed an overlapping expression pattern of CHL1 mRNA (Figure 18D) and CHL1 protein. However, the CHL1 mRNA expression level was very weak in cells of the molecular layer indicating that the intensive staining that was seen for protein expression in that particular layer was obviously more due to strong expression of CHL1 on dendrites of granule and Golgi cells than to the expression of CHL1 in basket or stellate cells. The specificity of the antibody was underlined by immunohistochemical detection of CHL1 using cerebellar cortex sections derived from CHL1 deficient mice (Figure 18C). No binding of the affinity-purified antibody at all was observed

after incubation of this particular tissue. The preparation of cryosections and all immunohistochemical experiments were performed by Bettina Rolf.

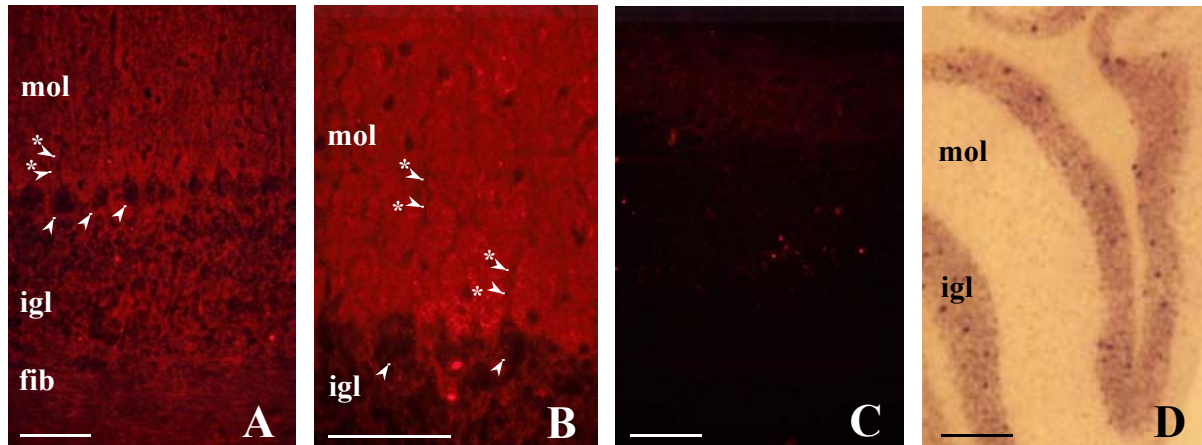


Figure 18: Localization of CHL1 in the cerebellar cortex by immunohistochemical detection using affinity-purified antibody and by *in situ* hybridization analysis

Cerebellar cortices were isolated either from wildtype (A/B, D) or from CHL1 deficient mice (C). Sections were prepared and immunohistochemical detection of CHL1 was carried out using an affinity-purified anti CHL1 antibody (A – C). *In situ* analysis was performed using a CHL1 specific anti sense probe (D). Molecular layer (mol); internal granular layer (igl); fiber layer (fib); somata of Purkinje cells are indicated by arrowheads (A/B); dendrites of Purkinje cells are depicted by arrowheads labeled with a star (A/B). Scale bars indicate 100 μm in (A) and 80 μm in (B).

(C): Cerebellar sections derived from CHL1 deficient mice revealed no unspecific binding of the affinity-purified antibody: Scale bar = 100 μm .

(D): Localization of CHL1 mRNA in sections of cerebellar cortex by *in situ* analysis demonstrated CHL1 mRNA expression in the internal granule layer (igl) and in the molecular layer (mol). Scale bar = 250 μm in (D).

To further check the specificity of the antibody, dissociated hippocampal neurons were prepared and the staining of the affinity-purified antibody (Figure 19A) was compared to that of an IgG fraction that was only purified using ProteinA sepharose (Figure 19B). Hippocampal neurons derived from CHL1 deficient mice were used as control for the specificity of antibody binding (Figure 19C). Finally, wildtype neurons were only stained with the fluorescence-labeled anti rabbit IgG antibody as a negative control for the secondary antibody (Figure 19D). The immunocytochemical detection of CHL1 in primary hippocampal cultures revealed a specific staining of CHL1 only in distinct subpopulations of hippocampal neurons. The affinity-purified antibody and the IgG fraction that was only ProteinA-purified

showed a similar staining pattern. Cells which expressed CHL1 displayed a strong staining on somata as well as on dendrites (Figure 19, A/B, indicated by arrowheads labeled with a pound sign). Cells which were only weakly stained in their somata but not on dendrites were also observed (Figure 19, A/B, indicated by arrowheads labeled with a star). This staining was due to unspecific binding of the secondary antibody since poor staining of the somata was also seen in cells derived from CHL1 $-/-$ mice (Figure 19C) and also after incubation of wildtype neurons with the secondary antibody alone (Figure 19D). Distinct expression of CHL1 in subpopulations of hippocampal neurons was previously described using an *in situ* analysis (Hillenbrand et al., 1999) and was confirmed here by the immunocytochemical detection of CHL1 using either the affinity-purified or the ProteinA-purified IgG fraction. Dissociated hippocampal cultures were kindly provided by Galina Dityateva.

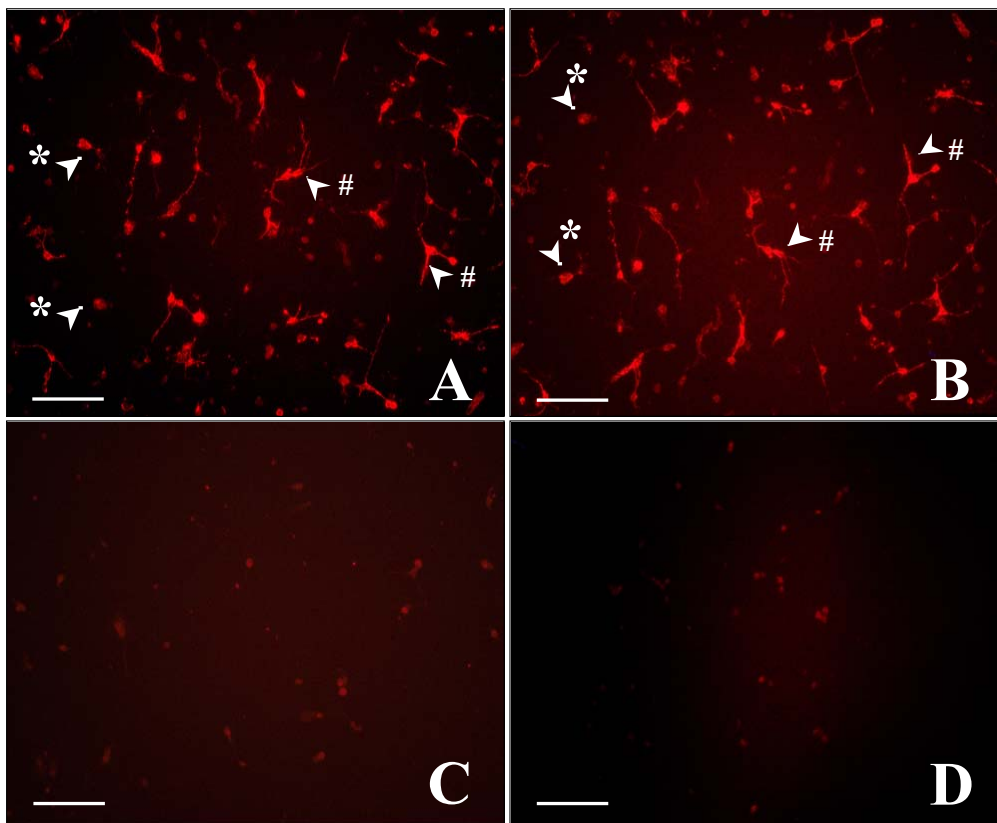


Figure 19: Expression of CHL1 in dissociated primary cultures of hippocampal neurons derived from wildtype mice or CHL1 knock-out mice

Dissociated hippocampal neurons were prepared either from wildtype mice expressing CHL1 (A/B and D) or from CHL1 deficient mice (C). Detection of CHL1 was carried out using an affinity-purified polyclonal antibody

(A) or a ProteinA-purified IgG fraction of the antibody (B). The secondary antibody was Cy3-conjugated and applied in a final dilution of 1/300. The specificity of the primary antibody was controlled by incubation of CHL1 deficient cells with the ProteinA-purified IgG fraction (C) and the secondary antibody was also tested for unspecific binding using wildtype cells as depicted in (D). Arrowheads labeled with a pound sign (#) (A/B) emphasize CHL1 expressing neurons while cells which were negative for expression of CHL1 are indicated with arrowheads labeled with a star (*). Scale bars = 80 μ m.

V.18.2. Stimulation of neuritogenesis of primary hippocampal neurons by the anti CHL1 antibody

The antiserum that was raised against the extracellular domain of CHL1 was investigated for the potential to stimulate CHL1-dependent neurite outgrowth. As mentioned before, the antibody binding is considered to mimic the binding of an extracellular interaction partner. For neuritogenesis, the crude serum was purified using ProteinA sepharose and the IgG fraction was immobilized to 96-well dishes. Non-immune rabbit IgG fraction (Sigma) and poly-L-lysine were used as negative controls. Dissociated hippocampal neurons were prepared from wildtype mice expressing CHL1 and cultured on the substrate-coated plastic wells. One representative assay is shown in Figure 20. Once, hippocampal neurons derived from CHL1 deficient mice were also prepared and tested for CHL1-dependent stimulation of neurite outgrowth after growing on anti CHL1 IgG fraction (data not shown). Cells were allowed to grow for 20 hours and afterwards they were fixed and visualized by toluidine blue staining. Cells were selected for analysis and neurites were measured in length according to previous published criteria (Haspel et al., 2000). Neurons were only analyzed which had no cell-cell-contacts and the longest neurite was only measured in length when the neurite was at least as long as or longer than the diameter of the cell. The statistical analysis of CHL1-dependent stimulation compared to negative controls was performed using the Mann Whitney test. The longest neurite of wildtype hippocampal neurons stimulated by the anti CHL1 antibody showed a significant elongation ($P < 0.0001$) to approximately 40 μ m in length for the both highest concentrations (Figure 20, black bars) while the negative control using poly-L-lysine showed a neurite length of only 20 μ m (Figure 20, grey bar). A dose-dependent effect of CHL1-dependent stimulation was also observed since for concentrations of 0.1 mg/ml and 0.01 mg/ml, a promotion of neurite outgrowth to 40 μ m was seen, whereas using a concentration of only 0.001 mg/ml of anti CHL1 antibody still significant stimulation ($P <$

0.0001) compared to poly-L-lysine was detectable, but compared to the higher antibody concentrations, only poor promotion of neurite outgrowth was visible. The non-immune rabbit IgG fraction also showed enhanced neurite outgrowth when it was coated with a concentration of 0.1 mg/ml. The stimulation was even weaker than stimulation with the lowest concentration of the anti CHL1 IgG fraction, but analyzed with the Mann Whitney test, the neurite length was still significantly enhanced ($P < 0.0001$) compared to poly-L-lysine. No significant alterations in neurite length compared to PLL was detected after immobilization of non-immune IgGs with lower concentrations (Figure 20, transversal striped). Hippocampal neurons derived from CHL1 deficient mice cultured on anti CHL1 IgG fraction revealed a neurite length that was comparable to neurite outgrowth of cells growing on low concentrations of rabbit IgG fraction or on poly-L-lysine (data not shown). The positive control using laminin showed extensively enhanced neuritogenesis even when compared to the anti CHL1 IgG fraction emphasizing that the stimulation of neurite outgrowth generated by the polyclonal antibody was not remarkably strong but significant when compared to poly-L-lysine and the non-immune Ig controls ($P < 0.0001$). For all following CHL1-dependent neurite outgrowth assays, the ProteinA-purified anti CHL1 IgG fraction was used with a concentration of 0.01 mg/ml since strongly enhanced neuritogenesis was observed for this concentration but no significant alterations in neurite length were observed when non-immune rabbit IgG was immobilized with this particular concentration.

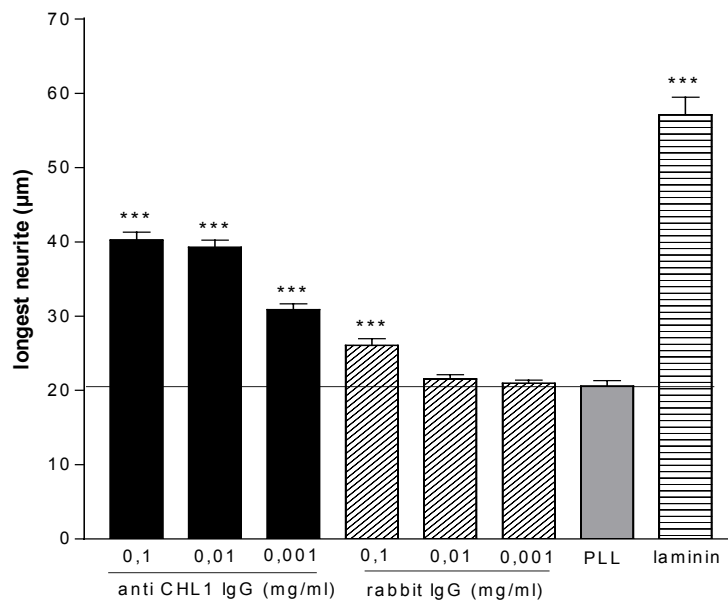


Figure 20: CHL1-dependent promotion of neurite outgrowth of primary hippocampal neurons

Primary hippocampal neurons were prepared from wildtype mice expressing CHL1 and seeded on coverslips which were previously coated with either anti CHL1 IgG fraction, non-immune rabbit IgG fraction or only with poly-L-lysine. Three different concentrations of ProteinA-purified anti CHL1 IgG fraction (black filled bars) and the non-immune rabbit IgG fraction (transversal striped bars) were used for stimulation. As a negative control, poly-L-lysine (0.025 %) was immobilized (grey filled bar) while laminin (0.01 %) was used as a positive control for promotion of neurite outgrowth (straight striped bars). Neurons were seeded with cell densities of approximately 5.000 – 7.500 cells/well and were allowed to extend neurites for 20 hours. Afterwards, neurite length was measured as described previously and analyzed using the Mann Whitney test.

V.18.3. CHL1-dependent stimulation of neurite outgrowth of CHL1 $-/-$ hippocampal neurons after transfection of either wildtype CHL1 or mutant CHL1 deleted in the hsc70 binding site

Hippocampal neurons derived from CHL1 deficient mice were prepared and cultured on coverslips which were coated either only with poly-L-lysine or with the anti CHL1 IgG fraction. At least eight hours after preparation, cells were transfected using the CaPO₄ method and afterwards cells were allowed to express the transfected protein overnight. On the second day, neurons were transfected again and cultured for further twelve hours. After this time period, cells were fixed and either stained with the anti CHL1 antibody to control CHL1 expression or cells were analyzed without staining procedure. Only cells which were cultured on poly-L-lysine were tested for CHL1 expression since CHL1 detection of cells growing on the anti CHL1 IgG fraction evoked high background due to the immobilized antibody fraction. To identify transfected cells without detection of CHL1, neurons were co-transfected with an expression vector encoding the enhanced green fluorescence protein (EGFP) and co-transfection was controlled on PLL coated coverslips. In Figure 21, a representative co-transfected neuron is shown revealing expression of EGFP (Figure 21A, green) as well as expression of CHL1 (Figure 21B, red). The overlay image shows expression of both proteins and suggests a partially overlapping expression indicated by the yellow pattern (Figure 21C). The light microscopic image emphasizes that the expressed proteins were distributed over the whole cell instead of a particular expression e.g. on dendrites or in the somata. All images point out that the transfected neurons showed a rather unusually round morphology and that

neurite outgrowth was nearly missing suggesting that the transfection procedure might be a harmful stressor.

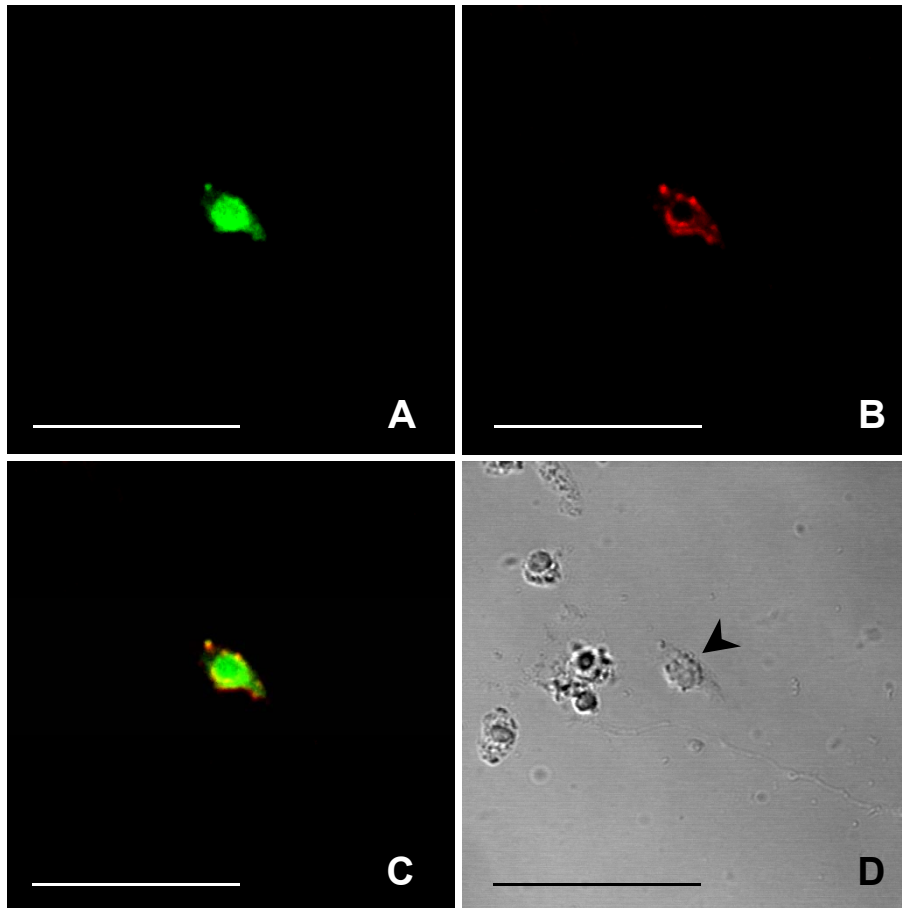


Figure 21: Transfection of hippocampal neurons derived from CHL1 knock-out mice using either wildtype CHL1 or CHL1 mutants.

Primary hippocampal neurons were prepared from CHL1 deficient mice and cultured on only poly-L-lysine coated coverslips for further detection of the CHL1 expression. Neurons were co-transfected twice using an expression vector encoding CHL1 and a further eucaryotic vector coding for the EGFP. After the second transfection, cells were allowed to grow for additional twelve hours. Afterwards, they were fixed and cells were either imaged only with a filter visualizing the green fluorescence generated by transfection of the EGFP (A) or detection of CHL1 was performed using the anti CHL1 IgG fraction derived from a polyclonal antiserum and further detected with Cy3-labeled secondary antibody (B). An overlay image confirms expression of both transfected proteins (C) while the light microscopic image (D) shows the transfected cell (indicated by an arrowhead) and also surrounding cells which were not transfected indicated by the fluorescence image. Pictures were analyzed using the Zeiss LSM510 argon-crypton confocal laser-scanning microscope. Scale bars = 50 μ m.

To answer the question whether the interaction of CHL1 and hsc70 is involved in CHL1-dependent neurite outgrowth, CHL1 deficient hippocampal neurons were transfected either with wildtype CHL1 or with the H1121Q mutant and D1123A mutant. These mutants were deleted in the hsc70 binding site provoking a disruption of the interaction of CHL1 and hsc70. Additionally, the CHL1 construct that is lacking the entire intracellular domain (CHL1 Δ ICD) was transfected as a negative control for the CHL1-dependent neurite outgrowth. Neurons were cultured on coverslips which were coated with the anti CHL1 IgG fraction as mentioned before and transfected twice. After fixation, cells were not stained for CHL1 expression but were visualized with regard to the co-transfection of EGFP. In Figure 22, a representative image of a neuron transfected with wildtype CHL1 (Figure 22, A/B) and a neuron transfected with CHL1 Δ ICD (Figure 22, C/D) is shown. For this picture, cells were selected which had developed extensive neurites. Nevertheless, the measurement of neurite length indicated no significant differences of CHL1-dependent neurite outgrowth comparing wildtype CHL1 transfected and mutant CHL1 (Δ ICD) transfected cells. No differences in neurite outgrowth were also observed after stimulation of cells which were transfected with CHL1 mutants deleted in the hsc70 binding site (images not shown). The summary of the results obtained from the neurite outgrowth stimulation reveals that in none of the stimulation assays an altered promotion of CHL1-dependent neurite outgrowth was observed. CHL1-dependent stimulation of neurite outgrowth after transfection of CHL1 mutants (Figure 22, C/D) did not show an impaired neuritogenesis when compared to wildtype transfected cells (Figure 22, A/B).

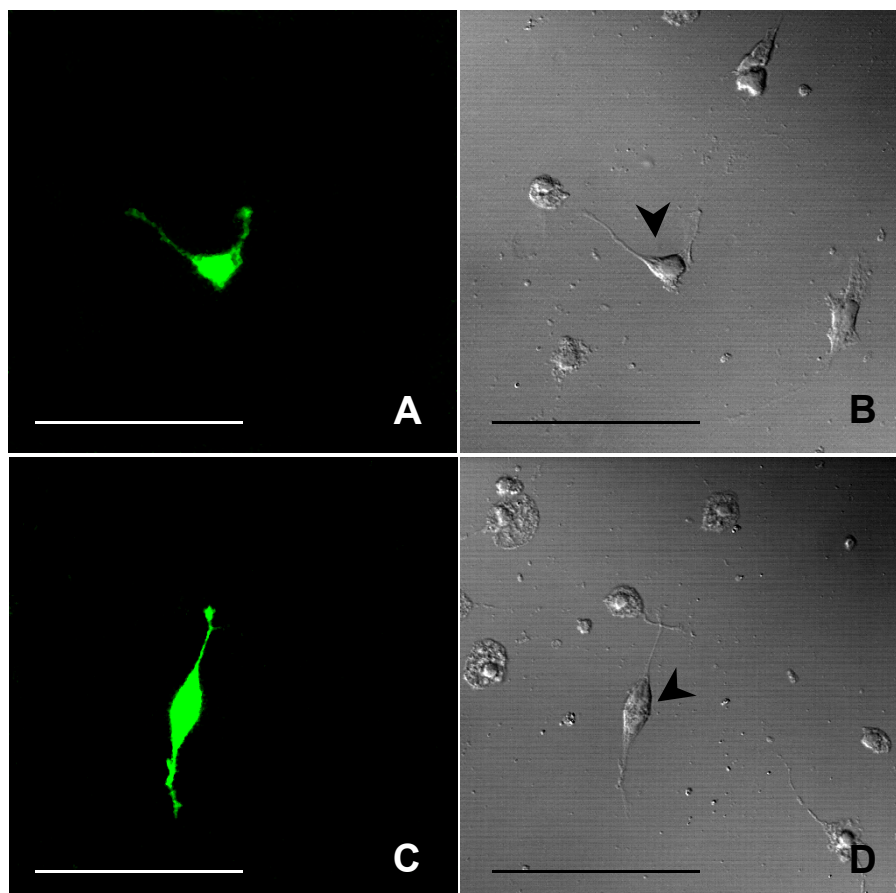


Figure 22: Transfection of primary hippocampal neurons derived from CHL1 $-/-$ mice and subsequent CHL1-dependent stimulation of neurite outgrowth

Primary hippocampal neurons were prepared from CHL1 deficient mice, cultured as described before and transfected twice with either wildtype CHL1 (A/B), CHL1 mutants deleted in the hsc70 binding motif (images not shown) or transfected with the CHL1 mutant that was lacking the entire intracellular domain (C/D). Transfected neurons were visualized by the expression of the enhanced green fluorescence protein to avoid immunocytochemical detection of coated CHL1. Images were analyzed using the Zeiss LSM510 argon-crypton confocal laser-scanning microscope. Scale bars indicate 50 μm .

The analysis of neurite outgrowth following transfection of either wildtype or mutant CHL1 could not confirm the hypothesis that the functional binding between CHL1 and hsc70 is required for the promotion of neuritogenesis in this experimental approach. But, since neurons were observed presenting an unusual morphology after transfection of these particular CHL1-constructs, an involvement of the functional interaction of both proteins in CHL1-dependent neurite outgrowth could not be excluded for the intact animal situation. This experimental

approach emerged to be not the appropriate system for analyzing the influence of a functional interaction between CHL1 – hsc70 on reorganization processes of the cytoskeleton since transfection of CHL1 constructs seemed to affect the vitality and thereby the morphology of the primary hippocampal neurons. In contrast to this, transfection of comparable constructs such as the pcDNA3/NCAM vector did not affect the appearance of primary neurons (Niethammer et al., 2002). After NCAM-transfection, such massive alterations in morphology were not observed as it was seen after transfection of primary neurons using the CHL1 constructs. In addition, an enhanced NCAM-dependent neurite outgrowth has been demonstrated following transfection of these constructs. This suggests that, in principle, the transfection did not affect basic cellular conditions of primary hippocampal neurons. Thus, the biological relevance of the CHL1 – hsc70 interaction remains to be elucidated with regard to a putative involvement in structural reorganization processes of the cytoskeleton followed by CHL1-dependent stimulation of neurite outgrowth in hippocampal neurons.

VI. Discussion

In the present work, a binding analysis of the neuronal cell adhesion molecule CHL1 was carried out in order to isolate an intracellular interaction partner. After separation of a non-detergent soluble fraction of a mouse brain using a two-dimensional gel electrophoresis, a single protein was observed that bound to the soluble intracellular domain of CHL1 (CHL1-ICD_{his6}) in an overlay assay. This particular protein revealed an apparent molecular mass of approximately 70 kDa and a slightly acidic isoelectric point of 5.5. The isolation of the protein from a silver stained gel and the analysis of the protein sequence by MALDI-MS identified this protein as the murine heat shock cognate 70, further abbreviated as hsc70 (GenBankTM accession number M19141) (Giebel et al., 1988).

VI.1. The heat shock cognate 70

The heat shock cognate 70 is a member of a subfamily of heat shock proteins which are induced in their expression by heat shock and other environmental stress. Members of the hsp70 family are subgrouped according to their molecular mass of approximately 70 kDa and they are highly conserved among a diverse number of organisms including bacteria like *Escherichia coli*, insects like *Drosophila melanogaster* as well as mammals. The hsp70 family has been recently reported to be composed of four members (Pelham, 1986), namely the hsp70, a protein that is strictly heat-inducible and that is predominantly localized in the nucleus and only rarely expressed in the cytoplasm of the cell. Furthermore, the hsc70 protein is also heat-inducible but shows high basal levels in the nucleus without cellular stressors. The third family member is the grp78 which is a glucose-regulated protein that has been identified only in secretory cells where it is restricted to the lumen of the ER. Finally, the fourth member of the hsp70 subfamily is the heat shock cognate 70 that was identified in the present work as a binding partner of the cell adhesion molecule CHL1.

The hsc70 protein implicates several functional features providing a variety of interesting opportunities with regard to the function of the CHL1 – hsc70 interaction. Hsc70 is the only heat shock protein of the 70 kDa subfamily that is expressed constitutively with high expression levels in growing cells and only poor expression in resting cell. Following heat

shock, the hsc70 expression is only slightly enhanced when compared to unstressed cells suggesting important functions of hsc70 during normal growth conditions of cells. One general feature of the hsc70 that is shared by other members of the hsp70 subfamily and additionally by other heat shock responding proteins such as hsp90, hsp40, Hip/Hap46, p60/Hop or p23 is the function as a molecular chaperone. Chaperones were originally defined as a group of unrelated proteins that mediate the acquisition of a distinct tertiary structure as well as the protein assembly including the formation of protein complex of either newly synthesized proteins or misfolded substrates. By definition, they are not themselves components of the final functional complex. Chaperone-mediated conformational changes are involved in protein folding as well as in protein translocation and degradation. Furthermore, the conformational alterations can regulate certain signal transduction pathways under normal growth conditions (Hartl, 1996). Studies on the mode of action of an individual chaperone revealed that in many cases, regulatory co-factors and related chaperones are involved indicating that different chaperone systems might cooperate in one folding mechanism. Recent findings emphasized that the substrate-binding of hsc70 is facilitated by the co-factor hsp40 in mammalian cells. The complex formation is regulated by the binding of ATP and the subsequent ATP-hydrolysis including the release of an ortho-phosphate residue from the hsc70 - hsp40 complex. Afterwards, hsp40 is detached and the hsc70 - substrate complex is stabilized by a further co-factor, the Hip/Hap46 protein. Subsequent complex dissociation appears to be initiated by the Hop/p60 protein that stimulates ADP/ATP nucleotide exchange resulting in the recycling of hsc70 and in the release of a folded substrate (Frydman and Höhfeld, 1997). Many of the hsc70 binding co-chaperones possess a so-called J-domain, a scaffold of four α -helices with an accessible loop that exposes the highly conserved HPD tripeptide that is essential for the binding of hsc70. They are termed DnaJ-like proteins according to the bacterial chaperone DnaJ that was originally identified as a J-domain-containing molecular chaperone. Others include structurally related tetratricopeptide repeats (TPR) which are involved in chaperone binding (Frydman and Höhfeld, 1997). Molecular chaperones occur ubiquitously and many of them are classified as stress proteins although some of them, as mentioned before for the hsc70, have essential functions under normal growing conditions.

Besides the function as a molecular chaperone, hsc70 is described to be involved in certain interactions with cytoskeletal structures. Both direct binding to microtubuli (Green and Liem,

1989) has been demonstrated for hsc70 and an indirect binding implicating an interaction of hsc70 with stathmin, a microtubuli (MT)-associated protein that is involved in the regulation of MT assembly (Manceau et al., 1999). Interestingly, the expression of stathmin was previously described to be growth-dependent emphasizing a possible function of the hsc70 – stathmin interaction during development (Balogh et al., 1996). Furthermore, a direct interaction between hsc70 and the intermediate filament protein vimentin was observed which was restricted to the Triton-insoluble fraction in diverse mammalian cell types (Napolitano et al., 1985). Finally, in procaryotic cells, hsc70 was identified as a component of an actin-related protein preparation that also contained alpha-actinin and spectrin (Guerrero-Barrera et al., 1999).

The subcellular localization of hsc70 to neuronal and non-neuronal vesicles and a synaptic localization of hsc70 in the nervous system provide novel insights in the function of the heat shock cognate. The analysis of the uncoating process of clathrin-coated vesicles (CVs) from various mammalian tissues revealed that the 70 kDa uncoating ATPase (UA) was identical to the hsc70 protein (Paddenberg et al., 1990). Further investigations confirmed the formation of a complex which includes clathrin and the UA/hsc70 with a binding stoichiometry of one molecule hsc70 per molecule of free clathrin (Prasad et al., 1994). The functional role of the UA/hsc70 in receptor-mediated endocytosis was addressed by an antibody raised against the putative clathrin-binding site that blocked the hsc70-mediated release of clathrin from isolated CVs. It was shown that the antibody interfered with the endocytosis of the ligand-receptor complex indicating that hsc70 is essential for the normal receptor-mediated endocytosis and that the heat shock cognate is presumably involved in the uncoating of CVs preceding their fusion with endosomes (Honing et al., 1994). Synaptic localization of hsc70 was investigated previously showing that hsc70 is a component of a rat brain synaptic junctional protein preparation (Langnaese et al., 1996). The presence of the heat shock cognate was immunohistochemically demonstrated in postsynaptic structures of rat brains (Suzuki et al., 1999) while a presynaptic localization of hsc70 has been confirmed by other studies (Bechtold et al., 2000). More recently, a functional role of hsc70 in the presynaptic release of neurotransmitter was investigated. In the presynapse, hsc70 does not function by itself but requires assistance from co-factors as mentioned before regarding chaperone functions. Hsc70 complexes with a further DnaJ-like protein that is localized in the presynapse, the cysteine-string protein (CSP), while other hsps like hsp60 or hsp90 do not interact with CSP (Stahl et

al., 1999). CSPs are evolutionarily conserved proteins which are associated with synaptic vesicles and other secretory organelles and which are implicated in the regulation of exocytosis. Furthermore, CSPs are proposed to be involved in the modulation of presynaptic calcium channel activity. They may act as molecular chaperones in association with hsc70 to direct the assembly or dissociation of multiprotein complexes at the calcium channel and thereby mediate the activity of presynaptic calcium channels (Seagar et al., 1999). A novel synapse-specific chaperone complex which is composed of the cysteine string protein, the heat shock cognate70 and a small glutamine-rich tetratricopeptide repeat (TPR)-containing protein (SGT) was recently identified. Alterations in the composition of the trimeric complex inhibit neurotransmitter release suggesting that the CSP/hsc70/SGT complex is important for the maintenance of a functional synapse (Tobaben et al., 2001).

Further insights in the functional role of hsc70 during nervous system development are revealed by the analysis of the expression pattern of hsc70 during neuronal differentiation. In very early studies, the F9 teratocarcinoma cell line was used as a model for murine development. It was clearly demonstrated that a down-regulation of hsc70 during F9 differentiation occurs at the transcriptional level. RNA and protein analyses of murine brains and of 14-day old embryos further suggest that hsc70 is very actively transcribed during early mouse embryogenesis whereas at later developmental stages a down-regulation of hsc70 RNA and protein levels was observed (Giebel et al., 1988). A more recent publication considered the distribution of hsc70 in the developing mouse brain between E9.5 and E17.5 demonstrating a specific spatial and temporal distribution pattern of hsc70 during embryonic mouse brain development (Loones et al., 2000). Interestingly, only hsc70 is expressed at significant levels in specific brain regions at early stages of the development (E9.5) whereas hsp70, hsp90 α or hsp25 were not detectable suggesting the importance of hsc70 during early neuronal development that was also shown in previous studies. The expression of hsc70 was observed in regions where the migration of longitudinal tracts appeared and at later developmental stages an enrichment of hsc70 expression was seen in descending and longitudinal fasciculi. These results indicated that hsc70 might be involved in the remodeling processes of cells during migration, adhesion or differentiation of the developing tissues. The extensive architectural alterations lead to structural reorganizations of the cytoskeleton in particular during migration processes. Since hsc70 has been shown to bind to cytoskeletal

elements, it was suggested that the heat shock cognate may regulate those filamentous reorganizations during early mouse brain development.

As mentioned before, the conformational alterations of substrate proteins generated by hsc70 can regulate signal transduction pathways. The involvement of hsc70 in certain signalling cascades was intensively investigated regarding the interaction of hsc70 with the anti-apoptotic protein Bag-1 (Takayama et al., 1997). It was shown that the formation of the hsc70/Bag-1 complex can regulate the activity of raf-1 by competitive binding of this serine/threonine kinase and subsequently the activity of the downstream extracellular signal-regulated kinases erk1 and erk2 is affected (Song et al., 2001). The hsc70 binding protein Bag-1 was also described to interact with the adaptor protein 14-3-3 that modulates signalling events between components of different pathways (Fountoulakis et al., 1999). Disruption of the 14-3-3 function revealed an impaired activation of the erk kinases but increases basal activation levels of the JNK1 kinase and the stress kinase p38 (Xing et al., 2000) suggesting a further signalling pathway that might be influenced by hsc70 in cooperation with Bag-1 and 14-3-3.

VI.2. Characterization of the CHL1 – hsc70 interaction

The identification of hsc70 as a binding partner of the neuronal cell adhesion molecule CHL1 was not expectable and not even reasonable since functional interactions between cell recognition molecules and heat shock proteins were not described before. Furthermore, the interaction between a cell adhesion molecule that is developmentally expressed during mouse brain development starting at rather late embryonic stages and a protein that is expressed in response to heat shock and other cellular stress was not obviously supposable. But, regarding the functional features of the heat shock cognate presented above, a putative interaction between these proteins became likely and interesting since hsc70 was identified as a constitutively expressed heat shock protein that showed an elevated expression level during early neuronal embryogenesis indicating an involvement of the heat shock cognate in developmental processes.

The specificity of the CHL1-binding to the heat shock cognate 70 was checked using the intracellular domains of L1 and NCAM180 as negative controls in the overlay binding assay.

Furthermore, the co-immunoprecipitation of hsc70 was additionally carried out by the use of a polyclonal anti L1 antiserum. Neither using L1-ICD nor using the intracellular domain of NCAM180 in the overlay assay and also not after immunoprecipitation of L1, an interaction with hsc70 was observed. A sequence analysis of CHL1 revealed the presence of the HPD tripeptide that is a highly conserved motif exposed in the J-domain of molecular chaperones within the intracellular portion of CHL1. This putative binding motif was identified to be the essential structure for the binding of CHL1 to hsc70 using a site-directed mutagenesis that led to a single amino acid exchange of the histidine or the aspartate residue. Deletion of only one amino acid in the HPD tripeptide resulted in a complete loss of hsc70 binding by mutant CHL1. An alignment of the intracellular domains of several L1-related molecules showed that the HPD binding motif is exclusively present in the sequence of CHL1 and not in the sequences of L1, NrCAM, NgCAM, neurofascin, neuroglian or the zebrafish L1-homologues L1.1 and L1.2 (Holm et al., 1996) suggesting that the interaction between a neuronal cell adhesion molecule and the heat shock cognate is an exclusive property of CHL1. Furthermore, the interaction of CHL1 and hsc70 was identified to be strictly ADP-dependent since no co-immunoprecipitation of hsc70 and CHL1 was observed in the presence of ATP but in the presence of ADP. Hsc70 includes an ATPase function and binding of either ADP or ATP was previously described as a functional feature of hsc70 for the recruitment of substrates or further co-chaperones that can influence the binding properties of the heat shock cognate.

Although the conditions prevailing during the binding assay that was used for the isolation of the CHL1 binding protein were rather denaturing, a strong and direct binding between CHL1 and hsc70 was observed in this approach. Interestingly, the direct binding under native conditions using recombinant fusion proteins failed to confirm the CHL1 – hsc70 association whereas the co-localization of both proteins that was observed in a distinct distribution pattern in hippocampal neurons was presumed as an indication for the binding between these proteins. The interaction was confirmed in an alternative binding approach using a co-precipitation of CHL1 and hsc70 from a crude cell lysates. Finally, the interaction of CHL1 and hsc70 was shown to be restricted to a distinct detergent-insoluble membrane subdomain that was assumingly a so-called raft fraction. Taking these results together, a specific conformation of CHL1 was proposed to be required for the binding to hsc70 that was mimicked by the denaturing conditions prevailing during the electrophoretic separation.

Interestingly, such a particular binding assay was used to verify the interaction of hsc70 with another binding partner indicating that the electrophoretic separation under denaturing conditions did not interfere with the binding properties of hsc70. The interaction between hsc70 and the anti-apoptotic protein Bag-1 was also revealed by this approach using ligand blotting of hsc70 and subsequent incubation of purified Bag-1 as a soluble probe (Höhfeld, 1998). The ELISA binding assay that was carried out in the present study to confirm the interaction of hsc70 and CHL1 also supported the assumption that the conformational status of the interaction partners might be a crucial factor for the binding. Recombinant Bag-1 and hsc70 were applied as a positive control. An interaction between these known binding partners was only seen when hsc70 was immobilized and Bag-1 was incubated as a soluble protein, whereas after immobilization of Bag-1 and subsequent incubation of soluble hsc70, no interaction was detectable. This result suggests that on one hand a distinct three-dimensional conformation of Bag-1 is an important prerequisite for the binding of hsc70 that is altered after the immobilization to the plastic surface (personal communication, Dr. U. Hartl, Munich). On the other hand, the immobilization of hsc70 also modifies the conformation of the protein without disturbing the binding to Bag-1 indicating that the immobilization even may contribute to a specific conformation of hsc70 that first provides the binding as it was previously seen in the overlay approach. In the cellular environment, this specific conformation of hsc70 is thought to be generated and also regulated by assisting proteins which may be co-chaperones of the hsc70. This presumption is supported by the immunocytochemical detection of hsc70 in primary hippocampal neurons revealing a distinct distribution pattern of the cytoplasmic protein in cellular subdomains. The co-localization of hsc70 and CHL1 was also detectable in specific areas indicating that the binding might be facilitated only in those distinct subdomains. The distribution analysis of hsc70 and CHL1 in membrane subfractions separated from an enriched synaptosomal preparation further supported the assumption that the binding of hsc70 and CHL1 may occur only in restricted subdomains since both proteins showed an overlapping distribution pattern in all subfractions which were analyzed. Finally, a co-immunoprecipitation of hsc70 and CHL1 that was exclusively observed in crude membranes as well as in the detergent-insoluble fraction of brain membranes confirmed the observation that the interaction of hsc70 and CHL1 is restricted to cellular subcompartment. The localization of the CHL1 – hsc70 interaction to subdomains may indicate that further proteins assist the interaction since in the non-detergent

soluble as well as in the Triton-soluble fraction both binding partners were present but no interaction was detectable, whereas in the detergent-insoluble fraction the expression of CHL1 was lower when compared to the soluble fractions but the co-precipitation was remarkably pronounced. An identification of such assisting proteins would be of outstanding interest for the further understanding by which mechanisms a complex formation containing hsc70 can promote and/or regulate the *in vivo* binding of CHL1 and hsc70.

Palmitoylation of serine residues that can influence the translocation of a fluid membrane protein to rafts (Kabouridis et al., 1997; Zhang et al., 1998) was addressed to be involved in the localization of CHL1 in cellular subdomains. A serine residue is not present in the intracellular domain of CHL1 but is localized immediately beyond the cytoplasmic part at position three within the transmembrane portion. This particular serine residue was affected by a site-directed mutagenesis. A decreased translocation of CHL1 to the detergent insoluble fraction was assumed that may reduce the facilitation of the CHL1 – hsc70 interaction since decreased levels of CHL1 should be present in the Triton X-insoluble fraction. Although CHL1 was only weakly detectable in the detergent insoluble fraction of CHO cell lysates and co-immunoprecipitations of CHL1 and hsc70 were performed using a Triton X-100 soluble fraction, the effect of the serine residue exchange was revealed indicated by a slightly reduced co-precipitation of hsc70. A decrease in the co-precipitation of hsc70 and the mutant affecting palmitoylation was seen in CHO cells as well as in N2A cells. In both cellular systems, the co-precipitation was carried out using either a detergent soluble or a crude lysate indicating that the localization of the binding partners to detergent insoluble subdomains is no prerequisite for the interaction of CHL1 and hsc70 in those particular cells. Nevertheless, the effect of the serine mutation that presumably reduces the translocation of CHL1 to rafts suggest that the interaction is also facilitated by a localization of CHL1 in the detergent insoluble fraction.

The conformation of the binding partners and thereby the translocation of both proteins to cellular subdomains obviously is a crucial factor for the facilitation of the CHL1 – hsc70 interaction. In addition to this, the immunocytochemical analysis of hippocampal cells demonstrated that the interaction between CHL1 and hsc70 depends on the developmental stage of the cells since a co-localization of CHL1 and hsc70 in distinct areas was only observed in hippocampal neurons derived from 4-day old animals and after culturing for three days, whereas in cells prepared from newborn animals cultured for only one day, co-

localization was only seen after co-capping of CHL1. This assumption was further investigated by biochemical analysis performing a co-immunoprecipitation of CHL1 and hsc70 from membrane fractions which were derived from either 5-day old or 3-weeks old mice. It was shown that the co-precipitation using crude membranes was much more pronounced in older animals when compared to younger animals although the expression levels of CHL1 were remarkably higher in the 5-day old mice. The crude membranes were further separated in detergent-soluble and insoluble fractions and the subsequent immunoprecipitation of CHL1 revealed a co-precipitation of hsc70 only in the detergent-insoluble fraction that was prepared from 3-weeks old animals. The co-immunoprecipitation using membrane fractions derived from animals of different ages confirmed the assumption that not only the conformation of the binding partners but also the developmental stage of the animals facilitate the interaction of CHL1 and hsc70. As mentioned before, hsc70 shows an elevated expression during early neuronal development, whereas CHL1 becomes weakly detectable at embryonic day 13 and shows the highest expression levels at rather late developmental stages from embryonic day 18 to postnatal day 7 (Hillenbrand et al., 1999). Furthermore, the biochemical analysis of the CHL1 – hsc70 binding that was carried out with regard to the age of the animals indicated that the interaction between both proteins was more pronounced in older animals than in 5-day old animals. Taken these observations together, a hsc70 function during early developmental stages in mice without an involvement of CHL1 is assumed whereas a functional interaction of CHL1 and hsc70 is facilitated at later developmental stages including the postnatal development in up to 3-weeks old animals and probably also in adults. Thereby, a possible function of the CHL1 – hsc70 interaction is proposed suggesting that the binding of both proteins at later developmental stages may confers stability and/or maintainance of cellular structures to neurons whereas during early development of the mouse brain, hsc70 is probably more involved in alterations of structural elements including conformational changes of cytoskeletal components.

VI.3. Functional analysis of the CHL1 - hsc70 interaction

Regarding the chaperone function that is implicated by hsc70, a functional analysis of the CHL1 – hsc70 interaction was carried out that addressed morphological and structural

reorganization processes of the cytoskeleton following CHL1-dependent neurite outgrowth. Primary hippocampal neurons derived from CHL1-deficient mice were transfected with either wildtype CHL1 or with CHL1 mutants which were deleted in the hsc70 binding site and neurite outgrowth of transfected cells was stimulated using the anti CHL1 antibody. Although no significant differences in CHL1-dependent neurite outgrowth after transfection of either wildtype or mutant CHL1 were observed in this cellular system, a participation of the interaction between CHL1 and hsc70 in structural alterations of the cytoskeleton can not be excluded. The experimental approach used in this work, namely the transfection of primary neurons using certain CHL1 constructs followed by CHL1-dependent neurite outgrowth, emerged to be a harmful stressor of the transfected neurons. Transfection of CHL1 constructs resulted in massive morphological changes of the cells including a round appearance and the lack of extended neurites that makes a functional analysis of the CHL1 – hsc70 interaction with regard to structural reorganization processes of the cytoskeleton impossible. The question whether the CHL1 – hsc70 interaction is involved in alterations of structure and composition of cytoskeletal elements is still open since this approach could not elucidate the requirement of a functional binding between CHL1 and hsc70 for the promotion of CHL1-dependent neurite outgrowth in primary hippocampal neurons.

As mentioned before, a putative role of the CHL1 – hsc70 interaction was assumed according to the observation that the interaction of both proteins is more facilitated with later developmental stages of the animals and that the localization of the binding is the more pronounced in detergent-insoluble cellular subdomains the older the animals are. Due to this results a functional role of the CHL1 – hsc70 binding was proposed that emphasized an involvement of the interaction in generating stability of intracellular structures. Further evidence that the maintenance of a neuron might be supported by the intracellular interaction of the transmembrane CHL1 with cytoskeletal elements mediated by the heat shock cognate 70 was provided since the interaction between L1 and the 440-kDa-isoform of ankyrinB (ankB) implicates such a function. L1 and ankB are co-localized in premyelinated axon tracts of the developing nervous system, a concomitant down-regulation of both proteins is revealed after myelination and ankB knock-out mice have reduced L1 expression levels in premyelinated axons of long fiber tracts. A functional importance of L1 and ankyrinB in these particular structures is strongly supposed. In fact, analysis of the ankB deficient mice revealed that the optic nerve fibers become dilated and degenerate by day 20 suggesting that the

ankyrinB – L1 interaction is essential for the maintenance of premyelinated axons in vivo (Scotland et al., 1998). Unfortunately, the hsc70 knock-out mouse is not available so far such that an involvement of the CHL1 – hsc70 interaction to the maintenance of cellular structures or the degradation of particular neurons is not accessible.

The overlapping distribution pattern of CHL1 and hsc70 in membrane subfractions which were derived from an enriched synaptosomal preparation provide further evidence for a putative functional role of the CHL1 – hsc70 interaction in synapses. In 7-day old animals and in adults, both proteins were present in a so-called raft fraction that was separated from the detergent-insoluble subfraction of synaptosomal membranes. Only in younger animals, a raft localization was identified that solely implicated further interactions to extracellular matrix and/or cytoskeletal structures whereas in adults CHL1 and hsc70 were detectable in rafts with but also without such interactions. Thereby, different functions were suggested for CHL1 and hsc70 in synapses according to the age of the animal. In younger animals, a linkage to structural elements like ECM proteins or cytoskeleton components was more pronounced for CHL1 and hsc70 whereas in adults both proteins implicate a further function that did not involve the interactions with such structural elements. The contribution of hsc70 to presynaptic complexes which are modulatory involved in the neurotransmitter release and the recycling of synaptic vesicles indicates that the interaction between CHL1 and hsc70 may participate in the generation or maintenance of a functional synapse.

VII. Summary

In the present study, a binding analysis of the neural cell adhesion molecule CHL1 (close homologue of L1) was carried out in order to isolate putative interaction partners of this recently described new member of the L1-related subfamily. An identification of an extracellular or intracellular receptor of CHL1 would provide novel insights in CHL1-mediated cell-cell contacts or in CHL1-dependent intracellular signalling mechanisms.

The extracellular and intracellular domains of CHL1 were subjected as recombinant fusion proteins to several biochemical binding studies. A single protein of the non-detergent soluble fraction of a mouse brain was observed to bind to soluble CHL1-ICD_{his6} in an overlay approach. This protein revealed a molecular mass of 70 kDa and an isoelectric point of 5.5. The putative binding partner of CHL1 was identified as the murine heat shock cognate 70 using MALDI-MS.

Co-immunoprecipitation of CHL1 and hsc70, ELISA binding assay and BIAcore™ SPR analysis failed to confirm the interaction of CHL1 and hsc70 under native conditions. However, localization studies of the putative binding partners in primary hippocampal neurons showed a distinct cellular co-distribution pattern of CHL1 and hsc70 indicating a facilitated interaction in membrane subdomains. In such domains, a specific conformational stage of the putative binding partners was assumed mediated by further assistant proteins and that has been mimicked under the prevailing conditions of the overlay approach. The co-localization in such subdomains was more pronounced in cells prepared from older animals than from newborn animals. This suggests that the developmental stage of the animal influences the localization of CHL1 and hsc70 to cellular subdomains and thereby the facilitation of the binding between CHL1 and hsc70.

CHL1 and hsc70 showed an overlapping distribution pattern in detergent-insoluble subfractions of enriched synaptosomal membranes. Taking all these observations into account, it was finally possible to co-precipitate CHL1 and hsc70 using crude fractions of a brain homogenate. Furthermore, hsc70 co-precipitated only in the presence of the co-factor ADP, but not in the presence of ATP. A precipitation of CHL1 using crude fractions from 5-day old mice and 3-weeks old mice demonstrated that the co-precipitation of hsc70 was more

pronounced in older animals and that the interaction was more translocated in a detergent-insoluble fraction in 3-weeks old mice.

Taking these results together, an ADP dependent interaction of CHL1 and hsc70 was identified that was localized in cellular subdomains where the interaction was assumingly facilitated by a specific conformational stage of the binding partner. The translocation of the CHL1 – hsc70 binding in detergent-insoluble fractions was further dependent on the developmental stage of the animals.

A putative binding site of hsc70 within the intracellular domain of CHL1 was identified, namely a HPD tripeptide that was originally described to be a hsc70 binding motif exposed in the J-domain of bacterial chaperones. Using a site-directed mutagenesis resulting in an amino acid exchange of either the histidine or the aspartate residue, it was demonstrated that the HPD tripeptide is essential for the binding of hsc70.

An involvement of the CHL1 – hsc70 interaction in structural alterations of the cytoskeleton was considered by CHL1-dependent neuritogenesis of primary hippocampal neurons of CHL1 $-/-$ mice stimulated after transfection with either wildtype or mutant CHL1. Evidence that the functional binding of CHL1 and hsc70 affects structural reorganization processes of the cytoskeleton during neuritogenesis could not be excluded since transfection of primary hippocampal neurons dramatically altered the morphology and vitality of the neurons. Thus, it was not possible to analyze the functional role of the CHL1 – hsc70 interaction.

This study could demonstrate for the first time a specific interaction between a cell adhesion molecule and a heat shock protein via the HPD tripeptide that is localized within the intracellular domain of CHL1. The interaction was characterized to be dependent on ADP as a co-factor for the binding. The binding was restricted to cellular subdomains and the localization was temporally dependent on the developmental stage of the animal. An involvement of the CHL1 – hsc70 in structural alterations of the cytoskeletal could not be excluded providing further opportunities for the investigation of the functional role of this interesting interaction between CHL1 and hsc70.

VII Zusammenfassung

In der vorliegenden Arbeit wurden Bindungsanalysen des neuronalen Zelladhäsionsmoleküls CHL1 (*close homologue of L1*) durchgeführt, die Interaktionspartner dieses kürzlich beschriebenen neuen Mitgliedes der L1-verwandten Unterfamilie isolieren sollten. Eine Identifizierung extra- oder intrazellulärer Rezeptoren von CHL1 könnte neue Einsichten in CHL1-vermittelte Zell-Zell-Kontakte oder in CHL1-abhängige intrazelluläre Signalkaskaden liefern.

Die extra- und intrazellulären Domänen von CHL1 wurden als rekombinante Fusionsproteine in verschiedene biochemische Interaktionsanalysen eingesetzt. Ein einzelnes Protein, das an die lösliche intrazelluläre Domäne von CHL1 in einem *overlay* Ansatz gebunden hat, konnte in der detergenten-freien löslichen Fraktion eines Maushirns nachgewiesen werden. Dieses Protein wies ein Molekulargewicht von 70 kDa und einen Isoelektrischen Punkt von 5.5 auf. Der mögliche Bindungspartner von CHL1 wurde mittels MALDI-MS als murines Hitzeschockprotein hsc70 identifiziert.

Ko-Immunpräzipitation von CHL1 und hsc70, ELISA Bindungsansatz und BIAcore™ SPR Analyse konnten die Interaktion von CHL1 und hsc70 unter nativen Bedingungen nicht bestätigen. Die immunzytochemische Lokalisation der beiden möglichen Bindungspartner in primären Hippokampus-Neuronen zeigte jedoch eine charakteristische distinkte Ko-Verteilung, die auf eine verstärkte Interaktion in membranösen Subdomänen hinweist. In solchen Domänen wurde eine bestimmte Konformation der Bindungspartner vorausgesetzt, die durch assistierende Proteine generiert werden kann und die durch die im *overlay* vorherrschenden Bedingungen kopiert wurde. Die Ko-Lokalisation in Subdomänen zeigte sich stärker in Zellen, die von älteren Tieren präpariert wurden als in Zellen von neugeborenen Tieren. Daraus lässt sich ableiten, dass der Entwicklungsstand des Tieres die Lokalisation der CHL1 – hsc70 Interaktion beeinflusst und damit auch die Interaktion fördert. CHL1 und hsc70 zeigten eine übereinstimmende Verteilung in detergenten-unlöslichen Subfraktionen angereicherter synaptosomaler Membranen. Unter Berücksichtigung aller vorherigen Beobachtungen war es schließlich möglich, CHL1 mit hsc70 aus einem kruden Homogenat zu präzipitieren. Hsc70 ko-präzipitierte allerdings nur, wenn ADP als Ko-Faktor der Bindung anwesend war, aber nicht in der Gegenwart von ATP. Eine Präzipitation aus kruden Homogenaten 5-Tage alter und 3-Wochen alter Mäuse zeigte, dass die Interaktion in

alten Tieren verstärkt war und die Präzipitation aus der detergenten-unlöslichen Fraktion nur bei 3-Wochen alten Tieren möglich war.

Zusammengefasst zeigen diese Ergebnisse eine ADP-abhängige Interaktion von CHL1 und hsc70. Diese konnte auf zelluläre Subdomänen beschränkt werden, in denen die Interaktion möglicherweise durch eine bestimmte Konformation der Bindungspartner erleichtert wurde. Die Translokation der Bindung in detergenten-unlöslichen Fraktionen hängt von dem Entwicklungsstand der Tiere ab.

Ein mögliches Bindungsmotiv für hsc70 in der intrazellulären Domäne von CHL1 konnte identifiziert werden: Ein HPD-Tripeptid, das ursprünglich als hsc70-Bindestelle in der J-Domäne von molekularen Faltungsproteinen beschrieben wurde. Eine gerichtete Mutagenese, die zum Aminosäureaustausch des Histidin- beziehungsweise Aspartatrestes führte, konnte zeigen, dass das HPD-Tripeptid essentiell für die Bindung von hsc70 ist.

Eine Beteiligung der CHL1 – hsc70 Interaktion an strukturellen Veränderungen des Zytoskeletts wurde anhand einer CHL1-abhängigen Stimulation des Neuritenwachstums primärer CHL1 -/- Hippokampus-Neurone untersucht, die entweder mit Wildtyp- oder mit mutiertem CHL1 transfiziert wurden. Hinweise, dass die Bindung von CHL1 und hsc70 an strukturellen Re-Organisationen des Zytoskeletts beteiligt ist, können nicht ausgeschlossen werden. Weil aber die Transfektion die Morphologie und Vitalität der Neurone dramatisch beeinflusste, war eine funktionelle Analyse der CHL1 – hsc70 Interaktion nicht möglich.

In dieser Arbeit konnte zum ersten Mal eine Interaktion zwischen einem Zelladhäsionsmolekül und einem Hitzeschockprotein demonstriert werden, die generiert wird über ein HPD-Tripeptid in der intrazellulären Domäne von CHL1. Diese Interaktion ist abhängig von dem Ko-Faktor ADP. Die Bindung konnte in zellulären Subdomänen lokalisiert werden und die Translokation der Interaktion war zeitlich abhängig vom Entwicklungsstand des Tieres. Eine Beteiligung der CHL1 – hsc70 Bindung an strukturellen Veränderungen des Zytoskeletts konnte nicht ausgeschlossen werden, wodurch sich interessante Möglichkeiten zur weiteren funktionellen Erforschung dieser Interaktion bieten.

VIII. Appendix

VIII.1. Oligonucleotides

	Oligonucleotides	Sequence	Remarks
N°1	CHL1-CT/SacI up	5'-CCC GAG CTC AAG AGG AAC AGA GGT-3'	amplification of intracellular domain
N°2	CHL1-CT/HindIII- dn	5'-CCC AAG CTT TCA TGC CCG GAG TGG-3'	amplification of intracellular domain
N°3	pQE primer „promotor region“	5'-CCC GAA AAG TGC CAC CTG-3'	for sequencing
N°4	L1-ICD/5'-NdeI	5'-GGA ATT CCA TAT GAA ACG CAG CAA GGG TGG-3'	amplification of intracellular domain
N°5	L1-ICD/3'-BamHI	5'-GGG GGA TCC ACT ATT CTA GGG CTA-3'	amplification of intracellular domain
N°6	T7 promotor primer	5'-TAA TAC GAC TCA CTA TAG G- 3'	for sequencing
N°7	T7 promotor primer	5'-TAA TAC GAC TCA CTA TAG G- 3'	amplification of CHL1/5' fragment in pcDNA3
N°8	CHL1 pos2665 Eco-dn	5'-TAA GTG GAA TTC ACT AAA GGG GTC TAG-3'	amplification of CHL1/5' fragment
N°9	CHL1 pos2665 Eco-up	5'-TTT AGT GAA TTC CAC TTA ACA GTC TTA-3'	amplification of CHL1/3' fragment in pcDNA3
N°10	CHL1 Stop Not-dn	5'-TTT GCG GCC GCT TCA TGC CCG GAG TGG GAA GGT-3'	amplification of CHL1/3' fragment
N°11	H1121Q-up	5'-AAG GAA GAT TTA CAA CCA GAT CCA GAA-3'	mutagenesis

VIII. Appendix

N°12	H1121Q-dn	5'-TTC TGG ATC TGG TTG TAA ATC TTC CTT-3'	mutagenesis
N°13	D1123A-up	5'-GAT TTA CAC CCA GCT CCA GAA GTT CAG-3'	mutagenesis
N°14	D1123A-dn	5'-CTG AAC TTC TGG AGC TGG GTG TAA ATC-3'	mutagenesis
N°15	C1102S/new-up	5'-TTG TTA ACT ATT TCC TTT GTG AAG AGG-3'	mutagenesis
N°16	C1102S/new-dn	5'-CCT CTT CAC AAA GGA AAT AGT TAA CAA-3'	mutagenesis
N°17	C1102S/stop-up	5'-TTG TTA ACT ATT TGA TTT GTG AAG AGG-3'	mutagenesis/deletion of intracellular domain
N°18	C1102S/stop-dn	5'-CCT CTT CAC AAA TCA AAT AGT TAA CAA-3'	mutagenesis/deletion of intracellular domain
N°19	CHL1 pos366-up	5'-A ATA GAG TTC ATA GTA CCA GGG GTT-3'	sequencing of full length clone
N°20	CHL1 I (BS)/522	5'-TGA ACA AGA TGA GAG AGT ATA CAT GAG C-3'	sequencing of full length clone
N°21	CHL1 pos976-up	5'-CAG TAG AAG AGC CTC CAG GCT GGA-3'	sequencing of full length clone
N°22	CHL1 II (BS)/1133	5'-GTG ACT TTA TGT TCC CCA GGG-3'	sequencing of full length clone
N°23	CHL1 pos1626-up	5'-CAT TTG AAA CAC AGT TTG AAG TTG-3'	sequencing of full length clone
N°24	CHL1 III (BS)/1823	5'-TCC TTG GTG TTG GAG ATC CGC CAG-3'	sequencing of full length clone
N°25	CHL1 pos2273-up	5'-GAA GAG TGG GAA GAA ATA GTT-3'	sequencing of full length clone
N°26	U-CHL1-3000 (BS)	5'-TCA CTT AAC AGT CTT AGC	sequencing of full

		CTA-3'	length clone
N°27	Sp6 reverse primer (Invitrogen)	5'-TAG TGT CAC CTA-3'	sequencing of full length clone

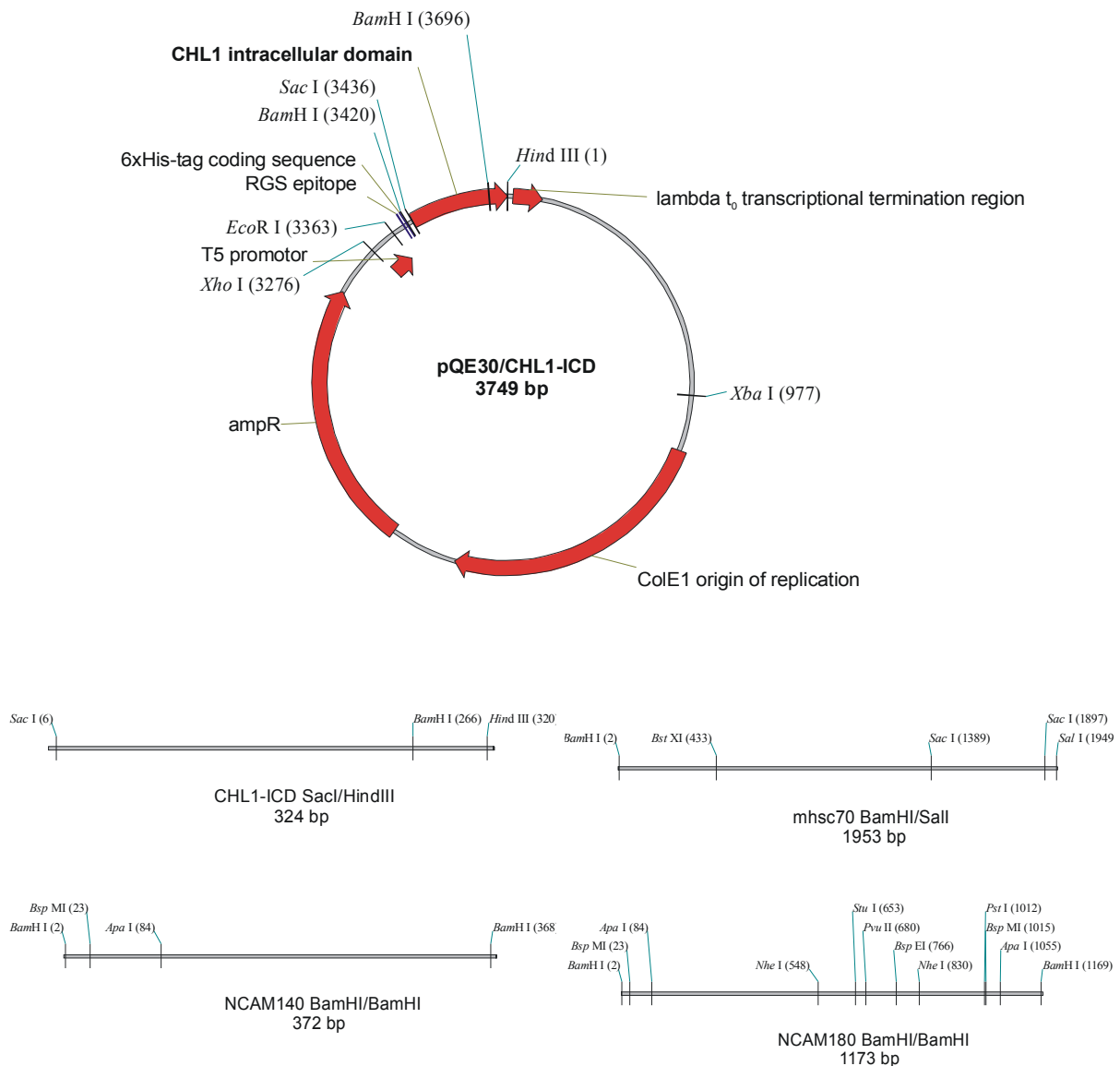
VIII.2. Accessionnumbers

Protein	Organism	Accession N°
CHL1	mouse	X94310
L1	mouse	X12875
NCAM 140	rat	X06564
NCAM 180	rat	not available
hsc 70	mouse	M19141

VIII.3. Plasmids

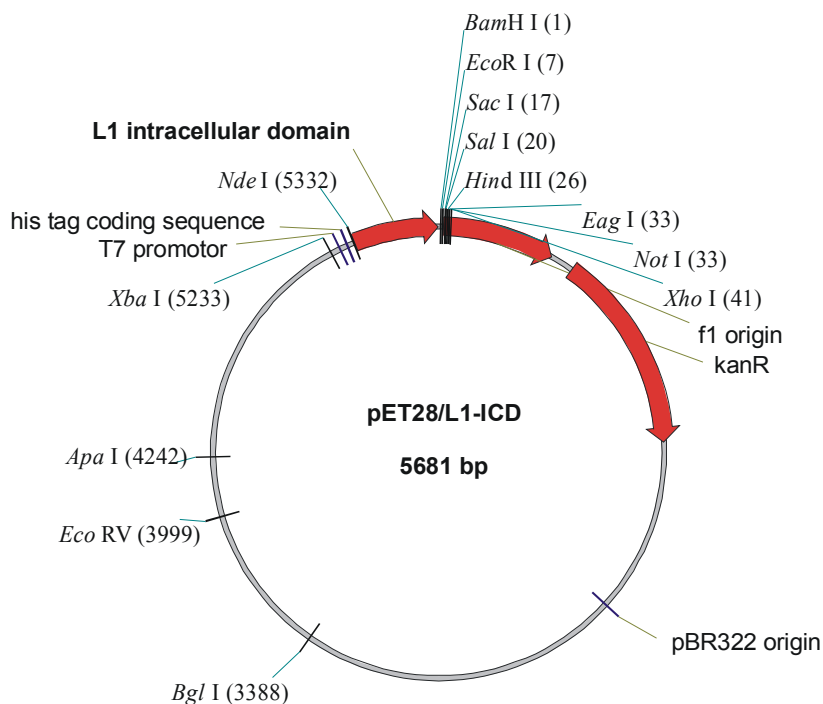
VIII.3.1. pQE30 constructs

The intracellular domain of CHL1 was amplified with primers referring to VIII.1, primers N° 1 and N° 2. Restriction sites were introduced by PCR and CHL1-ICD was ligated to pQE30 after digestion with the appropriate restriction enzymes BamHI/HindIII. Three additional pQE30 constructs were used for production of recombinant proteins which were provided as mentioned before. Inserts used for cloning into pQE30 are figured with terminal restriction sites.



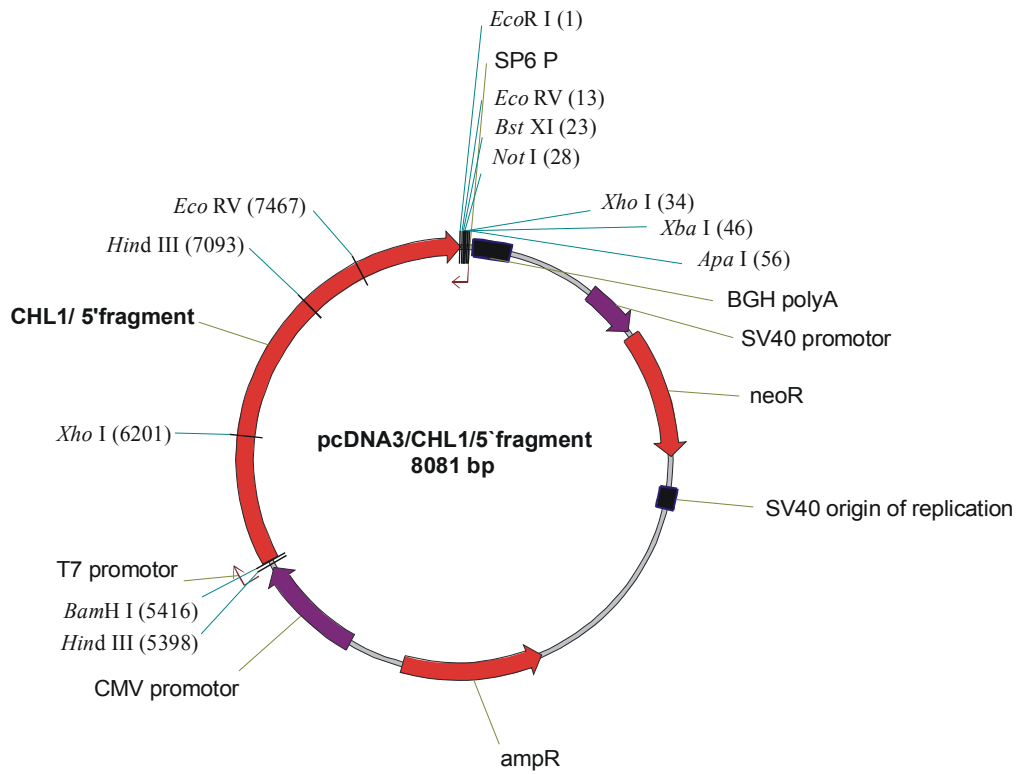
VIII.3.2. pET28 construct

L1 intracellular domain was originally cloned into pQE30, but L1-ICD was unable to be produced in that particular expression system. L1-ICD was thereby sub-cloned into pET28 after amplification and introduction of appropriate restriction sites with regard to pET 28. The target vector was digested with the corresponding restriction enzymes *Nde*I/*Bam*H I and religated with insert DNA.

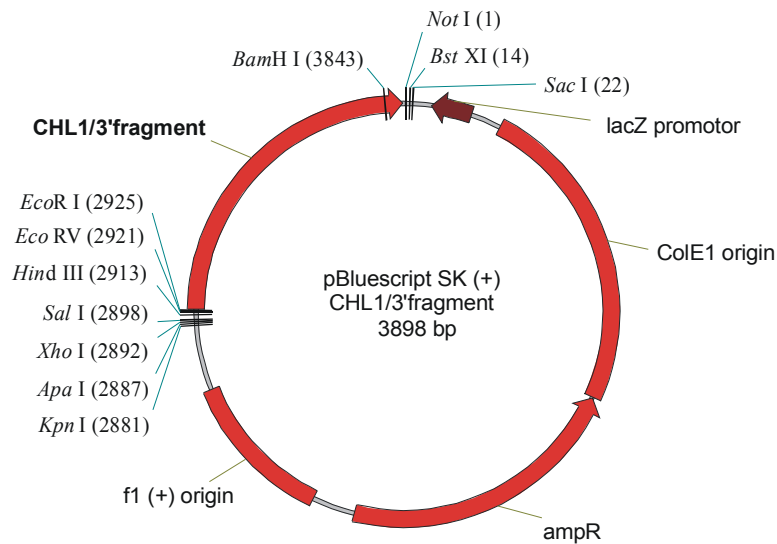


VIII.3.3. Site-directed mutagenesis

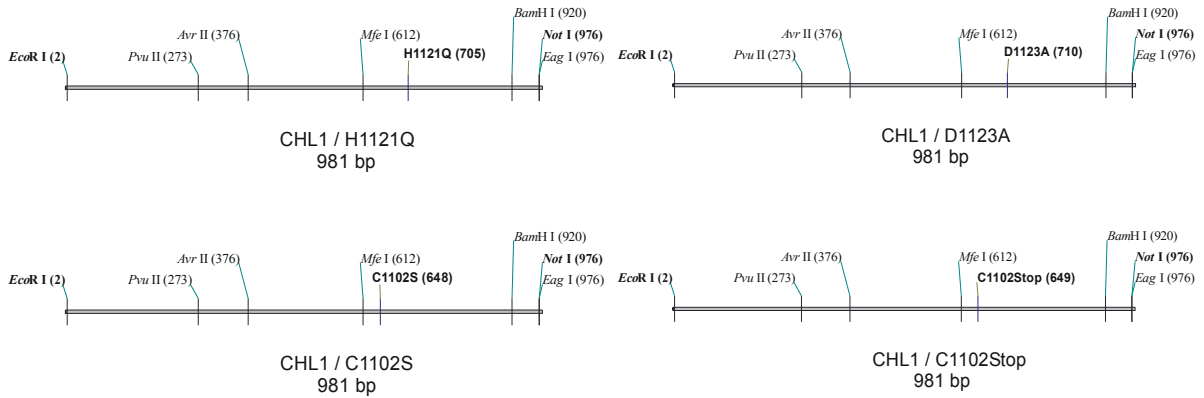
As a template for the site-directed mutagenesis of CHL1, a pcDNA3/full length CHL1 construct provided by Dr. Birthe Schnegelsberg was used. A large 5' end fragment (position 1 – 2660 bp) was amplified by PCR by introduction of a new EcoRI restriction site at position 2659 to 2664. The 5' end fragment was re-cloned in pcDNA3 after BamHI/EcoRI digestion. The 3' end fragment of approximately 1000 bp was re-amplified and subcloned into pBluescript after digestion with EcoRI and NotI. Competent DH5 α were transformed with pcDNA3/CHL1/5' fragment construct, plasmids were amplified and afterwards digested with EcoRI/NotI. The modified vector DNA was stored at -20°C until ligation with mutated CHL1/3' fragment.



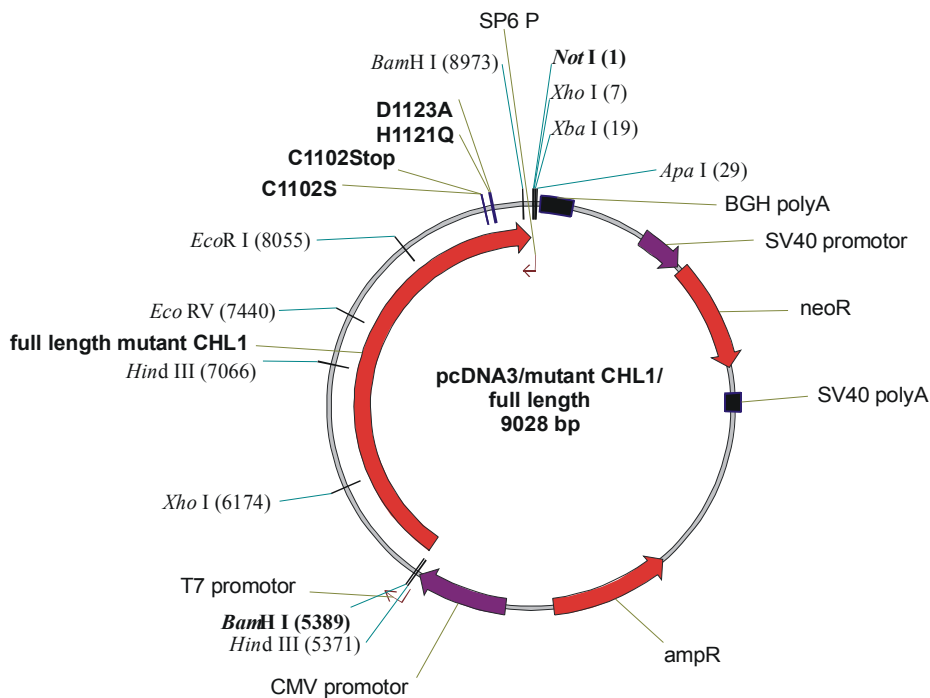
The 3' end fragment of approximately 1000 bp was amplified and subcloned into pBluescript after digestion with *Eco*RI and *Not*I. Competent DH5 α were transformed with the pBluescript construct, plasmids were amplified and purified and used as template for the site-directed mutagenesis.



Four different single amino acids were mutated in the intracellular domain of CHL1 (3x) and once in the transmembrane domain. For introduction of a single base pair mutation, primers were designed for each particular construct as cited in VIII.1 N° 11 – 18.



Inserts were digested with EcoRI/NotI as indicated and re-ligated to the previously digested pcDNA3/CHL1/5' fragment. The resulting construct is presented below after introduction of the mutations as mentioned before:



VIII.4. Abbreviations

μ	micro (10 ⁻⁶)
× g	g-force
°C	grad celsius
aa	amino acid
A	adenine
Acc.	accession number
Amp	ampicillin
APS	ammoniumperoxodisulfate
ADP	adenosine diphosphate
ATP	adenosine triphosphate
BCA	bicinchoninacid disodium salt
bp	base pairs
BSA	bovine serum albumine
C	cytosine
cDNA	complementary deoxyribonucleic acid
CHL1	close homologue of L1
CHO	Chinese Hamster Ovarian
CMV	cytomegalie virus
CTP	cytosine triphosphate
Da	dalton
dATP	2'-desoxyadenosinetriphosphate
dCTP	2'-desoxycytidinetriphosphate
DEPC	diethylpyrocarbonate
dGTP	2'-desoxyguanosinetriphosphate
DMSO	dimethylsulfoxide
DNA	deoxyribonucleic acid
DNase	desoxyribonuclease
dNTP	2'-desoxyribonucleotide-5'-triphosphate
DTT	dithiothreitol

<i>E. coli</i>	Escherichia coli
EDTA	ethylendiamintetraacetic acid
EGFP	enhanced green fluorescent protein
ELISA	enzyme-linked immunosorbent assay
erk 1/2	extracellular regulated kinases 1/2
<i>f.c.</i>	final concentration
FCS	fetal calf serum
g	gram
G	guanosine
h	human, hour
HBSS	Hank's buffered sodium chloride solution
HEPES	2-(4-(2-Hydroxyethyl)-piperzino)-ethansulfonic acid
his6	hexa histidine tag
HPD	histidine-proline-aspartate tripeptide
hsc70	heat shock cognate 70
hsp70	heat shock protein 70
ICD	intracellular domain
IEF	isoelectric focussing
IgG	immunoglobuline subclass G
IPG	immobilized pH gradient
IPTG	isopropyl- β -D-thiogalactoside
Kan	kanamycin
kb	kilo base pairs
l	litre
LB	Luria Bertani
m	milli (10^{-3})
MEM	minimal essential medium
MESNa	2-mercaptoethanesulfonic acid
min	minute
MOPS	(4-(N-morpholino)-propan)-sulfonic acid
mRNA	messenger ribonucleic acid

n	nano (10^{-9})
N2A	mouse neuroblastoma cell line 2A
NCAM	neural cell adhesion molecule
Nt	nucleotide(e)
OD _x	optic density
ORF	open reading frame
PAGE	polyacrylamide gel electrophoresis
PBS	phosphat-buffered saline
PCR	polymerase chain reaction
PEG	polyethylenglycol
PMSF	phenylmethanesulfonylfluoride
rpm	rounds per minute
RGS	arginine-glycine-serine tripeptide
RNA	ribonucleic acid
RNase	ribonuclease
RT	room temperature
s	second
SDS	sodium dodecyl sulfate
SPR	surface plasmon resonance
T	thymine
TABS	(N-tris(Hydroxymethyl)methyl-3-aminopropane-sulfonic acid
TE	tris-EDTA
TEMED	N,N,N',N'-tetraethylenamine
Tet	tetracycline
T _m	melting temperature
Tris	tris(-hydroxymethyl)-aminomethane
U	unit (enzymatic)
V	volt
v/v	volume per volume
Vol.	volume
w/v	weight per volume

IX. Bibliography

1. Amoureux M. C., Cunningham B. A., Edelman G. M., Crossin K. L. (2000) N-CAM binding inhibits the proliferation of hippocampal progenitor cells and promotes their differentiation to a neuronal phenotype. *J Neurosci* 20: 3631-3640.
2. Appel F., Holm J., Conscience J. F., Bohlen und H. F., Faissner A., James P., Schachner M. (1995) Identification of the border between fibronectin type III homologous repeats 2 and 3 of the neural cell adhesion molecule L1 as a neurite outgrowth promoting and signal transducing domain. *J Neurobiol* 28: 297-312.
3. Asai M., Ito Y., Iguchi T., Ito J., Okada N., Oishi H. (1992) Terminal deletion of the short arm of chromosome 3. *Jpn J Hum Genet* 37: 163-168.
4. Ausubel FM (1996) *Current Protocols in Molecular Biology*. New York: Greene Publishing Associates, Inc.
5. Balogh A., ege R. M., Sobel A. (1996) Growth and cell density-dependent expression of stathmin in C2 myoblasts in culture. *Exp Cell Res* 224: 8-15.
6. Bebbington C. R. (1991) Expression of antibody genes in nonlymphoid mammalian cells. *Methods Enzymol* 136-145.
7. Bechtold D. A., Rush S. J., Brown I. R. (2000) Localization of the heat-shock protein Hsp70 to the synapse following hyperthermic stress in the brain. *J Neurochem* 74: 641-646.
8. Beer S., Oleszewski M., Gutwein P., Geiger C., Altevogt P. (1999) Metalloproteinase-mediated release of the ectodomain of L1 adhesion molecule. *J Cell Sci* 112 (Pt 16): 2667-2675.
9. Beggs H. E., Soriano P., Maness P. F. (1994) NCAM-dependent neurite outgrowth is inhibited in neurons from Fyn-minus mice. *J Cell Biol* 127: 825-833.
10. Bieber A. J., Snow P. M., Hortsch M., Patel N. H., Jacobs J. R., Traquina Z. R., Schilling J., Goodman C. S. (1989) Drosophila neuroglian: a member of the immunoglobulin superfamily with extensive homology to the vertebrate neural adhesion molecule L1. *Cell* 59: 447-460.
11. Blaess S., Kammerer R. A., Hall H. (1998) Structural analysis of the sixth immunoglobulin-like domain of mouse neural cell adhesion molecule L1 and its interactions with alpha(v)beta3, alpha(IIb)beta3, and alpha5beta1 integrins. *J Neurochem* 71: 2615-2625.

IX. Bibliography

12. Brackenbury R., Thiery J. P., Rutishauser U., Edelman G. M. (1977) Adhesion among neural cells of the chick embryo. I. An immunological assay for molecules involved in cell-cell binding. *J Biol Chem* 252: 6835-6840.
13. Brewer G. J., Torricelli J. R., Evege E. K., Price P. J. (1993) Optimized survival of hippocampal neurons in B27-supplemented Neurobasal, a new serum-free medium combination. *J Neurosci Res* 35: 567-576.
14. Brümmendorf T., Kenwrick S., Rathjen F. G. (1998) Neural cell recognition molecule L1: from cell biology to human hereditary brain malformations. *Curr Opin Neurobiol* 8: 87-97.
15. Brümmendorf T., Lemmon V. (2001) Immunoglobulin superfamily receptors: cis-interactions, intracellular adapters and alternative splicing regulate adhesion. *Curr Opin Cell Biol* 13: 611-618.
16. Brümmendorf T., Rathjen F. G. (1993) Axonal glycoproteins with immunoglobulin- and fibronectin type III- related domains in vertebrates: structural features, binding activities, and signal transduction. *J Neurochem* 61: 1207-1219.
17. Brümmendorf T., Rathjen F. G. (1996) Structure/function relationships of axon-associated adhesion receptors of the immunoglobulin superfamily. *Curr Opin Neurobiol* 6: 584-593.
18. Brümmendorf T., Wolff J. M., Frank R., Rathjen F. G. (1989) Neural cell recognition molecule F11: homology with fibronectin type III and immunoglobulin type C domains. *Neuron* 2: 1351-1361.
19. Burgoon M. P., Hazan R. B., Phillips G. R., Crossin K. L., Edelman G. M., Cunningham B. A. (1995) Functional analysis of posttranslational cleavage products of the neuron-glia cell adhesion molecule, Ng-CAM. *J Cell Biol* 130: 733-744.
20. Chaisuksunt V., Campbell G., Zhang Y., Schachner M., Lieberman A. R., Anderson P. N. (2000) The cell recognition molecule CHL1 is strongly upregulated by injured and regenerating thalamic neurons. *J Comp Neurol* 425: 382-392.
21. Chamberlain L. H., Burgoyne R. D. (1997a) Activation of the ATPase activity of heat-shock proteins Hsc70/Hsp70 by cysteine-string protein. *Biochem J* 322 (Pt 3): 853-858.
22. Chamberlain L. H., Burgoyne R. D. (1997b) The molecular chaperone function of the secretory vesicle cysteine string proteins. *J Biol Chem* 272: 31420-31426.
23. Chang S., Rathjen F. G., Raper J. A. (1990) Neurite outgrowth promoting activity of G4 and its inhibition by monoclonal antibodies. *J Neurosci Res* 25: 180-186.

IX. Bibliography

24. Cheetham M. E., Jackson A. P., Anderton B. H. (1994) Regulation of 70-kDa heat-shock-protein ATPase activity and substrate binding by human DnaJ-like proteins, HSJ1a and HSJ1b. *Eur J Biochem* 226: 99-107.
25. Chen S., Mantei N., Dong L., Schachner M. (1999) Prevention of neuronal cell death by neural adhesion molecules L1 and CHL1. *J Neurobiol* 38: 428-439.
26. Connelly M. A., Grady R. C., Mushinski J. F., Marcu K. B. (1994) PANG, a gene encoding a neuronal glycoprotein, is ectopically activated by intracisternal A-type particle long terminal repeats in murine plasmacytomas. *Proc Natl Acad Sci U S A* 91: 1337-1341.
27. Cremer H., Chazal G., Goridis C., Represa A. (1997) NCAM is essential for axonal growth and fasciculation in the hippocampus. *Mol Cell Neurosci* 8: 323-335.
28. Crossin K. L., Krushel L. A. (2000) Cellular signaling by neural cell adhesion molecules of the immunoglobulin superfamily. *Dev Dyn* 218: 260-279.
29. Crossin, K. L., Prieto, A. L., and Mauro, V. P. The role of tenascin domains in developmental patterning, cell migration and gene expression. Crossin, K. L. Tenascin and counteradhesive molecules of the extracellular matrix, 23-46. 1-1-1996. Harwood Academic Publishers.
Ref Type: Serial (Book,Monograph)
30. Crossin K. L., Tai M. H., Krushel L. A., Mauro V. P., Edelman G. M. (1997) Glucocorticoid receptor pathways are involved in the inhibition of astrocyte proliferation. *Proc Natl Acad Sci U S A* 94: 2687-2692.
31. Cunningham B. A., Hemperly J. J., Murray B. A., Prediger E. A., Brackenbury R., Edelman G. M. (1987) Neural cell adhesion molecule: structure, immunoglobulin-like domains, cell surface modulation, and alternative RNA splicing. *Science* 236: 799-806.
32. Dahme M., Bartsch U., Martini R., Anliker B., Schachner M., Mantei N. (1997) Disruption of the mouse L1 gene leads to malformations of the nervous system. *Nat Genet* 17: 346-349.
33. Daniloff J. K., Levi G., Grumet M., Rieger F., Edelman G. M. (1986) Altered expression of neuronal cell adhesion molecules induced by nerve injury and repair. *J Cell Biol* 103: 929-945.
34. Davis J. Q., Bennett V. (1994) Ankyrin binding activity shared by the neurofascin/L1/NrCAM family of nervous system cell adhesion molecules. *J Biol Chem* 269: 27163-27166.

IX. Bibliography

35. Doherty P., Ashton S. V., Moore S. E., Walsh F. S. (1991) Morphoregulatory activities of NCAM and N-cadherin can be accounted for by G protein-dependent activation of L- and N-type neuronal Ca²⁺ channels. *Cell* 67: 21-33.
36. Doherty P., Fruns M., Seaton P., Dickson G., Barton C. H., Sears T. A., Walsh F. S. (1990) A threshold effect of the major isoforms of NCAM on neurite outgrowth. *Nature* 343: 464-466.
37. Doherty P., Walsh F. S. (1994) Signal transduction events underlying neurite outgrowth stimulated by cell adhesion molecules. *Curr Opin Neurobiol* 4: 49-55.
38. Doherty P., Walsh F. S. (1996) CAM-FGF Receptor Interactions: A Model for Axonal Growth. *Mol Cell Neurosci* 8: 99-111.
39. Doherty P., Williams E., Walsh F. S. (1995) A soluble chimeric form of the L1 glycoprotein stimulates neurite outgrowth. *Neuron* 14: 57-66.
40. Duczmal A., Schollhammer S., Katich S., Ebeling O., Schwartz-Albiez R., Altevogt P. (1997) The L1 adhesion molecule supports alpha v beta 3-mediated migration of human tumor cells and activated T lymphocytes. *Biochem Biophys Res Commun* 232: 236-239.
41. Dustin M. L., Springer T. A. (1991) Role of lymphocyte adhesion receptors in transient interactions and cell locomotion. *Annu Rev Immunol* 9: 27-66.
42. Ebeling O., Duczmal A., Aigner S., Geiger C., Schollhammer S., Kemshead J. T., Moller P., Schwartz-Albiez R., Altevogt P. (1996) L1 adhesion molecule on human lymphocytes and monocytes: expression and involvement in binding to alpha v beta 3 integrin. *Eur J Immunol* 26: 2508-2516.
43. Edelman G. M. (1993) A golden age for adhesion. *Cell Adhes Commun* 1: 1-7.
44. Edelman G. M., Crossin K. L. (1991) Cell adhesion molecules: implications for a molecular histology. *Annu Rev Biochem* 60: 155-190.
45. Edelman G. M., Cunningham B. A., Gall W. E., Gottlieb P. D., Rutishauser U., Waxdal M. J. (1969) The covalent structure of an entire gammaG immunoglobulin molecule. *Proc Natl Acad Sci U S A* 63: 78-85.
46. Faissner A., Teplow D. B., Kubler D., Keilhauer G., Kinzel V., Schachner M. (1985) Biosynthesis and membrane topography of the neural cell adhesion molecule L1. *EMBO J* 4: 3105-3113.
47. Felding-Habermann B., Silletti S., Mei F., Siu C. H., Yip P. M., Brooks P. C., Cheresch D. A., O'Toole T. E., Ginsberg M. H., Montgomery A. M. (1997) A single immunoglobulin-like domain of the human neural cell adhesion molecule L1 supports adhesion by multiple vascular and platelet integrins. *J Cell Biol* 139: 1567-1581.

48. Fischer D., Brown-Ludi M., Schulthess T., Chiquet-Ehrismann R. (1997) Concerted action of tenascin-C domains in cell adhesion, anti-adhesion and promotion of neurite outgrowth. *J Cell Sci* 110 (Pt 13): 1513-1522.
49. Fischer G., Kunemund V., Schachner M. (1986) Neurite outgrowth patterns in cerebellar microexplant cultures are affected by antibodies to the cell surface glycoprotein L1. *J Neurosci* 6: 605-612.
50. Fountoulakis M., Cairns N., Lubec G. (1999) Increased levels of 14-3-3 gamma and epsilon proteins in brain of patients with Alzheimer's disease and Down syndrome. *J Neural Transm Suppl* 57: 323-335.
51. Fransen E., Lemmon V., Van Camp G., Vits L., Coucke P., Willems P. J. (1995) CRASH syndrome: clinical spectrum of corpus callosum hypoplasia, retardation, adducted thumbs, spastic paraparesis and hydrocephalus due to mutations in one single gene, L1. *Eur J Hum Genet* 3: 273-284.
52. Frei T., Bohlen und H. F., Wille W., Schachner M. (1992) Different extracellular domains of the neural cell adhesion molecule (N- CAM) are involved in different functions. *J Cell Biol* 118: 177-194.
53. Frydman J., Höhfeld J. (1997) Chaperones get in touch: the Hip-Hop connection. *Trends Biochem Sci* 22: 87-92.
54. Furley A. J., Morton S. B., Manalo D., Karageorgos D., Dodd J., Jessell T. M. (1990) The axonal glycoprotein TAG-1 is an immunoglobulin superfamily member with neurite outgrowth-promoting activity. *Cell* 61: 157-170.
55. Fuss B., Wintergerst E. S., Bartsch U., Schachner M. (1993) Molecular characterization and in situ mRNA localization of the neural recognition molecule J1-160/180: a modular structure similar to tenascin. *J Cell Biol* 120: 1237-1249.
56. Garver T. D., Ren Q., Tuvia S., Bennett V. (1997) Tyrosine phosphorylation at a site highly conserved in the L1 family of cell adhesion molecules abolishes ankyrin binding and increases lateral mobility of neurofascin. *J Cell Biol* 137: 703-714.
57. Gennarini G., Cibelli G., Rougon G., Mattei M. G., Goridis C. (1989) The mouse neuronal cell surface protein F3: a phosphatidylinositol- anchored member of the immunoglobulin superfamily related to chicken contactin. *J Cell Biol* 109: 775-788.
58. Giebel L. B., Dworniczak B. P., Bautz E. K. (1988) Developmental regulation of a constitutively expressed mouse mRNA encoding a 72-kDa heat shock-like protein. *Dev Biol* 125: 200-207.
59. Green L. A., Liem R. K. (1989) Beta-internexin is a microtubule-associated protein identical to the 70-kDa heat-shock cognate protein and the clathrin uncoating ATPase. *J Biol Chem* 264: 15210-15215.

IX. Bibliography

60. Green P. J., Walsh F. S., Doherty P. (1996) Promiscuity of fibroblast growth factor receptors. *Bioessays* 18: 639-646.
61. Grumet M., Mauro V., Burgoon M. P., Edelman G. M., Cunningham B. A. (1991) Structure of a new nervous system glycoprotein, Nr-CAM, and its relationship to subgroups of neural cell adhesion molecules. *J Cell Biol* 113: 1399-1412.
62. Guerrero-Barrera A. L., de la G. M., Mondragon R., Garcia-Cuellar C., Segura-Nieto M. (1999) Actin-related proteins in *Actinobacillus pleuropneumoniae* and their interactions with actin-binding proteins. *Microbiology* 145 (Pt 11): 3235-3244.
63. Hall H., Liu L., Schachner M., Schmitz B. (1993) The L2/HNK-1 carbohydrate mediates adhesion of neural cells to laminin. *Eur J Neurosci* 5: 34-42.
64. Hall H., Vorherr T., Schachner M. (1995) Characterization of a 21 amino acid peptide sequence of the laminin G2 domain that is involved in HNK-1 carbohydrate binding and cell adhesion. *Glycobiology* 5: 435-441.
65. Hartl F. U. (1996) Molecular chaperones in cellular protein folding. *Nature* 381: 571-579.
66. Hasler T. H., Rader C., Stoeckli E. T., Zuellig R. A., Sonderegger P. (1993) cDNA cloning, structural features, and eucaryotic expression of human TAG-1/axonin-1. *Eur J Biochem* 211: 329-339.
67. Haspel J., Friedlander D. R., Ivgy-May N., Chickramane S., Roonprapunt C., Chen S., Schachner M., Grumet M. (2000) Critical and optimal Ig domains for promotion of neurite outgrowth by L1/Ng-CAM. *J Neurobiol* 42: 287-302.
68. Hassel B., Rathjen F. G., Volkmer H. (1997) Organization of the neurofascin gene and analysis of developmentally regulated alternative splicing. *J Biol Chem* 272: 28742-28749.
69. Haus U., Trommler P., Fisher P. R., Hartmann H., Lottspeich F., Noegel A. A., Schleicher M. (1993) The heat shock cognate protein from *Dictyostelium* affects actin polymerization through interaction with the actin-binding protein cap32/34. *EMBO J* 12: 3763-3771.
70. Hawley-Nelson P., Ciccarone V., Gebeyehu G., Jesse J., Felger P. (1993) *FOCUS* 15: 78.
71. Hemperly J. J., Edelman G. M., Cunningham B. A. (1986) cDNA clones of the neural cell adhesion molecule (N-CAM) lacking a membrane-spanning region consistent with evidence for membrane attachment via a phosphatidylinositol intermediate. *Proc Natl Acad Sci U S A* 83: 9822-9826.
72. Hennessy F., Cheetham M. E., Dirr H. W., Blatch G. L. (2000) Analysis of the levels of conservation of the J domain among the various types of DnaJ-like proteins. *Cell Stress Chaperones* 5: 347-358.

73. Hillenbrand R., Molthagen M., Montag D., Schachner M. (1999) The close homologue of the neural adhesion molecule L1 (CHL1): patterns of expression and promotion of neurite outgrowth by heterophilic interactions. *Eur J Neurosci* 11: 813-826.
74. Hoffman S., Sorkin B. C., White P. C., Brackenbury R., Mailhammer R., Rutishauser U., Cunningham B. A., Edelman G. M. (1982) Chemical characterization of a neural cell adhesion molecule purified from embryonic brain membranes. *J Biol Chem* 257: 7720-7729.
75. Holm J., Hillenbrand R., Steuber V., Bartsch U., Moos M., Lubbert H., Montag D., Schachner M. (1996) Structural features of a close homologue of L1 (CHL1) in the mouse: a new member of the L1 family of neural recognition molecules. *Eur J Neurosci* 8: 1613-1629.
76. Honing S., Kreimer G., Robenek H., Jockusch B. M. (1994) Receptor-mediated endocytosis is sensitive to antibodies against the uncoating ATPase (hsc70). *J Cell Sci* 107 (Pt 5): 1185-1196.
77. Honn K. V., Tang D. G. (1992) Adhesion molecules and tumor cell interaction with endothelium and subendothelial matrix. *Cancer Metastasis Rev* 11: 353-375.
78. Hortsch M. (1996) The L1 family of neural cell adhesion molecules: old proteins performing new tricks. *Neuron* 17: 587-593.
79. Hortsch M., Wang Y. M., Marikar Y., Bieber A. J. (1995) The cytoplasmic domain of the Drosophila cell adhesion molecule neuroglian is not essential for its homophilic adhesive properties in S2 cells. *J Biol Chem* 270: 18809-18817.
80. Höhfeld J. (1998) Regulation of the heat shock conjugate Hsc70 in the mammalian cell: the characterization of the anti-apoptotic protein BAG-1 provides novel insights. *Biol Chem* 379: 269-274.
81. Huang Y., Jellies J., Johansen K. M., Johansen J. (1997) Differential glycosylation of tractin and LeechCAM, two novel Ig superfamily members, regulates neurite extension and fascicle formation. *J Cell Biol* 138: 143-157.
82. Hynes R. O. (1992) Integrins: versatility, modulation, and signaling in cell adhesion. *Cell* 69: 11-25.
83. Ignelzi M. A., Jr., Miller D. R., Soriano P., Maness P. F. (1994) Impaired neurite outgrowth of src-minus cerebellar neurons on the cell adhesion molecule L1. *Neuron* 12: 873-884.
84. Itoh K., Stevens B., Schachner M., Fields R. D. (1995) Regulated expression of the neural cell adhesion molecule L1 by specific patterns of neural impulses. *Science* 270: 1369-1372.
85. Jensen O. N., Podtelejnikov A. V., Mann M. (1997) Identification of the components of simple protein mixtures by high- accuracy peptide mass mapping and database searching. *Anal Chem* 69: 4741-4750.

IX. Bibliography

86. Joergensen O. S. (1995) Neural cell adhesion molecule (NCAM) as a quantitative marker in synaptic remodeling. *Neurochem Res* 20: 533-547.
87. Jouet M., Rosenthal A., Kenwrick S. (1995) Exon 2 of the gene for neural cell adhesion molecule L1 is alternatively spliced in B cells. *Brain Res Mol Brain Res* 30: 378-380.
88. Kabouridis P. S., Magee A. I., Ley S. C. (1997) S-acylation of LCK protein tyrosine kinase is essential for its signalling function in T lymphocytes. *EMBO J* 16: 4983-4998.
89. Kadmon G., Altevogt P. (1997) The cell adhesion molecule L1: species- and cell-type-dependent multiple binding mechanisms. *Differentiation* 61: 143-150.
90. Kadmon G., Bohlen und H. F., Horstkorte R., Eckert M., Altevogt P., Schachner M. (1995) Evidence for cis interaction and cooperative signalling by the heat- stable antigen nectadrin (murine CD24) and the cell adhesion molecule L1 in neurons. *Eur J Neurosci* 7: 993-1004.
91. Kadmon G., Kowitz A., Altevogt P., Schachner M. (1990a) Functional cooperation between the neural adhesion molecules L1 and N- CAM is carbohydrate dependent. *J Cell Biol* 110: 209-218.
92. Kadmon G., Kowitz A., Altevogt P., Schachner M. (1990b) The neural cell adhesion molecule N-CAM enhances L1-dependent cell-cell interactions. *J Cell Biol* 110: 193-208.
93. Kamiguchi H., Lemmon V. (1997) Neural cell adhesion molecule L1: signaling pathways and growth cone motility. *J Neurosci Res* 49: 1-8.
94. Kanelakis K. C., Morishima Y., Dittmar K. D., Galigniana M. D., Takayama S., Reed J. C., Pratt W. B. (1999) Differential effects of the hsp70-binding protein BAG-1 on glucocorticoid receptor folding by the hsp90-based chaperone machinery. *J Biol Chem* 274: 34134-34140.
95. Kayyem J. F., Roman J. M., de la Rosa E. J., Schwarz U., Dreyer W. J. (1992) Bravo/Nr-CAM is closely related to the cell adhesion molecules L1 and Ng-CAM and has a similar heterodimer structure. *J Cell Biol* 118: 1259-1270.
96. Keilhauer G., Faissner A., Schachner M. (1985) Differential inhibition of neurone-neurone, neurone-astrocyte and astrocyte-astrocyte adhesion by L1, L2 and N-CAM antibodies. *Nature* 316: 728-730.
97. Kelley W. L., Georgopoulos C. (1997) Positive control of the two-component RcsC/B signal transduction network by DjIA: a member of the DnaJ family of molecular chaperones in *Escherichia coli*. *Mol Microbiol* 25: 913-931.
98. Kemler R., Ozawa M. (1989) Uvomorulin-catenin complex: cytoplasmic anchorage of a Ca²⁺-dependent cell adhesion molecule. *Bioessays* 11: 88-91.

IX. Bibliography

99. Kowitz A., Kadmon G., Eckert M., Schirmacher V., Schachner M., Altevogt P. (1992) Expression and function of the neural cell adhesion molecule L1 in mouse leukocytes. *Eur J Immunol* 22: 1199-1205.
100. Kowitz A., Kadmon G., Verschueren H., Remels L., De Baetselier P., Hubbe M., Schachner M., Schirmacher V., Altevogt P. (1993) Expression of L1 cell adhesion molecule is associated with lymphoma growth and metastasis. *Clin Exp Metastasis* 11: 419-429.
101. Kronenberg M., Siu G., Hood L. E., Shastri N. (1986) The molecular genetics of the T-cell antigen receptor and T-cell antigen recognition. *Annu Rev Immunol* 4: 529-591.
102. Krushel L. A., Tai M. H., Cunningham B. A., Edelman G. M., Crossin K. L. (1998) Neural cell adhesion molecule (N-CAM) domains and intracellular signaling pathways involved in the inhibition of astrocyte proliferation. *Proc Natl Acad Sci U S A* 95: 2592-2596.
103. Kuhn T. B., Stoeckli E. T., Condrau M. A., Rathjen F. G., Sonderegger P. (1991) Neurite outgrowth on immobilized axonin-1 is mediated by a heterophilic interaction with L1(G4). *J Cell Biol* 115: 1113-1126.
104. Kunemund V., Jungalwala F. B., Fischer G., Chou D. K., Keilhauer G., Schachner M. (1988) The L2/HNK-1 carbohydrate of neural cell adhesion molecules is involved in cell interactions. *J Cell Biol* 106: 213-223.
105. Kyte J., Doolittle R. F. (1982) A simple method for displaying the hydropathic character of a protein. *J Mol Biol* 157: 105-132.
106. Lander E. S., Linton L. M., Birren B., Nusbaum C., Zody M. C., Baldwin J., Devon K., Dewar K., Doyle M., FitzHugh W., Funke R., Gage D., Harris K., Heaford A., Howland J., Kann L., Lehoczky J., LeVine R., McEwan P., McKernan K., Meldrim J., Mesirov J. P., Miranda C., Morris W., Naylor J., Raymond C., Rosetti M., Santos R., Sheridan A., Sougnez C., Stange-Thomann N., Stojanovic N., Subramanian A., Wyman D., Rogers J., Sulston J., Ainscough R., Beck S., Bentley D., Burton J., Clee C., Carter N., Coulson A., Deadman R., Deloukas P., Dunham A., Dunham I., Durbin R., French L., Grafham D., Gregory S., Hubbard T., Humphray S., Hunt A., Jones M., Lloyd C., McMurray A., Matthews L., Mercer S., Milne S., Mullikin J. C., Mungall A., Plumb R., Ross M., Shownkeen R., Sims S., Waterston R. H., Wilson R. K., Hillier L. W., McPherson J. D., Marra M. A., Mardis E. R., Fulton L. A., Chinwalla A. T., Pepin K. H., Gish W. R., Chissoe S. L., Wendl M. C., Delehaunty K. D., Miner T. L., Delehaunty A., Kramer J. B., Cook L. L., Fulton R. S., Johnson D. L., Minx P. J., Clifton S. W., Hawkins T., Branscomb E., Predki P., Richardson P., Wenning S., Slezak T., Doggett N., Cheng J. F., Olsen A., Lucas S., Elkin C., Uberbacher E., Frazier M., Gibbs R. A., Muzny D. M., Scherer S. E., Bouck J. B., Sodergren E. J., Worley K. C., Rives C. M., Gorrell J. H., Metzker M. L., Naylor S. L., Kucherlapati R. S., Nelson D. L., Weinstock G. M., Sakaki Y., Fujiyama A., Hattori M., Yada T., Toyoda A., Itoh T., Kawagoe C., Watanabe H., Totoki Y., Taylor T., Weissenbach J., Heilig R., Saurin W., Artiguenave F., Brottier P.,

- Bruls T., Pelletier E., Robert C., Wincker P., Smith D. R., Doucette-Stamm L., Rubenfield M., Weinstock K., Lee H. M., Dubois J., Rosenthal A., Platzer M., Nyakatura G., Taudien S., Rump A., Yang H., Yu J., Wang J., Huang G., Gu J., Hood L., Rowen L., Madan A., Qin S., Davis R. W., Federspiel N. A., Abola A. P., Proctor M. J., Myers R. M., Schmutz J., Dickson M., Grimwood J., Cox D. R., Olson M. V., Kaul R., Raymond C., Shimizu N., Kawasaki K., Minoshima S., Evans G. A., Athanasiou M., Schultz R., Roe B. A., Chen F., Pan H., Ramser J., Lehrach H., Reinhardt R., McCombie W. R., de la B. M., Dedhia N., Blocker H., Hornischer K., Nordsiek G., Agarwala R., Aravind L., Bailey J. A., Bateman A., Batzoglou S., Birney E., Bork P., Brown D. G., Burge C. B., Cerutti L., Chen H. C., Church D., Clamp M., Copley R. R., Doerks T., Eddy S. R., Eichler E. E., Furey T. S., Galagan J., Gilbert J. G., Harmon C., Hayashizaki Y., Haussler D., Hermjakob H., Hokamp K., Jang W., Johnson L. S., Jones T. A., Kasif S., Kasprzyk A., Kennedy S., Kent W. J., Kitts P., Koonin E. V., Korf I., Kulp D., Lancet D., Lowe T. M., McLysaght A., Mikkelsen T., Moran J. V., Mulder N., Pollara V. J., Ponting C. P., Schuler G., Schultz J., Slater G., Smit A. F., Stupka E., Szustakowski J., Thierry-Mieg D., Thierry-Mieg J., Wagner L., Wallis J., Wheeler R., Williams A., Wolf Y. I., Wolfe K. H., Yang S. P., Yeh R. F., Collins F., Guyer M. S., Peterson J., Felsenfeld A., Wetterstrand K. A., Patrinos A., Morgan M. J., Szustakowki J. (2001) Initial sequencing and analysis of the human genome. *Nature* 409: 860-921.
107. Lane R. P., Chen X. N., Yamakawa K., Vielmetter J., Korenberg J. R., Dreyer W. J. (1996) Characterization of a highly conserved human homolog to the chicken neural cell surface protein Bravo/Nr-CAM that maps to chromosome band 7q31. *Genomics* 35: 456-465.
108. Langnaese K., Seidenbecher C., Wex H., Seidel B., Hartung K., Appeltauer U., Garner A., Voss B., Mueller B., Garner C. C., Gundelfinger E. D. (1996) Protein components of a rat brain synaptic junctional protein preparation. *Brain Res Mol Brain Res* 42: 118-122.
109. Letourneau P. C., Shattuck T. A. (1989) Distribution and possible interactions of actin-associated proteins and cell adhesion molecules of nerve growth cones. *Development* 105: 505-519.
110. Lindner J., Rathjen F. G., Schachner M. (1983) L1 mono- and polyclonal antibodies modify cell migration in early postnatal mouse cerebellum. *Nature* 305: 427-430.
111. Lipman D. J., Pearson W. R. (1985) Rapid and sensitive protein similarity searches. *Science* 227: 1435-1441.
112. Liu F. H., Wu S. J., Hu S. M., Hsiao C. D., Wang C. (1999) Specific interaction of the 70-kDa heat shock cognate protein with the tetratricopeptide repeats. *J Biol Chem* 274: 34425-34432.
113. Lochter A., Vaughan L., Kaplony A., Prochiantz A., Schachner M., Faissner A. (1991) J1/tenascin in substrate-bound and soluble form displays contrary effects on neurite outgrowth. *J Cell Biol* 113: 1159-1171.

114. Loones M. T., Chang Y., Morange M. (2000) The distribution of heat shock proteins in the nervous system of the unstressed mouse embryo suggests a role in neuronal and non-neuronal differentiation. *Cell Stress Chaperones* 5: 291-305.
115. Luders J., Demand J., Höhfeld J. (2000) The ubiquitin-related BAG-1 provides a link between the molecular chaperones Hsc70/Hsp70 and the proteasome. *J Biol Chem* 275: 4613-4617.
116. Lüthi A., Laurent J. P., Figueroa A., Müller D., Schachner M. (1994) Hippocampal long-term potentiation and neural cell adhesion molecules L1 and NCAM. *Nature* 372: 777-779.
117. Malhotra J. D., Tsiotra P., Karagogeos D., Hortsch M. (1998) Cis-activation of L1-mediated ankyrin recruitment by TAG-1 homophilic cell adhesion. *J Biol Chem* 273: 33354-33359.
118. Manceau V., Gavet O., Curmi P., Sobel A. (1999) Stathmin interaction with HSC70 family proteins. *Electrophoresis* 20: 409-417.
119. Mauro V. P., Wood I. C., Krushel L., Crossin K. L., Edelman G. M. (1994) Cell adhesion alters gene transcription in chicken embryo brain cells and mouse embryonal carcinoma cells. *Proc Natl Acad Sci U S A* 91: 2868-2872.
120. Mayer U., Nischt R., Poschl E., Mann K., Fukuda K., Gerl M., Yamada Y., Timpl R. (1993) A single EGF-like motif of laminin is responsible for high affinity nidogen binding. *EMBO J* 12: 1879-1885.
121. McGraw J., Hiebert G. W., Steeves J. D. (2001) Modulating astrogliosis after neurotrauma. *J Neurosci Res* 63: 109-115.
122. Mechtersheimer S., Gutwein P., Agmon-Levin N., Stoeck A., Oleszewski M., Riedle S., Fogel M., Lemmon V., Altevogt P. (2001) Ectodomain shedding of L1 adhesion molecule promotes cell migration by autocrine binding to integrins. *J Cell Biol* 155: 661-674.
123. Milev P., Friedlander D. R., Sakurai T., Karthikeyan L., Flad M., Margolis R. K., Grumet M., Margolis R. U. (1994) Interactions of the chondroitin sulfate proteoglycan phosphacan, the extracellular domain of a receptor-type protein tyrosine phosphatase, with neurons, glia, and neural cell adhesion molecules. *J Cell Biol* 127: 1703-1715.
124. Montgomery A. M., Becker J. C., Siu C. H., Lemmon V. P., Cheresch D. A., Pancook J. D., Zhao X., Reisfeld R. A. (1996) Human neural cell adhesion molecule L1 and rat homologue NILE are ligands for integrin alpha v beta 3. *J Cell Biol* 132: 475-485.

IX. Bibliography

125. Moos M., Tacke R., Scherer H., Teplow D., Fruh K., Schachner M. (1988) Neural adhesion molecule L1 as a member of the immunoglobulin superfamily with binding domains similar to fibronectin. *Nature* 334: 701-703.
126. Mortz E., Vorm O., Mann M., Roepstorff P. (1994) Identification of proteins in polyacrylamide gels by mass spectrometric peptide mapping combined with database search. *Biol Mass Spectrom* 23: 249-261.
127. Moscoso L. M., Sanes J. R. (1995) Expression of four immunoglobulin superfamily adhesion molecules (L1, Nr-CAM/Bravo, neurofascin/ABGP, and N-CAM) in the developing mouse spinal cord. *J Comp Neurol* 352: 321-334.
128. Müller-Husmann G., Gloor S., Schachner M. (1993) Functional characterization of beta isoforms of murine Na,K-ATPase. The adhesion molecule on glia (AMOG/beta 2), but not beta 1, promotes neurite outgrowth. *J Biol Chem* 268: 26260-26267.
129. Napolitano E. W., Pachter J. S., Chin S. S., Liem R. K. (1985) beta-Internexin, a ubiquitous intermediate filament-associated protein. *J Cell Biol* 101: 1323-1331.
130. Nayeem N., Silletti S., Yang X., Lemmon V. P., Reisfeld R. A., Stallcup W. B., Montgomery A. M. (1999) A potential role for the plasmin(ogen) system in the posttranslational cleavage of the neural cell adhesion molecule L1. *J Cell Sci* 112 (Pt 24): 4739-4749.
131. Niethammer P., Delling M., Sytnyk V., Dityatev A., Schachner M. (2002) Co-signaling of NCAM via lipid rafts and the FGF receptor is required for neuritogenesis. *J Biol Chem* submitted.
132. Nybroe O., Bock E. (1990) Structure and function of the neural cell adhesion molecules NCAM and L1. *Adv Exp Med Biol* 265: 185-196.
133. Orr H. T., Lancet D., Robb R. J., Lopez de Castro J. A., Strominger J. L. (1979) The heavy chain of human histocompatibility antigen HLA-B7 contains an immunoglobulin-like region. *Nature* 282: 266-270.
134. Owens G. C., Edelman G. M., Cunningham B. A. (1987) Organization of the neural cell adhesion molecule (N-CAM) gene: alternative exon usage as the basis for different membrane-associated domains. *Proc Natl Acad Sci U S A* 84: 294-298.
135. Paddenberg R., Wiegand C., Jockusch B. M. (1990) Characterization of the coated vesicle uncoating ATPase: tissue distribution, association with and activity on intact coated vesicles. *Eur J Cell Biol* 52: 60-66.

IX. Bibliography

136. Pancook J. D., Reisfeld R. A., Varki N., Vitiello A., Fox R. I., Montgomery A. M. (1997) Expression and regulation of the neural cell adhesion molecule L1 on human cells of myelomonocytic and lymphoid origin. *J Immunol* 158: 4413-4421.
137. Parise L. V. (1989) The structure and function of platelet integrins. *Curr Opin Cell Biol* 1: 947-952.
138. Pelham H. R. (1986) Speculations on the functions of the major heat shock and glucose- regulated proteins. *Cell* 46: 959-961.
139. Prasad K., Heuser J., Eisenberg E., Greene L. (1994) Complex formation between clathrin and uncoating ATPase. *J Biol Chem* 269: 6931-6939.
140. Prince J. T., Alberti L., Healy P. A., Nauman S. J., Stallcup W. B. (1991) Molecular cloning of NILE glycoprotein and evidence for its continued expression in mature rat CNS. *J Neurosci Res* 30: 567-581.
141. Ranscht B. (1988) Sequence of contactin, a 130-kD glycoprotein concentrated in areas of interneuronal contact, defines a new member of the immunoglobulin supergene family in the nervous system. *J Cell Biol* 107: 1561-1573.
142. Rathjen F. G., Schachner M. (1984) Immunocytological and biochemical characterization of a new neuronal cell surface component (L1 antigen) which is involved in cell adhesion. *EMBO J* 3: 1-10.
143. Reichardt L. F., Tomaselli K. J. (1991) Extracellular matrix molecules and their receptors: functions in neural development. *Annu Rev Neurosci* 14: 531-570.
144. Ren Q., Bennett V. (1998) Palmitoylation of neurofascin at a site in the membrane-spanning domain highly conserved among the L1 family of cell adhesion molecules. *J Neurochem* 70: 1839-1849.
145. Rieger F., Grumet M., Edelman G. M. (1985) N-CAM at the vertebrate neuromuscular junction. *J Cell Biol* 101: 285-293.
146. Ruoslahti E., Pierschbacher M. D. (1987) New perspectives in cell adhesion: RGD and integrins. *Science* 238: 491-497.
147. Ruppert M., Aigner S., Hubbe M., Yagita H., Altevogt P. (1995) The L1 adhesion molecule is a cellular ligand for VLA-5. *J Cell Biol* 131: 1881-1891.
148. Rutishauser U., Jessell T. M. (1988) Cell adhesion molecules in vertebrate neural development. *Physiol Rev* 68: 819-857.
149. Rutishauser U., Landmesser L. (1996) Polysialic acid in the vertebrate nervous system: a promoter of plasticity in cell-cell interactions. *Trends Neurosci* 19: 422-427.

150. Sadoul K., Sadoul R., Faissner A., Schachner M. (1988) Biochemical characterization of different molecular forms of the neural cell adhesion molecule L1. *J Neurochem* 50: 510-521.
151. Sadoul R., Kirchhoff F., Schachner M. (1989) A protein kinase activity is associated with and specifically phosphorylates the neural cell adhesion molecule L1. *J Neurochem* 53: 1471-1478.
152. Saffell J. L., Walsh F. S., Doherty P. (1992) Direct activation of second messenger pathways mimics cell adhesion molecule-dependent neurite outgrowth. *J Cell Biol* 118: 663-670.
153. Sambrook J, Fritsch EF, Maniatis T (1989) *Molecular Cloning: A Laboratory Manual*. New York: Cold Spring Harbor Laboratory, Cold Spring Harbor.
154. Sanes J. R. (1989) Extracellular matrix molecules that influence neural development. *Annu Rev Neurosci* 12: 491-516.
155. Schachner M., Martini R. (1995) Glycans and the modulation of neural-recognition molecule function. *Trends Neurosci* 18: 183-191.
156. Schaefer A. W., Kamiguchi H., Wong E. V., Beach C. M., Landreth G., Lemmon V. (1999) Activation of the MAPK signal cascade by the neural cell adhesion molecule L1 requires L1 internalization. *J Biol Chem* 274: 37965-37973.
157. Schmid R. S., Graff R. D., Schaller M. D., Chen S., Schachner M., Hemperly J. J., Maness P. F. (1999) NCAM stimulates the Ras-MAPK pathway and CREB phosphorylation in neuronal cells. *J Neurobiol* 38: 542-558.
158. Schneikert J., Hubner S., Martin E., Cato A. C. (1999) A nuclear action of the eukaryotic cochaperone RAP46 in downregulation of glucocorticoid receptor activity. *J Cell Biol* 146: 929-940.
159. Scholey A. B., Mileusnic R., Schachner M., Rose S. P. (1995) A role for a chicken homolog of the neural cell adhesion molecule L1 in consolidation of memory for a passive avoidance task in the chick. *Learn Mem* 2: 17-25.
160. Schuch U., Lohse M. J., Schachner M. (1989) Neural cell adhesion molecules influence second messenger systems. *Neuron* 3: 13-20.
161. Scotland P., Zhou D., Benveniste H., Bennett V. (1998) Nervous system defects of AnkyrinB (-/-) mice suggest functional overlap between the cell adhesion molecule L1 and 440-kD AnkyrinB in premyelinated axons. *J Cell Biol* 143: 1305-1315.

IX. Bibliography

162. Seagar M., Leveque C., Charvin N., Marqueze B., Martin-Moutot N., Boudier J. A., Boudier J. L., Shoji-Kasai Y., Sato K., Takahashi M. (1999) Interactions between proteins implicated in exocytosis and voltage-gated calcium channels. *Philos Trans R Soc Lond B Biol Sci* 354: 289-297.
163. Seilheimer B., Schachner M. (1987) Regulation of neural cell adhesion molecule expression on cultured mouse Schwann cells by nerve growth factor. *EMBO J* 6: 1611-1616.
164. Shevchenko A., Wilm M., Vorm O., Mann M. (1996) Mass spectrometric sequencing of proteins silver-stained polyacrylamide gels. *Anal Chem* 68: 850-858.
165. Shih P., Evans K., Schifferli K., Ciccarone V., Lichaa F., Masoud M., Lan J., Hawley-Nelson P. (1997) *FOCUS* 19: 52.
166. Small S. J., Akeson R. (1990) Expression of the unique NCAM VASE exon is independently regulated in distinct tissues during development. *J Cell Biol* 111: 2089-2096.
167. Small S. J., Haines S. L., Akeson R. A. (1988) Polypeptide variation in an N-CAM extracellular immunoglobulin-like fold is developmentally regulated through alternative splicing. *Neuron* 1: 1007-1017.
168. Song J., Takeda M., Morimoto R. I. (2001) Bag1-Hsp70 mediates a physiological stress signalling pathway that regulates Raf-1/ERK and cell growth. *Nat Cell Biol* 3: 276-282.
169. Sporns O., Edelman G. M., Crossin K. L. (1995) The neural cell adhesion molecule (N-CAM) inhibits proliferation in primary cultures of rat astrocytes. *Proc Natl Acad Sci U S A* 92: 542-546.
170. Springer T. A. (1990) Adhesion receptors of the immune system. *Nature* 346: 425-434.
171. Staatz W. D., Fok K. F., Zutter M. M., Adams S. P., Rodriguez B. A., Santoro S. A. (1991) Identification of a tetrapeptide recognition sequence for the alpha 2 beta 1 integrin in collagen. *J Biol Chem* 266: 7363-7367.
172. Stahl B., Tobaben S., Sudhof T. C. (1999) Two distinct domains in hsc70 are essential for the interaction with the synaptic vesicle cysteine string protein. *Eur J Cell Biol* 78: 375-381.
173. Suzuki T., Usuda N., Murata S., Nakazawa A., Ohtsuka K., Takagi H. (1999) Presence of molecular chaperones, heat shock cognate (Hsc) 70 and heat shock proteins (Hsp) 40, in the postsynaptic structures of rat brain. *Brain Res* 816: 99-110.
174. Takayama S., Bimston D. N., Matsuzawa S., Freeman B. C., Aime-Sempe C., Xie Z., Morimoto R. I., Reed J. C. (1997) BAG-1 modulates the chaperone activity of Hsp70/Hsc70. *EMBO J* 16: 4887-4896.

IX. Bibliography

175. Takeichi M. (1991) Cadherin cell adhesion receptors as a morphogenetic regulator. *Science* 251: 1451-1455.
176. Thiery J. P., Brackenbury R., Rutishauser U., Edelman G. M. (1977) Adhesion among neural cells of the chick embryo. II. Purification and characterization of a cell adhesion molecule from neural retina. *J Biol Chem* 252: 6841-6845.
177. Thor G., Probstmeier R., Schachner M. (1987) Characterization of the cell adhesion molecules L1, N-CAM and J1 in the mouse intestine. *EMBO J* 6: 2581-2586.
178. Tobaben S., Thakur P., Fernandez-Chacon R., Sudhof T. C., Rettig J., Stahl B. (2001) A trimeric protein complex functions as a synaptic chaperone machine. *Neuron* 31: 987-999.
179. Tongiorgi E., Bernhardt R. R., Schachner M. (1995) Zebrafish neurons express two L1-related molecules during early axonogenesis. *J Neurosci Res* 42: 547-561.
180. Van Der S. J., Kana B. D., Dirr H. W., Blatch G. L. (2000) Heat shock cognate protein 70 chaperone-binding site in the co- chaperone murine stress-inducible protein 1 maps to within three consecutive tetratricopeptide repeat motifs. *Biochem J* 345 Pt 3: 645-651.
181. Venter J. C., Adams M. D., Myers E. W., Li P. W., Mural R. J., Sutton G. G., Smith H. O., Yandell M., Evans C. A., Holt R. A., Gocayne J. D., Amanatides P., Ballew R. M., Huson D. H., Wortman J. R., Zhang Q., Kodira C. D., Zheng X. H., Chen L., Skupski M., Subramanian G., Thomas P. D., Zhang J., Gabor Miklos G. L., Nelson C., Broder S., Clark A. G., Nadeau J., McKusick V. A., Zinder N., Levine A. J., Roberts R. J., Simon M., Slayman C., Hunkapiller M., Bolanos R., Delcher A., Dew I., Fasulo D., Flanigan M., Florea L., Halpern A., Hannenhalli S., Kravitz S., Levy S., Mobarry C., Reinert K., Remington K., Abu-Threideh J., Beasley E., Biddick K., Bonazzi V., Brandon R., Cargill M., Chandramouliswaran I., Charlab R., Chaturvedi K., Deng Z., Di F., V, Dunn P., Eilbeck K., Evangelista C., Gabrielian A. E., Gan W., Ge W., Gong F., Gu Z., Guan P., Heiman T. J., Higgins M. E., Ji R. R., Ke Z., Ketchum K. A., Lai Z., Lei Y., Li Z., Li J., Liang Y., Lin X., Lu F., Merkulov G. V., Milshina N., Moore H. M., Naik A. K., Narayan V. A., Neelam B., Nusskern D., Rusch D. B., Salzberg S., Shao W., Shue B., Sun J., Wang Z., Wang A., Wang X., Wang J., Wei M., Wides R., Xiao C., Yan C., Yao A., Ye J., Zhan M., Zhang W., Zhang H., Zhao Q., Zheng L., Zhong F., Zhong W., Zhu S., Zhao S., Gilbert D., Baumhueter S., Spier G., Carter C., Cravchik A., Woodage T., Ali F., An H., Awe A., Baldwin D., Baden H., Barnstead M., Barrow I., Beeson K., Busam D., Carver A., Center A., Cheng M. L., Curry L., Danaher S., Davenport L., Desilets R., Dietz S., Dodson K., Doup L., Ferriera S., Garg N., Gluecksmann A., Hart B., Haynes J., Haynes C., Heiner C., Hladun S., Hostin D., Houck J., Howland T., Ibegwam C., Johnson J., Kalush F., Kline L., Koduru S., Love A., Mann F., May D., McCawley S., McIntosh T., McMullen I., Moy M., Moy L., Murphy B., Nelson K., Pfannkoch C., Pratts E., Puri V., Qureshi H., Reardon M., Rodriguez R., Rogers Y. H., Romblad D., Ruhfel B., Scott R., Sitter C., Smallwood M., Stewart E.,

IX. Bibliography

- Strong R., Suh E., Thomas R., Tint N. N., Tse S., Vech C., Wang G., Wetter J., Williams S., Williams M., Windsor S., Winn-Deen E., Wolfe K., Zaveri J., Zaveri K., Abril J. F., Guigo R., Campbell M. J., Sjolander K. V., Karlak B., Kejariwal A., Mi H., Lazareva B., Hatton T., Narechania A., Diemer K., Muruganujan A., Guo N., Sato S., Bafna V., Istrail S., Lippert R., Schwartz R., Walenz B., Yooseph S., Allen D., Basu A., Baxendale J., Blick L., Caminha M., Carnes-Stine J., Caulk P., Chiang Y. H., Coyne M., Dahlke C., Mays A., Dombroski M., Donnelly M., Ely D., Esparham S., Fosler C., Gire H., Glanowski S., Glasser K., Glodek A., Gorokhov M., Graham K., Gropman B., Harris M., Heil J., Henderson S., Hoover J., Jennings D., Jordan C., Jordan J., Kasha J., Kagan L., Kraft C., Levitsky A., Lewis M., Liu X., Lopez J., Ma D., Majoros W., McDaniel J., Murphy S., Newman M., Nguyen T., Nguyen N., Nodell M. (2001) The sequence of the human genome. *Science* 291: 1304-1351.
182. Volkmer H., Hassel B., Wolff J. M., Frank R., Rathjen F. G. (1992) Structure of the axonal surface recognition molecule neurofascin and its relationship to a neural subgroup of the immunoglobulin superfamily. *J Cell Biol* 118: 149-161.
183. von Bohlen und Halbach F., Taylor J., Schachner M. (1992) Cell-type specific effects of the neural cell adhesion molecules L1 and N-CAM on diverse second messenger systems. *Eur J Neuroscience* 4: 896-909.
184. Walsh F. S., Doherty P. (1997) Neural cell adhesion molecules of the immunoglobulin superfamily: role in axon growth and guidance. *Annu Rev Cell Dev Biol* 13: 425-456.
185. Wei M. H., Karavanova I., Ivanov S. V., Popescu N. C., Keck C. L., Pack S., Eisen J. A., Lerman M. I. (1998) In silico-initiated cloning and molecular characterization of a novel human member of the L1 gene family of neural cell adhesion molecules. *Hum Genet* 103: 355-364.
186. Wessel D., Flugge U. I. (1984) A method for the quantitative recovery of protein in dilute solution in the presence of detergents and lipids. *Anal Biochem* 138: 141-143.
187. Westermeier R (1993) *Electrophoresis in Practice*. VCH Verlagsgesellschaft mbH, Weinheim, Germany.
188. Whatley S. A., Leung T., Hall C., Lim L. (1986) The brain 68-kilodalton microtubule-associated protein is a cognate form of the 70-kilodalton mammalian heat-shock protein and is present as a specific isoform in synaptosomal membranes. *J Neurochem* 47: 1576-1583.
189. Williams A. F., Barclay A. N. (1988) The immunoglobulin superfamily--domains for cell surface recognition. *Annu Rev Immunol* 6: 381-405.
190. Williams E. J., Doherty P., Turner G., Reid R. A., Hemperly J. J., Walsh F. S. (1992) Calcium influx into neurons can solely account for cell contact- dependent neurite outgrowth stimulated by transfected L1. *J Cell Biol* 119: 883-892.

IX. Bibliography

191. Williams E. J., Furness J., Walsh F. S., Doherty P. (1994a) Activation of the FGF receptor underlies neurite outgrowth stimulated by L1, N-CAM, and N-cadherin. *Neuron* 13: 583-594.
192. Williams E. J., Mittal B., Walsh F. S., Doherty P. (1995) FGF inhibits neurite outgrowth over monolayers of astrocytes and fibroblasts expressing transfected cell adhesion molecules. *J Cell Sci* 108 (Pt 11): 3523-3530.
193. Williams E. J., Walsh F. S., Doherty P. (1994b) The production of arachidonic acid can account for calcium channel activation in the second messenger pathway underlying neurite outgrowth stimulated by NCAM, N-cadherin, and L1. *J Neurochem* 62: 1231-1234.
194. Wong E. V., Schaefer A. W., Landreth G., Lemmon V. (1996a) Casein kinase II phosphorylates the neural cell adhesion molecule L1. *J Neurochem* 66: 779-786.
195. Wong E. V., Schaefer A. W., Landreth G., Lemmon V. (1996c) Involvement of p90rsk in neurite outgrowth mediated by the cell adhesion molecule L1. *J Biol Chem* 271: 18217-18223.
196. Wong E. V., Schaefer A. W., Landreth G., Lemmon V. (1996b) Involvement of p90rsk in neurite outgrowth mediated by the cell adhesion molecule L1. *J Biol Chem* 271: 18217-18223.
197. Xing H., Zhang S., Weinheimer C., Kovacs A., Muslin A. J. (2000) 14-3-3 proteins block apoptosis and differentially regulate MAPK cascades. *EMBO J* 19: 349-358.
198. Yoshihara Y., Kawasaki M., Tamada A., Nagata S., Kagamiyama H., Mori K. (1995) Overlapping and differential expression of BIG-2, BIG-1, TAG-1, and F3: four members of an axon-associated cell adhesion molecule subgroup of the immunoglobulin superfamily. *J Neurobiol* 28: 51-69.
199. Yoshihara Y., Kawasaki M., Tani A., Tamada A., Nagata S., Kagamiyama H., Mori K. (1994) BIG-1: a new TAG-1/F3-related member of the immunoglobulin superfamily with neurite outgrowth-promoting activity. *Neuron* 13: 415-426.
200. Zetter B. R. (1990) The cellular basis of site-specific tumor metastasis. *N Engl J Med* 322: 605-612.
201. Zhang H., Kelley W. L., Chamberlain L. H., Burgoyne R. D., Lang J. (1999) Mutational analysis of cysteine-string protein function in insulin exocytosis. *J Cell Sci* 112 (Pt 9): 1345-1351.
202. Zhang W., Tribble R. P., Samelson L. E. (1998) LAT palmitoylation: its essential role in membrane microdomain targeting and tyrosine phosphorylation during T cell activation. *Immunity* 9: 239-246.
203. Zhang Y., Roslan R., Lang D., Schachner M., Lieberman A. R., Anderson P. N. (2000) Expression of CHL1 and L1 by neurons and glia following sciatic nerve and dorsal root injury. *Mol Cell Neurosci* 16: 71-86.

IX. Bibliography

204. Zimmerman G. A., Prescott S. M., McIntyre T. M. (1992) Endothelial cell interactions with granulocytes: tethering and signaling molecules. *Immunol Today* 13: 93-100.
205. Zuellig R. A., Rader C., Schroeder A., Kalousek M. B., Bohlen und H. F., Osterwalder T., Inan C., Stoeckli E. T., Affolter H. U., Fritz A., . (1992) The axonally secreted cell adhesion molecule, axonin-1. Primary structure, immunoglobulin-like and fibronectin-type-III-like domains and glycosyl-phosphatidylinositol anchorage. *Eur J Biochem* 204: 453-463.

Acknowledgement / Danksagung

Die experimentellen Arbeiten dieser Dissertation wurden am Institut für Biosynthese Neuraler Strukturen am Zentrum für Molekulare Neurobiologie Hamburg (ZMNH) durchgeführt. Frau Prof. Dr. Melitta Schachner möchte ich für die Überlassung des interessanten Themas, für die Bereitstellung des Arbeitsplatzes und für ihre stete Hilfs- und Diskussionsbereitschaft danken.

Für die Übernahme der Betreuung und die Korrektur der externen Dissertation möchte ich ausdrücklich Herrn Priv. Doz. Joerg W. Bartsch danken, da mir seine Bereitschaft, mich als Externe zu betreuen, nicht als Selbstverständlichkeit, sondern als große Hilfe und Entgegenkommen erscheint.

Special thanks I would like to address to Bernhard Kuester, D.Phil. from the laboratory of Prof. Matthias Mann (Center of Experimental Bioinformatics, Odense University, Denmark) for performing the MALDI-MS analysis by which an important factor for the ongoing of this work was provided.

Dr. Ralf Kleene danke ich des weiteren für die Hilfestellung und Diskussionsbereitschaft während der Doktorarbeit und für das kritische und produktive Korrekturlesen während des Zusammenschreibens. Außerdem möchte ich Dr. Frank Plöger danken, der mich vor allem in molekularbiologischen Fragen ausgezeichnet betreut hat. Dr. Catharina G. Becker danke ich für das aufmerksame Korrekturlesen der letzten Version und ihre sinnvollen und hilfreichen Verbesserungsvorschläge.

Darüberhinaus möchte ich den folgenden Personen danken:

- Bettina Rolf für die immunhistochemischen Untersuchungen zur Spezifität des CHL1 Antikörpers und für die großzügige Überlassung der Graphen. Desweiteren für ihren Anteil an Organisation und Kontrolle der L1/CHL1 Doppel-k.o. Mauslinie und für die Bereitstellung von CHL1-defizienten Zuchtpaaren.
- Dr. Astrid Rollenhagen für die Einweisung und Hilfe am konfokalen Lichtmikroskop.
- Galina Dityateva für die Präparation der hippokampalen Primärneurone.

- Vladimir Sytnyk für die Einführung und Hilfestellung bei der Transfektion der Primärneurone und die Auswertungen am Laser Scanning Microscope.
- Sandra Schmidt für die statistische Auswertung der Neuritenwachstumsmessungen primärer Hippokampusneurone.
- Dr. Markus Delling für die produktive Hilfestellung bei Planung und Durchführung der Mutagenesen.
- Dr. Matthias Evers für die ständige Hilfsbereitschaft in allen Computerfragen und auch allen sonstigen Belangen des Laboralltags.
- allen namentlich nicht zu nennenden Mitarbeitern des Instituts und der Serviceeinrichtungen des Zentrums (Tierstall, Sequenzierung, Biacore).

Allen Kollegen/-innen des Instituts für Biosynthese Neuraler Strukturen möchte ich für die hilfsbereite und produktive Arbeitsatmosphäre in dieser Arbeitsgruppe danken, die vieles erleichtert hat. Im Besonderen möchte ich denen Kollegen danken, die mich während der ganze Zeit auch freundschaftlich begleitet haben: Die „Kantinengruppe“ Dr. Matthias Evers, Dr. Ulrich Bormann, Dr. Markus Delling, Kai Wesche, Joern Schweitzer und Dr. Michael Kutsche. Sowie Dr. Birthe Schnegelsberg , Tanja Schneegans, Bettina Rolf und Sandra Schmidt für Freundschaft und Motivation in und ausserhalb des Labors.

Letztendlich gilt mein größter Dank meiner Familie - meinen Eltern und meiner Großmutter – und allen Freunden, die mich über die ganze Zeit unterstützt und bestärkt haben in meinen Zielen. Und auch an Julian für mehr als den IT-support in den letzten schweren Stunden des Zusammenschreibens.

Curriculum vitae

Name: Melanie Richter

Geburtsdatum: 12.02.1971

Geburtsort: Herford

Bildungsweg:

Mai 1990 Abitur am Gymnasium am Markt in Bünde/Westfalen

Oktober 1990-
Oktober 1992 Philipps-Universität zu Marburg, Grundstudium
Diplomstudiengang Chemie

November 1992 Vordiplomsprüfung Chemie

Oktober 1993 Universität Bielefeld, Quereinstieg in den Diplomstudiengang
Biologie

Oktober 1993-
Juli 1994 Grundstudium

Mai 1995 Vordiplom Teilprüfung Biologie

Oktober 1994-
Februar 1996 Hauptstudium

April 1996-
Juli 1996 Nebenfach Klinische Psychologie an der Fakultät für Psychologie
und Sportwissenschaften der Universität Bielefeld

November 1996-
Februar 1997 Diplomprüfung Biologie

April 1997-
Mai 1998 Diplomarbeit am Institut für Biosynthese Neuraler Strukturen bei
Frau Prof. Dr. Melitta Schachner, Zentrum für Molekulare
Neurobiologie Hamburg (ZMNH) des Universitätskrankenhauses
Eppendorf

seit Juli 1998 Promotion am obengenannten Institut bei Frau Prof. Dr. Melitta
Schachner